



Gels with sense: supramolecular materials that respond to heat, light and sound

Christopher D. Jones^a and Jonathan W. Steed^{*a}

Received 00th January 20xx,
Accepted 00th January 20xx

DOI: 10.1039/x0xx00000x

www.rsc.org/

Advances in the field of supramolecular chemistry have made it possible, in many situations, to reliably engineer soft materials to address a specific technological problem. Particularly exciting are “smart” gels that undergo reversible physical changes on exposure to remote, non-invasive environmental stimuli. This review explores the development of gels which are transformed by heat, light and ultrasound, as well as other mechanical inputs, applied voltages and magnetic fields. Focusing on small-molecule gelators, but with reference to organic polymers and metal-organic systems, we examine how the structures of gelator assemblies influence the physical and chemical mechanisms leading to thermo-, photo- and mechano-switchable behaviour. In addition, we evaluate how the unique and versatile properties of smart materials may be exploited in a wide range of applications, including catalysis, crystal growth, ion sensing, drug delivery, data storage and biomaterial replacement.

1. Introduction

Gels are an important component of many human technologies, both modern and ancient. Natural gels of pectin, gelatine and agar have been utilised in food products since medieval times. Today, gels are also found in products such as lubricants, adhesives, soaps, cosmetics, medical implants and explosives.¹ The diverse and widespread application of gels may be attributed to their unique physical properties: like conventional solids, gels are able to support weight and retain their shape, yet they exhibit fluid-like behaviour under stress and can be moulded, printed and injected as required.²

A gel is defined by IUPAC³ as “a colloidal network that is expanded throughout its whole volume by a fluid.” Gels may be formed from water,⁴ organic solvents⁵ or ionic liquids⁶ and are termed hydrogels, organogels and ionogels accordingly. Gels in which the fluid phase is a gas, meanwhile, are termed aerogels. In general, liquid constitutes the vast majority of the material’s mass. The solid network, in which the liquid is encapsulated, consists of fibrous aggregates of polymers⁷ or small molecules, commonly referred to as low-molecular-weight gelators (LMWGs).⁸ It is worth noting that the definition of a gel does not require that a material be commonly identified as such. Indeed, this family of materials arguably encompasses even complex biological systems lacking the archetypal appearance of a gel, such as cytoskeletons, blood clots, microbial colonies and swollen cellular tissues.

Although it is normal practice to identify a gel by visual inspection, there are a number of other, more quantifiable physical properties that are typically exhibited by materials of this type. The popular inversion test, in which a gel is

characterised by its resistance to flow in an upturned vial, delivers a positive result for the majority of gels but is difficult to apply consistently due to the dependency on container size and composition.⁹ Furthermore, the test is poorly suited to the identification of weak and partial gels and may yield false positive results if applied to viscous liquids, suspensions and strongly adhered solids. A more reliable approach is to categorise materials based on their rheological behaviour.¹⁰ Gels undergo characteristic changes when subjected to tensile and compressive stresses but are more often identified based on their responses to oscillatory shear. In a typical experiment, the strain of a gel should vary only weakly with frequency, exhibit a similar phase to the imposed stress, and increase dramatically if the stress exceeds the yield point of the material, defined as the threshold value beyond which liquefaction takes place.

Historically, discoveries of new gelators have relied heavily on serendipity. However, burgeoning interest in the patterns of interactions between molecules has led to an improved understanding, at the molecular level, of the factors contributing to gel formation.^{11, 12} Particular pairs of functional groups that assemble into robust supramolecular synthons may be deliberately incorporated into a small molecule¹³ or polymer¹⁴ to target aggregates with the desired morphology. In gels, strongly hydrogen-bonding moieties such as ureas and amides are often exploited to generate fibrous structures,^{15, 16} though species containing aromatic rings or extended lipophilic moieties may also produce suitable architectures.⁵

One potentially useful feature of supramolecular gels is their sensitivity to chemical stimuli. Hydrogen-bonding motifs are strongly influenced by pH, so supramolecular gels often collapse or dissolve when an acid or base is added.¹⁷⁻²¹ A gel-sol transition is not, however, the only response that can arise from stimulation of a gel. Changes in gel structure may also affect

^a Durham University, South Road, DH1 3LE, UK. E-mail jon.steed@durham.ac.uk

properties such as colour,²² fluorescence,²³ viscosity,²⁴ conductivity²⁵ or magnetic susceptibility.^{26, 27} Furthermore, it is possible for gelator molecules to reassemble into an alternative aggregate, such as another gel,²⁸⁻³⁴ a non-gel micellar phase,³⁵⁻³⁷ or a precipitate of crystals^{38, 39} or amorphous solid.^{29, 35, 40-43} Supramolecular gels which respond to chemical cues, and their uses as sensors for specific molecules and ions, are the subject of a number of reviews.⁴⁴

Switchable behaviour may also be induced by physical stimuli such as changes in heat, light and mechanical forces. For example, Liu *et al.* reported that gels of azobenzene dendron **1** in polar solvents may be obtained through either ultrasound treatment or thermal cycling, and disrupted by heating, shaking, or UV illumination (Fig. 1).⁴⁵ Unlike chemical changes, these stimuli can be applied remotely and non-invasively, potentially allowing for rapid cycling between different gel and sol phases without contamination or degradation of the active material. The aim of this review is to offer a comprehensive summary of thermo-, photo- and mechano-switchable behaviour in supramolecular gels, with a particular focus on “smart” systems displaying multiple well-defined physical states that can be reliably interconverted. We consider in detail how such responses arise from thermal effects, variations in gel morphology and changes to the molecular structure of the gelator. In addition, the technological uses of responsive gels are described, with a brief evaluation of their advantages and limitations.

2. Gels that respond to heat

2.1 Switchable gelation

A gel is typically prepared by dissolving a gelator in a heated solvent and cooling the resulting solution. The temperature at which the gel forms is termed the gelation temperature, T_{gel} .^{46, 47} Given the labile nature of supramolecular motifs, gels based on LMWGs are frequently thermoreversible, reverting to the parent solution when heated above a threshold temperature. In

rare cases, however, a thermoreversible gel may be obtained by raising, rather than lowering, the temperature: the gel is “heat-set” and dissolves upon cooling.^{29, 48-55} Reversible heat-setting is often the result of an entropically-favoured molecular transformation. For example, a metallopolymer reported by de Hatten *et al.* forms a reversible gel at 140 °C due to a ligand-exchange reaction, in which the material dissociates into free trioctylphosphine-copper(I) complexes and neutral organic polymers that can more readily aggregate.⁵³ Likewise, Kuroiwa *et al.* created a gel by heating a cobalt(II) coordination polymer to induce an octahedral-to-tetrahedral transition, with concomitant release of the triazole ligand.⁵⁵ The entropic drive for gelation may also be provided by the aggregation process itself. Although the gelator experiences a loss of disorder during self-assembly, this can be offset by an increase in the entropy of a polar solvent, which must form ordered solvation shells while the compound remains in solution. An effect of this nature is commonly displayed by partly or wholly hydrophobic species such as β -cyclodextrin, calixarenes and non-polar peptides, and can be enhanced by the addition of kosmotropic salts such as lithium chloride.^{49, 56, 57}

A comprehensive summary of the influence of heating on gel formation can be found in a recent review by Li and Liu.⁵⁸ Crucially, the stability of a gel has been shown to depend on the number of junctions between the constituent fibres.⁵⁹ In some gels, fibres become entangled, physically crossing over each other to form transient junctions.⁶⁰ Alternatively, self-assembly may proceed in multiple directions such that fibres are connected via rigid branch points, known as permanent junctions.⁶¹ Gels containing permanent junctions are typically stronger than those containing only transient junctions,^{59, 62, 63} as quantified by their storage moduli and yield points.⁶⁴ Indeed, introducing covalent or robust intermolecular crosslinks between gel fibres is an established method for preventing disassembly of the aggregate state.⁶⁵ Branching may also affect the size, volume and connectivity of pores and, in gels of conductive materials such as poly(thiophene)s⁶⁶ and iodine-doped tetrathiafulvenes,⁶⁷ facilitate electron transport through the fibre network.

Formation of permanent junctions is highly dependent on gelator concentration.⁶⁸ At low levels of supersaturation, branching is limited and occurs mainly on the slowly growing side-faces of fibres. By contrast, highly supersaturated solutions favour extensive branching from both the side and tip surfaces.⁶⁹ Raising the level of supersaturation in a gelator solution can serve to enhance the mechanical strength and thermal stability of the gel produced. However, increased supersaturation results in more frequent nucleation, giving rise to a larger number of separate networks connected only by transient junctions (Fig. 2).⁷⁰ In addition, fibres with many permanent junctions may form dense spherulites, in which close packing of branches prevents the interpenetration of adjacent networks.⁷¹ To maximise the stability and strength of a gel, supersaturation must therefore be carefully controlled to establish an optimum balance between nucleation, fibre growth and branching.^{62, 72}

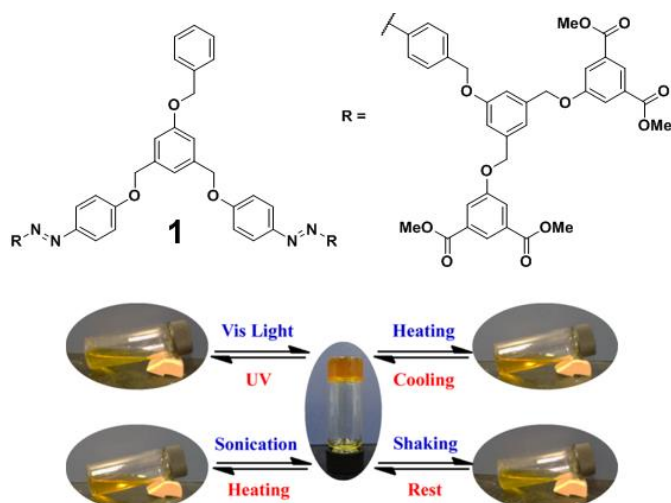


Fig. 1 Gel-sol and sol-gel transitions of a multiaddressable dendron **1** in 2-methoxyethanol. Image adapted with permission from ref. 45. Copyright 2012 American Chemical Society.

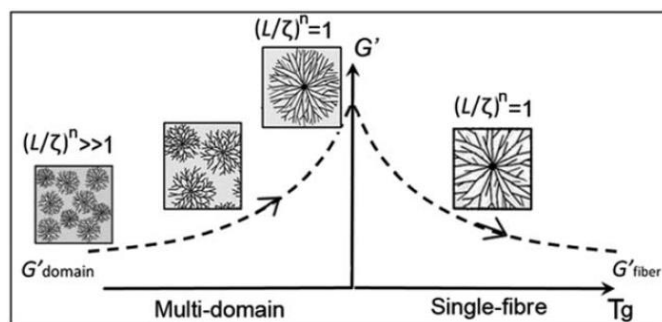


Fig. 2 Schematic plot showing the variation of network structure and storage modulus, G' , with T_g , the temperature of the gelling solution (where $T_g < T_{gel}$). (L/z) is the ratio of the gel volume to the volume of a single fibre-growth domain. Gel strength is maximised at levels of supersaturation giving small numbers of highly branched spherulites. Image adapted from ref. 62 with permission from The Royal Society of Chemistry.

Supersaturation varies in proportion to the solubility of the gelator. If solubility increases with temperature in a typical fashion, cooling a gelling solution raises the level of supersaturation and increases the mass of fibres and degree of branching in the final material.^{61, 69, 71} Branching can also be promoted by subjecting the solution to a higher rate of cooling.^{63, 73} It has been proposed that crystalline ordering is lost at permanent junctions, and that accelerated cooling facilitates this mismatch by reducing the time available for self-assembly.⁶¹ This theory was explored by Lam *et al.* in a study of the gelation kinetics of 12-hydroxystearic acid in mineral oil under non-isothermal conditions.⁷⁴ Intriguingly, at cooling rates below 5 K/min, fibres in a 2.5 wt.% solution exhibit nearly constant persistent lengths of 90–100 μm and fractal dimensions of approximately 1.0, indicative of extremely limited branching. At higher cooling rates, however, the persistence length is reduced to 20–40 μm and branching becomes more prevalent, producing fractal dimensions in the range 1.1–1.4. Fourier-transform infrared (FT-IR) analysis reveals that increased branching coincides with divergence in the formation rates of supramolecular synthons. Whereas hydrogen bonding by hydroxyl groups scales in proportion to gel formation, the rate of carboxyl dimerization plateaus at cooling rates above 5 K/min, suggesting that molecules under these conditions are forced to interact in a suboptimal fashion.

To fully understand the mechanism of a gel's formation, the kinetics of self-assembly must be quantitatively assessed.⁷⁵ If the rate of growth is constant near the start of gelation but falls thereafter, it is likely that successive stages of aggregation are similarly favoured and the process may be referred to as isodesmic. Conversely, the existence of a significant induction period suggests that nucleation and early propagation steps occur more slowly than subsequent growth. Mathematical models have been developed to describe and distinguish between these regimes, but characterisation of real systems may be complicated by changes in kinetic behaviour over time or under varying conditions. For example, Jonkheijm *et al.* found that an oligo(*p*-phenylenevinylene) (OPV) in cooled alkane solutions undergoes isodesmic self-assembly to form small disordered nuclei, before developing into larger helical structures via a cooperative nucleation-elongation pathway.⁷⁶

The stability of a reversible self-assembled aggregate may generally be gauged from the maximum temperature at which it forms. In a gel, this threshold temperature T_{gel} is variously defined as the point at which the material becomes more opaque, experiences a marked increase in elastic modulus, becomes capable of supporting a ball bearing at its surface or resists flow under gravity when the container is inverted. The onset of the reverse transitions is associated with the melting temperature of the gel, T_{melt} , but this value can vary depending on the temperature at which the gel is formed, T_f . Thus, T_{melt} is more reliably defined as the point at which T_f converges with the observed melting temperature, and can be obtained by linear extrapolation of measurements at $T_f \ll T_{melt}$ on a Hoffman-Weeks plot. Malik *et al.* adopted this approach in a study of gel formation by a synthetic tripeptide in *o*-dichlorobenzene, and found that the initial rate of gelation, approximated as the reciprocal of t_{gel} , exhibits a thermal dependency characteristic of fibrillar crystallisation.⁷⁷ Specifically, the logarithm of t_{gel} scales linearly with the ratio of T_{melt} to the product of T_f and the degree of undercooling, $(T_{melt} - T_f)$. It is worth noting, however, that this thermodynamic model does not fully capture the complexity of the gelation process. Turbidity measurements and microscopic observations indicate that gelation is preceded by a process of spinoidal decomposition, in which the solvent and peptide undergo spontaneous demixing to produce separate liquid phases. Furthermore, it is suspected that crystallisation involves the complexation of four solvent molecules by each molecule of tripeptide, as gels with this composition exhibit the largest melting enthalpies per mass of gelator.

The value of T_{gel} is largely determined by the strength of the supramolecular interactions in the material, and is thus highly sensitive to the structure of the gelator. Indeed, T_{gel} may be affected substantially by differences in enantiomeric excess,^{78, 79} chain length^{15, 45, 80, 81} or even the positions of functional groups.^{82–84} It is interesting to note that varying a simple molecular characteristic such as polarity, solubility or flexibility can lead to marked changes in nucleation and growth processes. For example, Rogers *et al.* found that while 6-, 8-, 10-, 12- and 14-hydroxystearic acids form gels easily in mineral oil, isomers hydroxylated in the 2 and 3 positions typically afford a small number of large, fibrous crystals.⁸³ This difference was explained in terms of the rate of crystal formation: separating the hydroxyl and carboxylate groups increases the activation barrier to nucleation, as it becomes more entropically costly to direct both polar functionalities towards the face of a growing crystallite.

Another factor governing the stability of a gel is the concentration of the gelling solution. Typically, the value of T_{gel} increases with concentration above the critical gelator concentration (CGC) until a saturation value is reached. Given that the onset of gelation depends on the solubility of the gelator, the stability of the final material is largely dictated by the solvent present. However, it may be possible in some cases to alter the solubility of a compound, and thus the value of T_{gel} , without the use of a different solvent. The chaotropic salt guanidinium chloride was shown by Nebot *et al.* to increase the

aqueous solubility of bolaamphiphile gelator **2**, but the guanidinium-amide interactions responsible for this effect are weakened by heating (Fig. 3).⁸⁵ Thus, addition of the salt to a solution of **2** above its usual CGC affords a heat-set gel with an elastic modulus that varies inversely with temperature. Such gels are only kinetically stable at room temperature, and may thus be utilised for the release of entrapped small molecules in a slow and controllable fashion.

Gelator concentration may also influence the rate of gel formation. Malik *et al.* found that the reciprocal of gelation time, t_{gel}^{-1} , scales approximately as the square root of concentration in excess of the CGC.⁷⁷ Whilst the proposed link to percolation theory is highly tentative, this formula usefully captures the effect of supersaturation on the kinetics of self-assembly, and demonstrates how additives and solvents that produce a change in CGC may inhibit or accelerate the gelation process. It is important to note, however, that the temperature dependency of the CGC does not fully account for the impact of solvent on gelation rate. For example, the dihydrazide gelator **3** was shown by Zhang *et al.* to gel chloroform far more rapidly than toluene, even though it is substantially less soluble in the latter above 20 °C (Fig. 4).⁸⁶ Furthermore, increasing the temperature of the chloroform system leads to more transparent gels with higher T_{melt} values and lower rates of formation, whereas gelation in toluene is accelerated by heating and always produces an opaque material of high thermal stability. Attempts to estimate the fractal dimensionality, D_f , of the gels from dynamic fluorescence data are of uncertain validity as the claimed correspondence with the Dickinson model of gelation⁸⁷ is not clearly justified. Nonetheless, a somewhat⁸⁸ more robust analysis based on the Avrami equation⁸⁹ suggests that D_f values of the chloroform gels increase slightly as the temperature is raised. In toluene, meanwhile, D_f values rise sharply partway through the gelation process and scale dramatically with temperature, with representative maxima of 1.7 and 3.0 at 5 and 35 °C respectively. These changes suggest that the aggregates in both systems become more interconnected with increasing temperature, and in toluene form via a two-stage process, undergoing one-dimensional growth before assembling into more densely packed fibrous bundles.

Although the environment of a gelator can influence both the rate of aggregation and mode of self-assembly, correlations between the gelation time and physical properties of a gel are

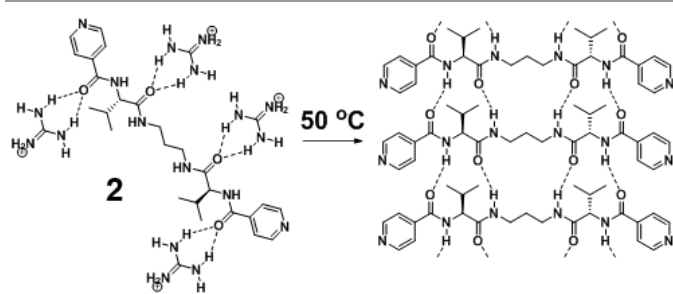


Fig. 3 Example of heat-induced gelation triggered by the loss of hydrogen bonding interactions with a chaotropic cation. Image adapted with permission from ref. 85. Copyright 2014 John Wiley and Sons.

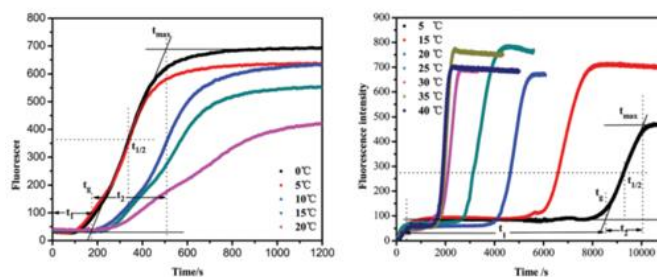
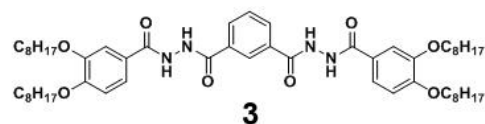


Fig. 4 Changes in fluorescence of **3** during gel formation in chloroform (left) and toluene (right). The time for gelation to begin (t_1) and reach completion (t_2) are both shorter in chloroform below 20 °C. However, the rate of gelation increases with temperature in toluene, whilst in chloroform it decreases. Image adapted from ref. 86 with permission from The Royal Society of Chemistry.

not always straightforward. Cholesterol-polyoxometalate hybrids were found by Su *et al.* to form gels comprising branched and intertwining ribbons in 17:3 toluene-DMF mixtures, and shorter, straighter assemblies at higher toluene concentrations.⁹⁰ Whilst increasing the concentration of toluene, a relatively poor solvent, initially reduces gelation time, volume fractions beyond 0.9 result in less rapid gel formation. By contrast, both fibre length and gel strength increase with toluene concentration. Similarly divergent trends in gelation kinetics and gel stability were described by Rohner *et al.*, in a study of 1:1 toluene gels of phenylethylamine and a range of peptide carboxylic acids.⁹¹ The least soluble peptides exhibited the lowest CGC values and gelation times as expected, but converted to sols at roughly the same temperature as more soluble analogues, due to a tendency for more enthalpically favoured structures to exhibit larger entropies of dissociation.

There has been some progress in predicting the outcomes of gelation experiments from the known physical properties of the gelator and solvent. In one notable study, Xu *et al.* showed that for gels containing solvents with comparable solubility parameters, T_{gel} correlates well with the solvent's viscosity and molecular volume.⁹² In addition, it has been shown that molecules are more likely to gel a given solvent if they display large enthalpies and entropies of dissolution,⁹³ and strongly favour low-dimensionality assemblies in crystal-structure predictions.⁹⁴ However, even in systems with simple compositions and calculable bulk properties, accurate estimation of a gel's thermal behaviour is often made difficult by complex, heat-induced changes at the molecular scale. A good illustration of the effect of molecular transformations on gel stability was provided by Ke *et al.*³⁶ Alternating treatments with heat and ultrasound cause aggregates of **4** in THF-water to interconvert between vesicular and gel-forming fibrous structures, due to a reversible transition between two U-shaped conformations of the gelator (Fig. 5).

Further variability in gel characteristics may arise if self-assembly can produce a range of products. The influence of even subtle changes in supramolecular interactions was strikingly demonstrated by Zhou *et al.*, who reported that a

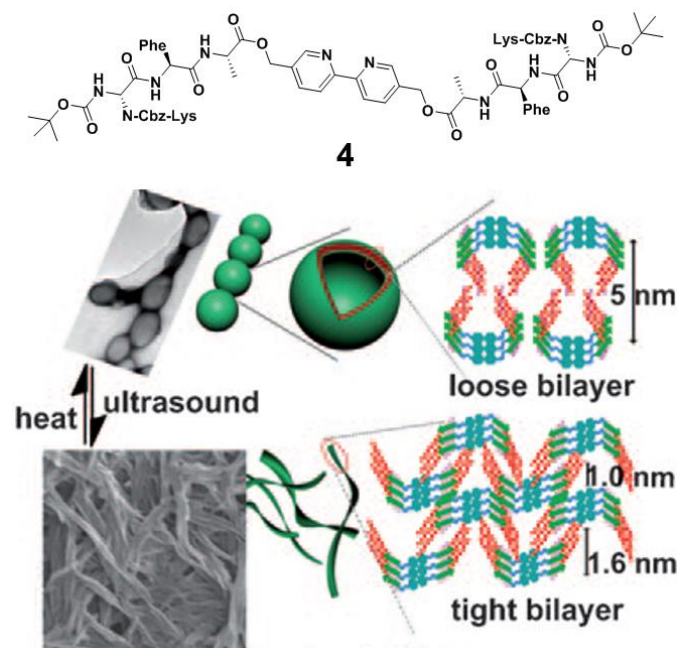


Fig. 5 SEM images and schematic representations of the morphological transitions induced by heating and sonication of **4** in THF-water. Shown right are the proposed packing modes of the gelator in its different conformations. The bipyridine core, drawn in blue, is connected to the tripeptide chains (red) via alkyl ester groups (green). Image reproduced with permission from ref. 36. Copyright 2011 John Wiley and Sons.

chiral calix[4]arene diamine gels cyclohexane if heated in the presence of D-2,3-dibenzoyletartaric acid but exhibits the reverse behaviour if the L-isomer is used.⁹⁵ Gelation in the second case is attributable to the formation of fibres with a lamellar structure, while heat-setting in the alternative system occurs because mismatched interactions between the co-gelators favour discrete, egg-shaped vesicles at lower temperatures. Discrimination between aggregate morphologies is thought to arise because cooling strengthens and shortens intermolecular interactions and thus promotes curvature in growing lamellae, to optimise packing of the chiral species. It should be noted that such dramatic changes in self-assembly outcome can also be achieved by mixing a chiral gelator with the enantiomeric species. According to one general mechanism, known as the chiral bilayer effect, an enantiopure amphiphile forms more stable micellar gels than the corresponding racemate, because crystallisation of the latter can more readily preserve the head-head and tail-tail interactions of the micelle assemblies.⁹⁶

In the competition between self-assembly pathways, kinetic effects are especially important. Thus, an effective method for controlling the aggregation outcome is through variation in the rate of change in temperature. Murata *et al.* demonstrated that rapidly cooling solutions of an azobenzene-linked cholesteryl gelator produces right-handed helices, whereas gradual cooling favours left-handed structures.⁹⁷ The chirality of the rapidly cooled system may be inverted by gentle heating, but the reverse transition cannot occur without dissolution of the gel. It may be deduced that the right-handed aggregate is a kinetically favoured but metastable state, which persists only if the cooling rate exceeds the rate of formation of the thermodynamic product.

A more common consequence of gel metastability is collapse of the material due to crystallisation.^{39, 94, 98-100} This change in phase may involve a salting-out process,^{101, 102} rearrangement of hydrogen bonds^{94, 98, 103} or recombination of labile metal-ligand interactions.^{104, 105} The relative stabilities of products are often highly sensitive to the environment of the gelator, and in particular the solvent, which in some multicomponent systems might be temperature-dependent. For example, Vidyasagar and Sureshan report a series of carbohydrate-derived gelators with 1,3-diol motifs that can interact to form linear supramolecular assemblies.¹⁰⁶ Remarkably, aggregation in petrol containing fewer moles of water than gelator affords a strong gel made up exclusively of non-hydrated fibres, while increasing the water concentration beyond one equivalent results in hydrated crystals with no concomitant gel. Although the authors do not explore the effect of temperature, it is feasible that the balance between gelation and crystallisation could be tuned by gradual evaporation of the more volatile co-solvent, or through heat-induced dehydration of a water-containing additive. Comparable dynamic control of the aggregation process has been realised in phase-separating colloidal suspensions, which may afford a kinetically trapped gel material before coalescing into a more compact equilibrium arrangement.¹⁰⁷

The mechanism of degelation may also exhibit unexpected complexity. A common observation is that the temperature of the gel-sol transition exceeds T_{gel} , due to the kinetic stability of the aggregate state.¹⁰⁸⁻¹¹¹ Breakup of the gel may be preceded by interconversion of polymorphic assemblies, with relative stabilities dictated by the structure of the gelator and the solvent being gelled. Such transformations need not reflect the pathway of self-assembly during formation of the gel. Indeed, differential scanning calorimetry studies by Čaplár *et al.* found that one series of isomeric chiral alkylamides can undergo as many as three endothermic transitions upon heating, but often display fewer exothermic transitions when cooled.⁸⁴ The temperatures of the transitions rarely coincide, and are strongly affected by even small changes in the polarity of the solvent, or the ionisation state or enantiopurity of the gelator. This behaviour is typical of a chiral amphiphilic gelator that can access a range of bilayer arrangements, the energies of which vary subtly in accordance with the symmetry, packing efficiency and chemical environment of the self-assembled molecules.

Many applications of supramolecular gels are dependent on the reversibility of gel-sol and sol-gel transitions. However, while thermoreversibility in small-molecule gels is common, such materials do not always form a simple gelator solution upon heating.¹¹² Wang *et al.* described a gel that appears to dissolve at a temperature T_{clear} , but retains residual nuclei up to a significantly higher temperature T_{soln} .⁶⁹ When the system is heated to between T_{clear} and T_{soln} and cooled, the surviving nuclei facilitate regelation, resulting in a higher-than-expected value of T_{gel} . Penaloza *et al.* similarly found, via FT-IR, fluorescence microscopy and small-angle X-ray scattering experiments, that the amphiphilic gelator N-palmitoyl-Gly-Gly-Gly-His trifluoroacetate forms fibrous aggregates in both the gel and sol states.¹¹³ Notably, the presence of such intact structures

in a sol may lead to the development of new aggregates, with the result that cycles of gel formation and destruction cannot be repeated indefinitely.^{29, 35}

Where ready interconversion between gel and sol states is possible, supramolecular materials may be usefully employed as temporary catalyst supports.^{114, 115} Small-molecule gels have been successfully utilised in the *in situ* preparation of gold, palladium and platinum nanoparticles for use in a range of liquid- and gas-phase processes. Moreover, a number of studies have shown that gelation can be used to boost the catalytic activity of gelators themselves. For example, Rodríguez-Llansola *et al.* reported that gelator **5** can effectively catalyse Henry nitroaldol reactions only in the gel state, wherein interactions between L-proline residues serve to enhance the basicity of the material (Fig. 6).¹¹⁶ Inducing dissolution of the gel was found to reduce both conversion and selectivity: a rise in temperature from 5 to 50 °C was needed to match the reaction rate in the gel, and the yields of side-reactions, such as nitroalkene generation, were markedly increased.

The formation of a gel might alternatively lead to a fall in catalytic turnover. Bachl *et al.* illustrated such an effect in the photooxidation of 1-(4-methoxyphenyl)ethanol by riboflavin acetate.¹¹⁷ When carried out within a gel, the reaction progressed at a rate 30-60% lower than in a non-stirred solution, and utilising the flavin catalyst as a co-gelator led to deactivation by almost 90%. Notwithstanding these limitations, the use of gels as reaction media did offer some benefits: the catalyst was protected from photodegradation, and in one case the reaction could be conducted without the proton-transfer agents needed in solution. The study additionally demonstrates the advantages of supramolecular gels over many other solid supports. In particular, the transparency of gels permits light-mediated reactions to be performed, and the ability to induce gel-sol transitions allows for easy recycling of the catalyst and gelator.

Switchable gelation has been exploited in a number of other applications. Due to their large surface areas, fibrous gels can serve as supports for catalytic particles, enzymes or quantum dots, or as tuneable media for controlling crystallisation and nanofabrication processes.^{39, 118-124} Precipitation in a gel may deliver materials with unusual crystal structures or particle

morphologies, which can subsequently be collected by simply dissolving the gel and filtering. Polymer gels exhibiting sol-gel transitions have also proven useful in medical products. In particular, a compound which forms a heat-set hydrogel near the temperature of the body (37 °C) may be administered to a patient as a liquid, but thereafter develop into a functional material with solid-like properties. As described in thorough reviews by Moon *et al.* and Hirst *et al.*, gels of this type have been used in controllable drug delivery systems, internal wound dressings and biocompatible scaffolds to replace, and aid the regeneration of, damaged tissues.^{125, 126}

2.2 Swelling effects

Insofar as gel formation and disassembly processes are dependent on temperature, all supramolecular gels may be described as thermoresponsive. Arguably more interesting are gels which, upon heating, exhibit varying physical properties without reverting to sols. One property that could be thermally sensitive is the volume of the gel network. Raising the temperature is likely to affect the intrinsic size and shape of gel fibres,¹²⁷ but it may also induce changes in their interactions with solvent molecules, causing substantial amounts of liquid to enter or leave the material.¹²⁸

A simple method for inducing a deswelling response is to remove solvent from a gel by means of heat or reduced pressure. Gels consisting of narrow interconnected fibres can often be dried to impressively porous materials in which the original fibrous structures can still be observed. In a study by Zhang *et al.*, desolvating an ethanol sonogel of **6** afforded a fibrous xerogel with a Brunauer-Emmett-Teller (BET) surface area of 266 cm² g⁻¹, whereas a powdered material prepared by thermal treatments exhibited a BET area of just 165 cm² g⁻¹ (Fig. 7).¹²⁹ Drying can, however, lead to collapse of an aggregate framework due to the surface tension at moving liquid-vapour interfaces, and may thus be highly undesirable prior to imaging of a gel or exploitation of its porous structure. Fortunately, such an outcome may be avoided by displacing the solvent of the gel with liquid carbon dioxide, which can be converted to a gas via

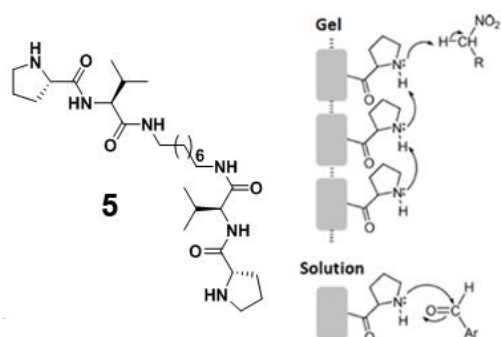


Fig. 6 Structure of L-proline-based gelator **5** and reaction schemes illustrating the dominant reaction pathways in its gels and sols. Proton transfer between proline residues in the gel promotes deprotonation of the nitroalkane reagent, which may subsequently react with an aldehyde to yield a nitroaldol product. In solution, the catalyst is considerably less basic and thus acts as a soft nucleophile, directly attacking the aldehyde to form an imine. Further reactions lead to nitroalkenes and dinitroalkanes as products. Images adapted with permission from ref. 116. Copyright 2009 American Chemical Society.

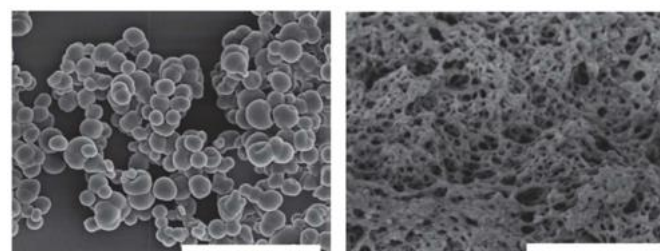
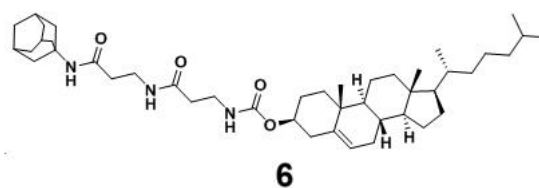


Fig. 7 SEM micrographs of aggregates of **6** prepared by drying of an ethanol sol (left, scale bar 5 μm) or sonogel (right, scale bar 1 μm). The fibrous aggregate appears more porous and exhibits a BET surface area that is approximately 60% larger. Images adapted from ref. 129 with permission from The Royal Society of Chemistry.

a supercritical fluid state to bypass the formation of destructive phase boundaries. Supercritical drying is most commonly applied to polymer gels and delicate inorganic materials such as mesoporous silicas, but may also be of use in preparing porous materials from small-molecule gels. Indeed, Shi *et al.* observed that bis(urea) gelators with perfluorinated end groups can gel carbon dioxide directly at concentrations of 1–6 wt.% and a pressure of 300 atm.¹³⁰ The resulting aerogels are over 97% less dense than the parent materials and exhibit micron-sized pores, making them ideal supports for heterogeneous catalysis or molecular sensing applications.

Less trivial swelling and deswelling phenomena, involving the reversible transport of fluid without a change in phase, occur frequently in polymer-based gels and have been reviewed in detail.¹³¹ Transitions of this nature occur spontaneously in response to varying environmental conditions and are thus differentiated from other processes affecting material volume, such as the injection of gas to generate a gel-stabilised foam.¹³² Generally, expulsion of liquid is linked to decreasing solubility of the gelator or, equivalently, increased aggregation of the gel fibres. The effect of heating is dependent on the supramolecular interactions present in the gel. Gels comprising hydrophobic gelators and a polar solvent typically undergo substantial deswelling with increasing temperature, because ordering of the solvent molecules around gel fibres is entropically disfavoured.¹³³ Conversely, hydrogen bonds between gel fibres are weakened by heating, inducing uptake of solvent and swelling of the gel.^{134–136}

Supramolecular gels may also exhibit swelling phenomena.¹³⁴ However, gel-solvent interactions are commonly (with some exceptions¹³⁷) important for the stability of the fibrous network,⁷⁶ so removal of even a fraction of the solvent may lead to destruction of gel-like properties. For example, Kiyonaka *et al.* found that heating a hydrogel of **7a** to 65 °C produces reversible shrinkage with visible expulsion of water, but heating to 69 °C results in the complete loss of solvent to give a white precipitate (Fig. 8).⁴³ Deswelling is highly sensitive to the structure of the gelator. In the gel of **7b**, a sharp phase transition occurs at 40 °C, while the gel of **7c** undergoes

a more gradual transition between 30 and 40 °C. Gelator **7d**, meanwhile, forms a gel that does not exhibit deswelling at all, instead undergoing a gel-sol transition when heated.

Another example of swelling supramolecular gels was provided by Krieg *et al.*¹³⁸ Gelator **8** forms gels in mixtures of tetrahydrofuran and water, with π - π stacking of the planar pyrene moieties leading to the formation of elongated fibres. These self-assembled structures are stable even at 100 °C. However, adjacent fibres interact predominantly via polyethylene glycol (PEG) chains (Fig. 9), which exhibit lower polarity at higher temperatures due to increased conformational flexibility.^{139, 140} Heating therefore causes the fibres to become more hydrophobic, resulting in increased aggregation and expulsion of solvent beyond 70 °C. The swollen gel can be regenerated slowly by cooling or, more rapidly, through redox-induced sol-gel and gel-sol transitions.

It is worth emphasising that swelling and aggregation processes are closely connected. While marked volume transitions in supramolecular gels are reported only occasionally, transitions between fibres and thicker ribbons or tapes are common.^{17, 51, 141–145} The dimensions of a polymer lamella were shown by Armon *et al.* to dictate the pitch, curvature and diameter of the resulting fibre, with wider and thinner sheets producing more condensed, tubular helices and higher elastic energies.¹²⁷ Thermal treatment can lead to morphological changes by inducing growth or shrinkage of lamellae and shifting the optimal balance between stretching and bending deformations. Such behaviour was observed by Qiao *et al.* in coordination polymers consisting of cholate and lanthanum ions.³¹ Scanning and transmission electron microscopy images reveal the dominant structures at 4 °C to be nanotubes with diameters of 5–23 nm, but increasing the temperature to 15 °C produces ribbons with widths of 10–60 nm and a right-handed helical morphology. Heating to 50 °C,

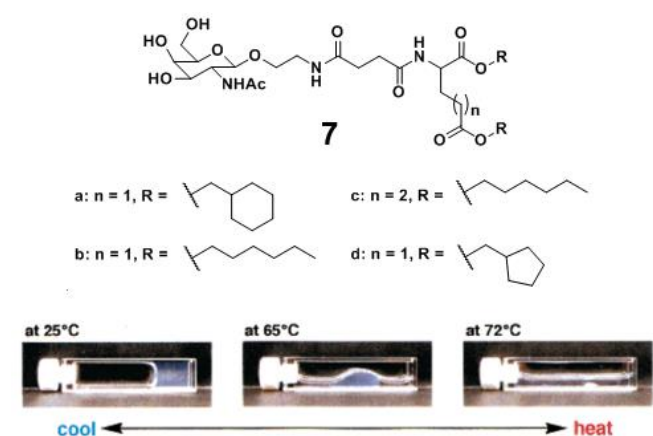


Fig. 8 Structures of N-acetyl galactosamine derivatives **7a–d** and photographs of the **7a** hydrogel at different temperatures. Shrinkage of the gel is visible at 65 °C (centre bottom). At 72 °C (bottom right), complete degelation has occurred and the gelator has reverted to a white precipitate. Images adapted with permission from ref. 43. Copyright 2002 American Chemical Society.

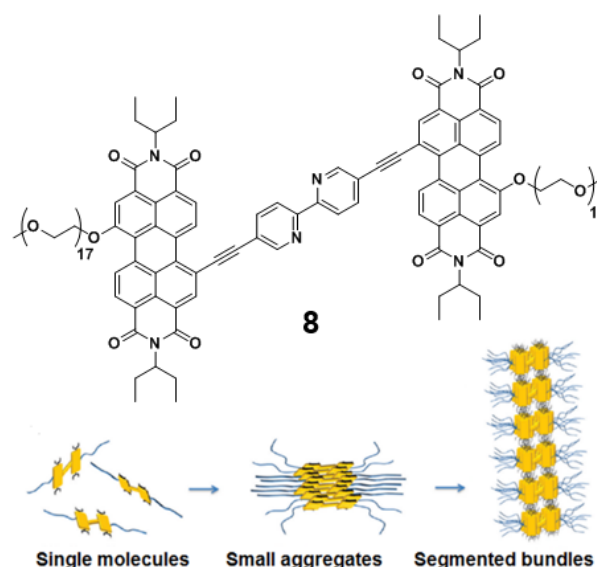


Fig. 9 Schematic representation of the aggregation mechanism of gelator **8**, a perylene diimide chromophore. Gelation occurs through π - π stacking of the perylene moieties, followed by coalescence of the pendant PEG chains to produce fibrous bundles. Solvent may also interact with the PEG chains, separating bundles to generate a swollen gel. However, heating weakens the PEG-solvent interactions, inducing a deswelling response. Images adapted with permission from ref. 138. Copyright 2009 American Chemical Society.

meanwhile, yields untwisted tapes with widths of 30-150 nm. It is unsurprising that enhanced aggregation, caused by the weakening of hydrogen bonds between water and cholate, results in a loss of curvature in the gel fibres, since both bending and stretching energies scale with the width and thickness of a tape.¹²⁷ Interestingly, however, changes in aggregate size also correlate with the rate of gelation: at 25 °C, a 3 mM solution fully gelled in less than a minute, whereas a solution with the same concentration at 4 °C formed a complete gel only after 2-3 days.

One useful feature of swelling gels is their ability to act as tuneable sponges, absorbing or releasing liquids in response to environmental cues. Such behaviour has been harnessed in a range of medical and bioengineering applications. Polymer hydrogels are particularly useful as they are compatible with the body's aqueous internal environment and often biologically inert. Furthermore, the swelling properties of polymer gels can be adjusted to suit a specific situation. For example, the rate of swelling can be reduced by use of larger or less spherical gel particles;¹⁴⁶ the magnitude of liquid uptake can be modified by including crosslinks between the gel fibres;^{14, 65, 147, 148} and ionic functionalities can be added to produce a volume transition that occurs more discontinuously upon heating.¹⁴⁹⁻¹⁵² Modifications of this nature also affect the rheological properties of the gel and must therefore be carefully chosen to ensure mechanical compatibility with the treatment site. Bai *et al.* succeeded in matching the strengths of thermally responsive poly(*N*-isopropylacrylamide) (pNIPA) hydrogels to those of bone and cartilage by incorporating β -cyclodextrin moieties, crosslinking these with adamantane-decorated poly(amidoamine) dendrimers, and adding to this network two additional polymers with furfuryl and maleimide termini.¹⁵³ Following injection into a bone fracture, the hydrogel undergoes rapid reinforcement due to cycloaddition of the furfuryl and maleimide groups, but prolonged incubation in the physiological environment leads to reversal of this crosslinking and replacement of the material with biological tissue.

Swelling of gels has also been exploited in medicine to deliver drugs in a controlled manner.^{19, 154, 155} If a drug is to be released slowly, the polymer support must be designed to exhibit gradual deswelling and high stability in its working environment, such as the acidic fluid of the stomach.¹⁵⁶ Conversely, rapid drug release may be achieved by the use of super-disintegrators, wherein extensive swelling weakens the polymer to facilitate dissolution.^{155, 157} Comparable drug release from gels comprising LMWGs has been explored,^{43, 158, 159} especially in topical applications.^{160, 161} LMWGs offer a number of advantages over polymeric gelators: they are often simpler to synthesise, boast useful features such as rapid low-temperature interconversion between sol and gel states, and can be controllably modified to enable specific and varied interactions with other molecules, such as an encapsulated drug.^{16, 135, 162} However, the widespread use of LMWGs in medical products has yet to be realised, due to the difficulty of designing sufficiently stable and biocompatible supramolecular gels with the desired properties.¹⁶³

In addition to enabling the release of a trapped guest, swelling behaviour may be harnessed to modulate the physical and chemical characteristics of a functional gel. Loss of solvent serves to increase the elastic potential energy of the system, which may be released through motion or deformation on a macroscopic scale. The nature of the response is dictated by the temperature distribution in the gel and can thus, in principle, be tuned to perform a useful mechanical function. A simple and practical approach, demonstrated by Yu *et al.* in thermally collapsible pNIPA hydrogels, is to supply heat via a deformable electrode mesh embedded in the gel sample (Fig. 10).¹⁶⁴ Although the rate of deswelling may be lower than if the gel were immersed in a heated solvent, this method allows different regions of the material to be heated in isolation, affording complex, asymmetric structures in a predictable and reproducible fashion.

An alternative strategy for controlling gel deformation is to manufacture a material that exhibits strain preferentially at the desired locations. Klein *et al.* showed that a pNIPA disc displays radial symmetry and positive Gaussian curvature on deswelling if the gelator is concentrated towards the centre of the structure.¹⁶⁵ A radially increasing concentration gradient, meanwhile, prescribes a negative curvature, necessitating the formation of wrinkles or creases that eliminate radial symmetry. More complex morphologies may be targeted by establishing less symmetric concentration distributions,¹⁶⁶ or through the use of three-dimensional starting geometries such as cylinders, which display wrinkling only if the curvature exceeds a threshold value. In addition, folding may be induced through successive cycles of heating and cooling, along axes of curvature dictated by the initial gel geometry.¹⁶⁷ Careful crafting of a gel may engender mechanical responses akin to those in biological systems, allowing the material to be implemented in artificial muscles and other actuator devices.¹⁶⁸ Studying the interplay of composition, geometry and thermal responsiveness may also assist in understanding the evolution of curvature at a microscopic level, which can lead to twisting or scrolling of aggregates or favour fibrous and lamellar assemblies over three-dimensional crystallites.

Changes in the shape and texture of a gel are often the most visible consequences of a volume transition. Of course, it is inevitable that a gel undergoing a decrease in volume will also exhibit changes in its bulk properties. In general, aggregation associated with deswelling leads to a reduction in the average distance between gel fibres. This effect usually enhances the stiffness of the gel^{31, 50} and may, in some systems, strengthen interactions between gelator molecules or adsorbed species.¹⁶⁹

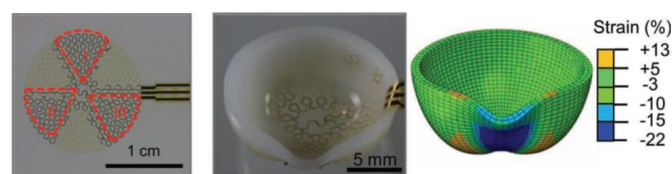


Fig. 10 Embedding three radial heater meshes in a pNIPA gel permits heat-induced shrinkage to be achieved in a localised fashion. Activating one heater creates a non-uniform strain distribution (estimated via a finite element simulation, right), such that a hemispherical gel is converted to a less symmetrical structure (centre). Image adapted with permission from reef. 164. Copyright 2013 John Wiley and Sons.

The usefulness of such changes was demonstrated by Wang *et al.*, who found that basic vinylimidazole moieties incorporated into a pNIPA gel are more active towards the hydrolysis of *p*-nitrophenyl esters when the gel is in its collapsed, hydrophobic high-temperature state.¹⁷⁰ By contrast, osmium-based complexes tethered to hydrogels of poly(vinylpyridine) were found by Heller *et al.* to undergo electron-transfer reactions less readily after deswelling, because aggregation disfavours the folded conformations needed to bring together neighbouring metal centres.²⁵

Intuitively, swelling processes should be particularly useful for controlling reactions that are diffusion-limited. As solvent is expelled during deswelling, the volume fraction of the gelator, ϕ , increases. This renders the system less permeable, since mass transport through gel fibres is less rapid than through a solvent. For a model distribution of impermeable spheres in a solvent matrix, it can be shown that diffusion of small solutes decreases roughly linearly with increasing ϕ if ϕ is small.¹⁷¹ In gels, it is more common to apply the Carman-Kozeny model, in which the pores between fibres are cylindrical and randomly distributed.¹⁷² This approach leads to a more complicated relationship between ϕ and diffusion rate, but the trend is still approximately linear for small ϕ . Indeed, some studies^{173, 174} have indicated that mass transport is dependent only on ϕ and the sizes¹⁷⁵ of the gel pores: geometric details such as fibre orientation are of relatively little importance.

As ϕ increases, the pores between gel fibres become narrower, and increasingly exert a drag force on the mobile solution.¹⁷¹ The rate of diffusion decreases as the ratio of the solute's hydrodynamic radius to the pore radius increases.¹⁷⁶⁻¹⁷⁹ In gels with low ϕ , drag is predominantly caused by viscous flow of solvent against the pore walls, so this is typically the only contribution included in models of diffusion.¹⁸⁰ It is clear, however, that adsorption,^{181, 182} electrostatic forces^{181, 183} and direct collisions with the pore wall^{184, 185} may further impede diffusion, particularly if the pore is very narrow, or the solute is charged^{186, 187} or bulky.¹⁸⁸⁻¹⁹⁰ In addition, drag may be amplified if the gel fibres are themselves ionised,^{187, 191} or present a rough or corrugated surface to the diffusing fluid.^{192, 193}

Phillips,¹⁹⁴ Pluen¹⁷⁷ and co-workers have attempted to summarise the major contributions to diffusion in a single formula. In practice, diffusion is often found to be lower than predicted by a factor of 1.5 to 3.0.¹⁷⁷ This result may partly be due to effects not accounted for in the models, such as structural heterogeneity at the external surface of the gel.¹⁹⁵ Typically, however, discrepancies are attributed to tortuosity: the fact that, for a given linear displacement, solutes in gels must travel further than those in solution in order to circumnavigate the impermeable gel fibres.^{177, 196} Tortuosity results from both the internal geometry of the gel and the inability of large molecules to pass through constricted spaces between fibres.^{178, 185, 197} Deswelling is likely to increase tortuosity, as solutes in a shrunken gel must travel through narrower channels and are thus more likely to encounter steric obstructions.¹⁹¹

Overall, shrinkage of a gel can reduce the rate of diffusion by as much as two orders of magnitude.¹⁹⁸ Such a decrease is

likely to diminish the activity of a supported catalyst, but this effect may be partly compensated for by an increase in reagent concentration. In a study by Zhang *et al.*, deswelling of a pNIPA gel was found to cause the internal concentration of a ferrocene complex to increase by roughly 4.5 times.¹⁹⁸ Similarly, Poggendorf *et al.* observed that PEG in pNIPA gels becomes so concentrated upon deswelling that transport of the solute is apparently enhanced, even though resistance to diffusion is increased.¹⁹⁹ Notably, as regions of high solute concentration develop, large local concentration gradients are established, which may serve to facilitate diffusion.¹⁹⁹ Indeed, it has been shown that diffusion in gels is particularly sensitive to solute concentration, as disruption of solute-solute interactions by gel fibres leads to more rapid transport along concentration gradients.²⁰⁰ Binding of solvent by gelator molecules may also play a role, since the loss of interactions between solvent molecules may reduce the average size of solvent clusters and their overall resistance to diffusion processes.²⁰¹

Additional complexity may arise due to interactions between reagents and the swelling gel, especially if the material can form multiple directional interactions with the adsorbed species. Oya *et al.* prepared a pNIPA gel with cationic side chains and found that the affinity of the gel for multiply charged pyranine anions scaled linearly with side chain density in the swollen state.²⁰² After thermal deswelling, however, a cubic or quartic relationship was observed, depending on the number of anionic sulfate groups present in the guest. This behaviour is consistent with a transition from single-point to multiple-point binding between the guest and gel fibres, and may be exploited to trigger guest release despite an increase in volume of encapsulated solvent. The existence of specific interactions also reinforces non-directional electrostatic forces, known as the Donnan potential, which can be as much as three orders of magnitude weaker under high-salt conditions and is less strongly affected by binding site concentration.²⁰³

Of further note are swelling events which not only influence the efflux of a guest, but display a feedback response as diffusion proceeds. In the aforementioned study by Poggendorf *et al.*, increasing the concentration of PEG in the pNIPA gels was found to both amplify the degree of swelling and lower the temperature at which the transition occurred. Interestingly, inward diffusion of PEG also induced reswelling of some gels after an initial shrinking event.¹⁹⁹ A similar, but more prolonged self-oscillating effect can be achieved by coupling ruthenium(II) tris(2,2'-bipyridine) to a pNIPA gel and utilising the material as a supported catalyst for the Belousov-Zhabotinsky (BZ) reaction.²⁰⁴ In this reaction, malonic acid reacts with bromate ions in acidic solution, forming bromide ions, carbon dioxide and water via a complicated redox sequence. Acting as a catalyst, ruthenium complexes are initially oxidised, causing the gel to swell due to increased hydration of the functionalised fibres. As the local oxidant is consumed, the catalyst is reduced and dehydrated, and the gel shrinks once more. The BZ reaction produces waves of oxidant, and the gel is thus stimulated to swell and contract in an oscillatory manner along the axis of wave propagation. It can be seen that chemical energy is converted to mechanical work, which in some gel geometries

may facilitate movement of the reacting solution through the material (Fig. 11).²⁰⁵ Because the BZ reaction influences the frequency of the swelling cycle, it effectively controls reagent transport and is thus indirectly self-regulating.²⁰⁶ Heating is not needed to produce this effect, but it does serve, below the volume-transition temperature of the gel, to increase the velocity of the waves of oxidation and diffusion rates of the reactants.

Since swelling involves structural modifications on a colloidal scale, it may be accompanied by changes in the colour or transparency of the material. In fact, swelling is just one of many mechanisms by which the optical properties of a gel can vary. Due to the ease with which small-molecule gelators can be designed, synthesised and derivatised, supramolecular gels have proven popular in the development of novel chromic systems, and for obtaining insights into the influence of intermolecular interactions on photophysical processes. These efforts have highlighted the subtle electronic effects that may be imparted by even small alterations of a self-assembled material, in response to thermal inputs and other changes in its physical environment.

2.3 Optical responses

It has long been known that aggregation can lead to substantial changes in the optical properties of a material. The mechanisms responsible for these phenomena may be subdivided according to their spectroscopic outcomes. In supramolecular assemblies, it is usual to compare the frequencies of absorption signals in the solid state with the corresponding frequencies in solution. A red-shift is termed a bathochromic effect and attributed to J-aggregation, while a blue-shift, or hypsochromic effect, is indicative of H-aggregation.

Molecules produce colour largely by absorption of photons, which causes electrons to be promoted from their ground state S_0 to an excited state S_1 .²⁰⁷ These are singlet configurations, as the number of antiparallel electron spins is maintained during the excitation. In a coloured organic compound, the highest occupied orbital of S_0 is typically a filled π bonding or non-bonding MO, while that of S_1 is a low-lying π^* MO with single occupancy. Fluorescence occurs when, following an $S_1 \leftarrow S_0$ transition, an excited molecule returns to the S_0 state and

releases its excess energy in the form of a photon. Alternatively, an electron may relax non-radiatively, releasing energy as heat via internal conversion. The balance between radiative and non-radiative deactivation in a molecule is largely determined by its electronic structure, but may also be influenced by environmental factors. For example, heating usually reduces fluorescence by promoting quenching effects such as molecular vibrations and solvent collisions.²⁰⁸

Although S_0 and S_1 are quantised, the energy of a transition can vary over a wide range, as each electronic state is coupled to molecular vibrations to produce a ladder of quantised vibronic energy levels. As a result, molecular absorption and emission spectra display broad continuous signals, with maxima arising from the most favourable vibronic transitions. Since electrons may relax non-radiatively to lower vibrational states after a transition, and the $S_1 \rightarrow S_0$ transition need not involve the ground vibrational state of S_0 , absorption spectra span higher energies than the corresponding emission spectra. This separation in energy, as measured between the global maxima of the two spectra, is termed the Stokes shift. Like absorption frequency, the Stokes shift can be significantly affected by aggregation: in particular, H-aggregation tends to increase the shift observed, while J-aggregation produces shifts of low or even zero magnitude.

An explanation for aggregation effects was first proposed by Kasha,²⁰⁹ who noted that dimerisation replaces each vibronic state with one higher in energy and another lower (Fig. 11).²¹⁰ These energy levels correspond to the two possible configurations of transition dipoles in the dimer. Crucially, electrons are only promoted to states in which the transition dipoles are aligned in-phase. If arrangements of this type are lowest in energy, $S_1 \leftarrow S_0$ transitions in the dimer require less energy than in the monomer, and the material exhibits bathochromic behaviour. A hypsochromic effect, by contrast, arises when out-of-phase pairing is favoured. Fluorescence primarily involves the most stable S_1 vibronic energy level which, in H-aggregates, corresponds to an out-of-phase state. Electrons promoted to an in-phase state must therefore relax non-radiatively before emission, producing a large Stokes shift.

Given that the allowed transitions in a dimer are dictated by the orientations of the monomer dipoles, the optical characteristics of the system must be closely linked to the mode of self-assembly. For rod-like molecules, bathochromic effects tend to result from strong end-to-end interactions, while hypsochromic effects require a side-on molecular arrangement. Less ideal structures, in which molecules are tilted or offset relative to their neighbours, may exhibit both J- and H-type absorption (Fig. 12).²¹⁰ These relationships are highly robust, and applicable even to extended aggregates such as supramolecular polymers. Thus, any stimulus that alters the packing of molecules in a material is likely to alter its spectroscopic properties.

In general, gelators exhibit the most pronounced optical changes when moving between solution and the solid state. It is thus unsurprising that many thermal chromic responses are associated with sol-gel or gel-sol transitions. For example, Yao *et al.* reported that merocyanine dye **9** forms supramolecular

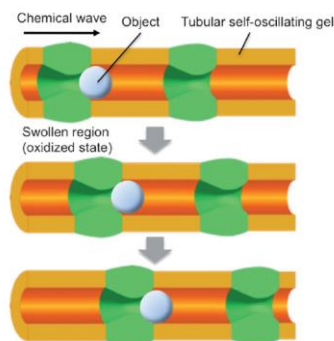


Fig. 11 Peristalsis-like motion of a tubular gel coupled with a redox-sensitive catalyst. The Belousov-Zhabotinsky reaction generates waves of oxidant, inducing the gel to swell and contract along its pore axes. This process can forcibly transport objects (represented as a blue circle here) through the gel. The frequency and velocity of swelling can be controlled via the temperature. Image reproduced with permission from ref. 205. Copyright 2012 John Wiley and Sons.

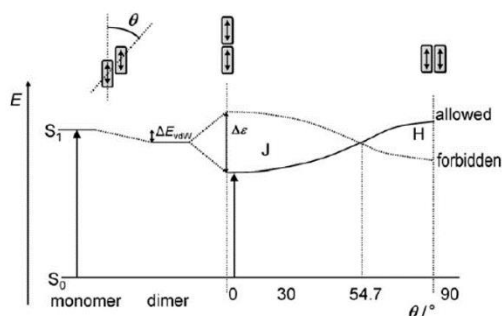


Fig. 12 Schematic diagram showing the variation in energy of the allowed and forbidden S_1 states as the angle between molecules, θ , is varied. Note that splitting does not affect ΔE_{vib} , the average energy of dimer states relative to the monomer. Image reproduced with permission from ref. 210. Copyright 2011 John Wiley and Sons.

polymers with distinctive blue-shifted absorption signals (Fig. 13).²¹¹ The polymers are stabilised by dipolar π - π stacking motifs and bundle together at high concentration to generate interconnected gel fibres. However, in the presence of solvents more polar than alkanes such as THF, the molecules assemble into dimers and monomers, producing absorption maxima at higher wavelengths. Intriguingly, polymers formed in the moderately polar solvent trichloroethene are metastable, so undergo a chromic transition through gradual disassembly into smaller clusters. This transition occurs over a period of days below 30 °C, but may be greatly accelerated by heating: in accordance with an Arrhenius-type relationship, the rate roughly doubles for an increase in temperature of 7–9 °C.

Another example of a thermoresponsive gel with variable absorption was provided by Das *et al.*²⁸ In non-polar solvents, dialkoxynaphthalene and naphthalene-diimide derivatives form co-gels in which the different naphthalene moieties are stacked in an alternating fashion. Since the frontier orbitals of the π systems differ greatly in energy, aggregation is associated with the formation of intensely absorbing charge-transfer complexes. The co-gels appear bright red or orange at 0 °C but assume permanent yellow colorations when warmed to room temperature, due to separation of the gelators into single-

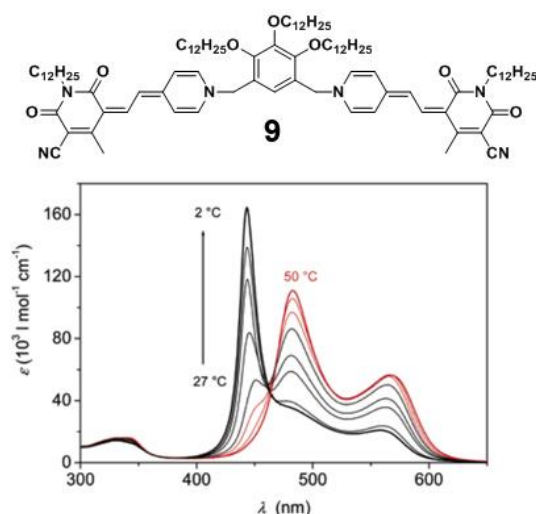


Fig. 13 UV-vis absorption spectra of **9** in a mixture of THF and methylcyclohexane over a range of temperatures. Maxima at 440, 490 and 570 nm are attributed to polymers, dimers and monomers of **9** respectively. Image adapted with permission from ref. 211. Copyright 2004 American Chemical Society.

component gels. The thermal dependency of the process is characteristic of a supramolecular material that is kinetically favoured but lacks thermodynamic stability. Thus, the study illustrates how rate-controlled gel formation can produce a material that is preconfigured to display thermochromic behaviour, due to the metastability of the self-assembled states.

Thermally induced structural changes can also affect fluorescence. Emission responses involving π - π interactions are particularly common, as stacking of aromatic rings may lead to exchange of excitation energy between neighbouring π systems. Energy transfer may occur through dipole-dipole interactions (the Förster mechanism) or, in materials displaying very small π - π separations, direct orbital overlap (the Dexter mechanism). Both the Förster and Dexter processes quench the fluorescence of the donor system by providing non-radiative pathways for electron relaxation. The acceptor, meanwhile, becomes more strongly emissive, typically fluorescing at a lower frequency than the unquenched donor.

Excitation energy transfer can be modulated by varying the separation or orientation of the interacting π systems. Praveen *et al.* demonstrated this principle by incorporating rhodamine, a charge acceptor, into a dodecane-chloroform gel of an OPV.²¹² Förster transfer induces the rhodamine to fluoresce at 625 nm, while quenching the gelator signal at 530–570 nm. Raising the temperature, however, leads to the disappearance of the rhodamine emissions and re-emergence of the gelator signal at 450 nm. The blue-shift in the fluorescence of the gelator results from disaggregation of the gel fibres, accompanied by loss of dipole-dipole coupling and divergence of the S_0 and S_1 states. Evidently, disassembly of the material acts as a switch for the donor-acceptor interaction, triggering a reversible and thermally controllable chromic response.

The study by Praveen *et al.* demonstrates the effects of π - π coupling on the wavelength and intensity of a fluorescence signal. While self-assembly often serves to strengthen such interactions, the mobility and conformational freedom of the aggregating species are greatly reduced. An excited molecule in solution may dissipate its energy through vibrations, rotations or intermolecular collisions. By contrast, the components of a supramolecular polymer are restricted to a small range of positions and geometries, and relatively isolated from the surrounding solvent molecules. Aggregation reduces the ability of electrons to relax via non-radiative pathways, so the lifetime of the excited state is extended and the efficiency of radiative deactivation markedly increased. This phenomenon, sometimes referred to as aggregation-induced enhanced emission (AIEE), occurs in a variety of supramolecular gel systems and is the subject of a number of recent reviews.^{23, 213}

Clearly, AIEE can only take effect if the systems responsible for fluorescence are formed or retained during aggregation. Even minor structural changes can lead to a pronounced alteration of the emission spectrum. For example, fluorescence of pyrene moieties at wavelengths of 450–500 nm is indicative of dimerization, as π - π stacking of these groups generates an emissive excited-state complex, or excimer.²¹⁴ Aggregation commonly promotes excimer formation by reducing the

separation of the pyrenyl species,^{111, 215-217} but the opposite effect – sometimes termed aggregation-caused quenching, or ACQ – may occur under some circumstances.^{41, 213, 218} In pyrene-based aggregates, ACQ arises when π systems self-organise into a non-overlapping arrangement, such that the bonding interactions of the excimer are no longer possible. The lack of π - π coupling may be compensated for by a strengthening of other interactions such as the hydrogen bonds of **10** (Fig. 14)^{41, 218, 219} or, if steric constraints allow for a range of packing modes, an increase in entropy.²²⁰

ACQ frequently occurs during the self-assembly of highly conjugated molecules. Indeed, non-emissivity appears to be a general feature of H-aggregates, in which serial face-to-face stacking of π systems is a common structural motif. According to the theory of Kasha,²⁰⁹ fluorescence in these materials is disfavoured because the most populated S_1 states correspond to out-of-phase dipole configurations, which typically exhibit small $S_1 \rightarrow S_0$ transition moments. Quenching increases with the size of the π - π stacked arrays and may thus be used to monitor the growth of self-assembled aggregates.⁹⁹ Exceptions may arise, however, where electrons can access weakly coupled triplet states to dissipate energy in the form of phosphorescent emissions.²²¹ Intersystem crossing between singlet and triplet states is promoted by the presence of heavy atoms such as Pt^{221, 222} and Br,²²³ and leads readily to radiative relaxation when coupled with AIEE effects.

A factor more commonly responsible for emission enhancement is the displacement of π systems from the ideal face-to-face stacking arrangement. Rösch *et al.* have shown that torsion angles as small as 10° are sufficient to enable strong fluorescence in merocyanine dyes, which otherwise behave as classical H-aggregates.²²⁴ Similarly, Cigáň *et al.* reported that H-aggregates of one bicyclic system are emissive because the molecules are offset to minimise separation of the electron-rich and electron-deficient rings.²²⁵ If the relative displacement of rings is very large, an assembly of π systems may even display the enhanced fluorescence, small Stokes shift and red-shifted

absorption characteristic of a J-aggregate.²¹⁰ The occurrence of J-aggregation in gels is often strongly dependent on the presence of directional interactions other than π - π stacking. For example, Ajayaghosh and Praveen found that OPV derivatives terminated with one or more hydroxyl groups give gels with J-aggregate structures, whereas derivatives terminated with cholesteryl esters produce H-aggregate materials.²²⁶

The balance between H- and J-aggregation may be influenced by environmental changes, such as exposure to heating or sonication,²²⁷ variation in the solvent²²⁸⁻²³⁰ or addition of a strongly binding additive.²³¹ According to Würthner *et al.*,²¹⁰ the synthetic route is particularly important when aggregation is governed by non-directional van der Waals interactions, as in the stacking of pseudocyanine dyes. In some cases, the self-assembly pathway may lead to a product which is kinetically favoured but thermodynamically unstable, such that the optical properties of the system may continue to evolve even after the material has formed.^{28, 232, 233} This effect was exemplified in a study by Lohr *et al.*, wherein a helical H-aggregate of a chiral bis(merocyanine) dye was found to convert over time to a different H-aggregate comprising more twisted fibres.²³⁴ As expected, the rate of the rearrangement process is controllable by heating: the initial aggregate is almost completely lost after 7000 min at 20 °C, but may be trapped for weeks if the temperature is lowered.

Direct conversion between J- and H-aggregates can also be achieved. Cho *et al.* reported that carboxylated porphyrin **11** forms hypsochromic metallo gels when sonicated in the presence of palladium(II) ions, but these break up into bathochromic aggregates when heated above T_{gel} , and further disassemble to give monomeric species at 60 °C (Fig. 15).²²⁷ The reverse process, conversion from J- to H-aggregates, can be induced through subsequent sonication of the sol. Switching between phases is associated with changes in both colour and fluorescence: the thermally generated metallo gel is green and exhibits the non-emissivity typical of H-aggregates, whereas the J-aggregate is red and more strongly fluorescent than both the original gel and the dissolved monomer. Although the metallo gel displays a highly amorphous sheet-like morphology, the J-aggregate adopts the form of cubic crystals, affording an X-ray structure in which the expected staggered molecular arrangement is clearly visible.

Optical properties in gels may be further modulated through swelling effects. The thermally induced collapse of a gel can dramatically reduce its transparency,^{43, 235} and may also be harnessed to control the structural colour of suspended particles or pores.²³⁶ In one study, close-packed silica beads were used to template an optical diffraction grating consisting of a porous pNIPAA gel, the dimensions of which could be varied under pH or temperature control to emit any colour in the visible spectrum.²³⁷ Swelling may further be associated with changes in aggregate morphology, which can in turn affect the colour or fluorescence of a material. For example, hydrogels based on a pyrenyl conjugate of phenylalanine were shown by Nanda *et al.* to contain helical fibres between 30 and 55 nm in diameter and emit strongly at 398 and 489 nm under neutral conditions.¹⁷ By contrast, gels at pH 14 contain non-helical tape-

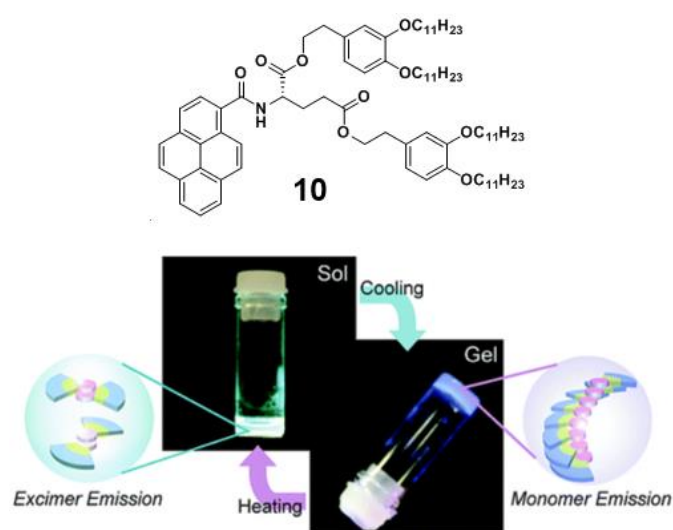


Fig. 14 Thermoreversible excimer emission of **10**. Gelation produces an ACQ effect because the close π - π stacking of the excimer cannot occur in the hydrogen-bonded structure of the gel. Image adapted with permission from ref. 218. Copyright 2007 American Chemical Society.

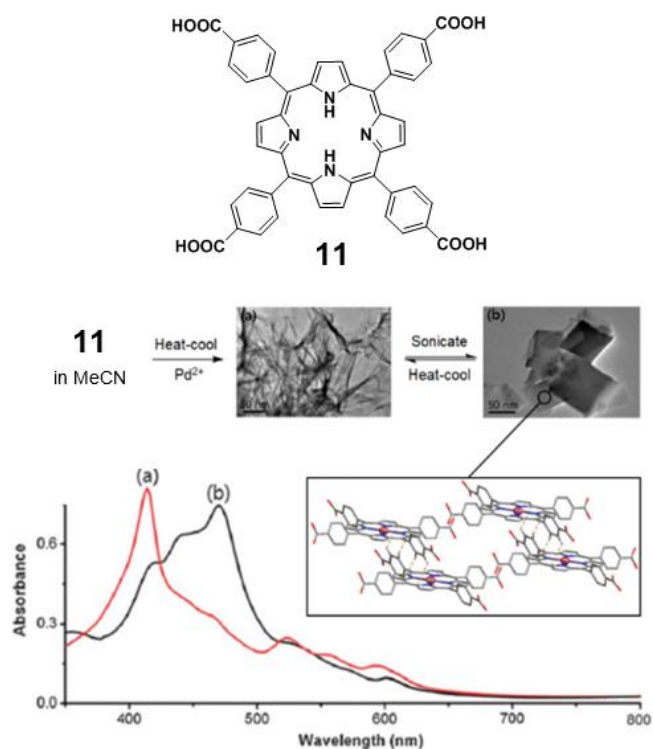


Fig. 15 Thermal formation of H-aggregated gel (a) from palladium(II) porphyrin complex **11** in acetonitrile, and the subsequent sonication-induced conversion to J-aggregates (b). The UV-vis absorption spectra of the two aggregates are shown. Inset is the X-ray crystal structure of **11** obtained in DMF. Images adapted from ref. 227 with permission from the Centre National de la Recherche Scientifique (CNRS) and The Royal Society of Chemistry.

like fibres 80 to 210 nm in width and are far less emissive at 398 nm, due to greater incorporation of monomeric pyrene groups into excimer assemblies.

Even if swelling does not induce optical transitions in the gel itself, such changes may result from the uptake or expulsion of a visible guest. The rate of diffusion of a guest into or out of the material is dictated by the size of the guest and the density and flexibility of the gel network. Sutton *et al.* demonstrated that hydrogels of Fmoc-phenylalanine prepared by a gradual decrease in pH can freely release even a 20 kDa fluorescently labelled dextran 5 nm in diameter.²³⁸ Fmoc-tyrosine, however, is less ionised at the point of gelation and capable of stronger hydrogen bonding interactions, so produces stronger gels with less labile fibre junctions. Accordingly, the diffusion rates of 358 Da Naphthol Yellow and 676 Da Direct Red were found to be lower by 8 and 84% respectively, and a 4 kDa dextran 2 nm in diameter showed no appreciable diffusion whatsoever. Willis-Fox *et al.* exploited such restrictions in solute transport to establish localised concentrations of a poly(fluorene) conjugated polyelectrolyte (CPE) in a matrix of diureasils, polymeric bis(urea)s crosslinked via terminal triethoxysilane moieties.²³⁹ Whilst adding CPEs to the diureasils during their sol-gel preparation caused them to be uniformly distributed throughout the material, swelling a preformed diureasil film in a CPE solution produced a dense layer of the fluorophore within 12–14 μm of the surface. Confining a guest to the surface of diureasil films may improve their performance as luminescent solar concentrators for photovoltaic devices, by reducing their

cost and minimising losses in efficiency due to self-absorption effects.²⁴⁰

A more esoteric consequence of restricted diffusion in gels is the emergence of complex, wave-like patterns within the solute distributions. Convection in liquid systems, driven by heat, light or an electric potential, can produce remarkably ordered dissipative structures including rolls, dendrites and pseudo-crystalline lattices.²⁴¹ Spatiotemporal patterns responsive to chemical interactions, however, are possible only if the transport rates of reagents are substantially mismatched. Effects of this nature, known as Turing instabilities, have been realised through the multicomponent reaction of iodide, chlorite, malonic acid and starch in acidic polymer hydrogels.²⁴² Interaction of the iodine product with both the polymer network and starch indicator dramatically lower its diffusion coefficient, generating standing wave oscillations in the reagent concentrations to establish a three-dimensional lattice of coloured spots. Similar reaction-diffusion coupling in gel-phase BZ reactions can break the symmetry of the initial reagent distributions to produce spots, bands and spiral waves.²⁴³ An important feature of such instabilities is that they are sensitive not only to the reagent concentrations and container geometry but also to environmental inputs such as heat, light, mechanical disturbances and even gravity.²⁴⁴ Patterns may be controlled by varying catalytic activity with gradients in temperature, pH or illumination, or through controlled swelling of a gel with suitable stimuli-responsive characteristics. Observations of these artificial systems could offer insight into comparable diffusion-limited patterning of biological systems, which has been implicated in symmetry-breaking cellular differentiation during tissue morphogenesis and embryo development.²⁴⁵

Additional environmental sensitivity is possible in gel networks containing d- or f-block metals.^{44, 246–248} Heating or cooling may alter the coordination environment of a metal, potentially inducing gel disassembly and/or a chromic response.^{53, 55} For certain metals, the change in coordination may occur via a spin-crossover mechanism, wherein a high-spin configuration of electrons converts to a low-spin state. Transitions of this type have been reported in gels comprising iron(II) complexes of triazole ligands.^{27, 249} Reversible conversion from diamagnetic low-spin to paramagnetic high-spin states is typically marked by a loss of colour and substantial increase in magnetic susceptibility. Spin-crossover temperatures are roughly constant in a given solvent, but stress-strain moduli and melting temperatures vary with gelator concentration (Fig. 16). Thus, the mechanical properties of the gels may be adjusted to suit a particular application, without reducing the efficacy of the desired switching response.

Electronic transitions may also affect the covalent structure of a gelator. The resulting molecule may pack and interact differently to its precursor, leading to changes in the stability, morphology and physical characteristics of the aggregate. Provided the reactive group responds to a specific stimulus and undergoes a well-defined transformation, it may be utilised as a molecular switch to convert between materials in a rapid and

quantitative manner. The mechanisms and applications of such switches will be outlined in the following section.

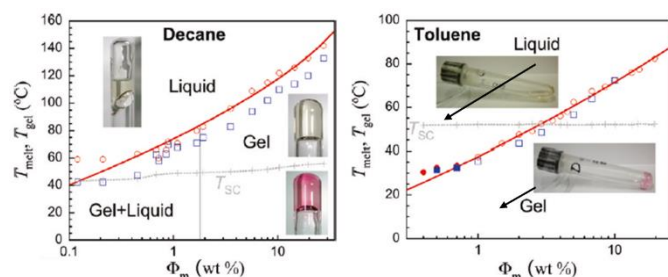


Fig. 16 Pseudo phase-diagrams of an iron(II)-triazole complex in decane and toluene. The measured T_{gel} value at each gelator concentration, Φ_m , is marked in blue squares and the melting temperature, T_{melt} , in red circles. Empty and full symbols denote gels prepared by cooling to 20 °C and 1 °C respectively. The recorded spin-crossover temperature, T_{SC} , is shown in grey. Spin-crossover clearly leads to a change from pink to colourless in both solvents, while heating above T_{melt} produces a colourless sol. Images adapted with permission from ref. 27. Copyright 2010 American Chemical Society.

3. Gels that respond to light

3.1 Conformational changes

Changes in molecular conformation are a common phenomenon in supramolecular materials. Flexible gelators can often access a number of packing modes with comparable energies, in which bond angles vary but the connectivity of atoms remains fixed. One such transformation, reported by Ke *et al.* and involving a change in the relative orientation of tripeptide chains around a bipyridine core, was mentioned in section 2.1 (Fig. 5).³⁶ Yan *et al.* invoked a similar process to rationalise the heat-setting of a nickel(II) metallogel of a bis(terpyridine) cyclam, noting that conversion of the U-shaped ligand to a more linear conformation would allow neighbouring coordination polymers to form bundle-like assemblies.⁵⁰ In these and many other systems, molecular deformation is associated with the growth or break-up of the gel network, but it is not unusual for a gelator to produce a different fibrous material in each conformational state. For example, Wu *et al.* found that the molecular arrangement of a cholesteryl gelator in *p*-xylene gels varies according to the gelation procedure.²⁵⁰ Molecular-geometry calculations suggest that molecules in gels obtained by thermal treatment display a straightened conformation with relatively little intramolecular hydrogen-bonding, whereas those in gels generated by sonication are bent in order to maintain the intramolecular interactions. This structural variation, though slight, translates to stark differences in the morphology and surface wettability of the aggregates formed.

Further conformational control can be achieved by altering the molecular structure of the gelator. One approach, which mimics the enzymatic processes governing self-assembly in biological systems,²⁵¹ is to incorporate a labile moiety that inhibits folding of the molecule into a gel-forming conformation. Haines *et al.* employed this strategy in the development of a synthetic 20-residue peptide that forms hydrogels on exposure to UV light.²⁵² In the absence of protecting groups, the molecule adopts a β -hairpin structure that can self-assemble laterally through the formation of

intermolecular hydrogen bonds, and facially through the association of hydrophobic faces. Protection of a cysteine residue with an α -carboxy-2-nitrobenzyl group, however, results in a random coil conformation unsuited to the formation of an extended supramolecular network. It is proposed that introduction of a charged residue on the valine-rich face disrupts hydrophobic interactions and provides steric hindrance to disfavour the formation of intramolecular hydrogen bonds. Deprotection can be achieved in just 30 minutes with a hand-held UV lamp, and affords hydrogels at basic pH with rheological properties comparable to those of a fresh unprotected peptide gel (Fig. 17). This photo-initiation methodology, sometimes referred to as caging, is preferable to the use of a photoreactive additive since it may be executed without significantly perturbing the pH of the system, and yields a by-product that has little effect on the strength or biocompatibility of the resulting gel.

Photocleavage of a gelator precursor represents an effective and elegant method for initiating a self-assembly process, but is impractical in systems that cannot be suitably functionalised or must be capable of reverting *in situ* to their original state. A more popular strategy is to exploit functional groups that remain intact upon illumination, but undergo switching between two or more rigid conformations. As a means of controlling gel properties, the use of species with intramolecular switching behaviour offers a number of advantages. Many popular reactive groups can tolerate a wide range of temperatures and solvents, and may be easily integrated into existing classes of gelator without greatly diminishing their propensity for gelation. Switching often occurs only in response to particular sets of stimuli and may thus be triggered as required, without affecting other sensitive functionalities present in the material. Finally, in many cases, a switching response may be tailored to suit a particular application: it may be made rapid and quantitative, or targeted to a product state with the required optical, mechanical and reactive properties.^{8, 30, 253, 254}

A variety of molecular switches have been incorporated into LMWGs, but common patterns of reactivity may be identified (Table 1). *Cis-trans* isomerisations are particularly popular, as they deliver a reversible conversion between two well-defined and chemically similar states that are both conformationally locked. Transformations of this type are most frequently realised in gels by stimulation of an azobenzene group, which is isomerised from the *trans* form to the *cis* by UV radiation near

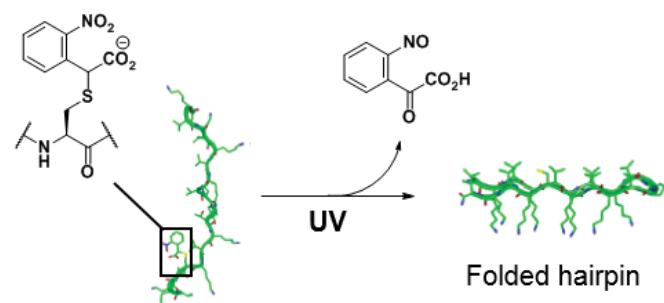


Fig. 17 Protection of a cysteine residue in a 20-residue peptide prevents the formation of a fibrous gel. Upon UV illumination, the protecting group is removed as a molecule of 2-nitrosoglyoxylic acid, allowing the peptide to fold into a β -

hairpin structure. Subsequent stacking of hairpins affords a network of fibrils. Image adapted with permission from ref. 252. Copyright 2005 American Chemical Society.

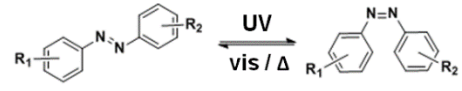
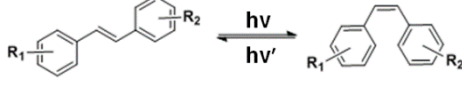
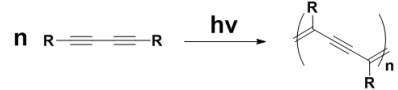
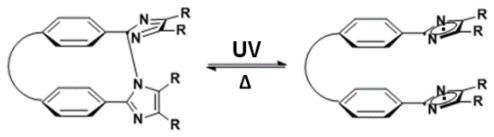
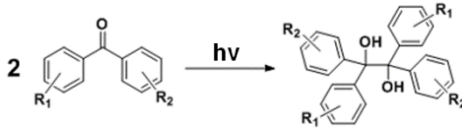

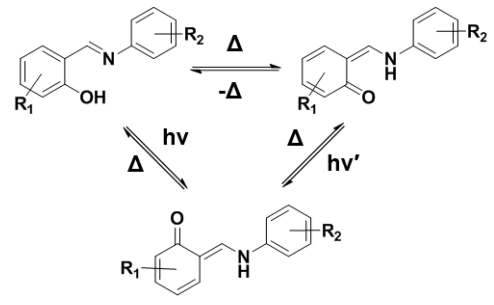

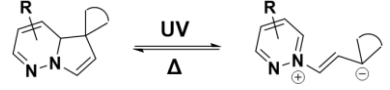
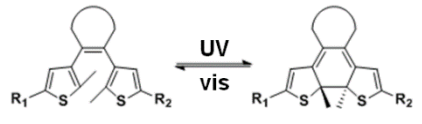
Reaction class	Example	Equation
<i>Trans-cis (E-Z)</i> isomerisation	Azobenzene	
	Stilbene	
Polymerisation	Diacetylene	
Dimerisation	Imidazole	
	Benzophenone	
Cycloaddition	Anthracene	
Tautomerisation	N-salicylidene aniline (anil)	
Electrocyclic reaction	Spiropyran	
	Dihydroindolizine	
	Dithienylethene (DTE)	

Table 1 Examples of photoresponsive functionalities that have been incorporated into LMWGs. R groups indicate common derivatisation patterns but are not exhaustive.

360 nm in wavelength. The reverse reaction can normally proceed to completion in a few hours at room temperature, but it may also be facilitated by visible light, with optimal wavelengths ranging from 430 to 450 nm.²⁵⁵

One use of the azobenzene switch is to produce a marked optical response. The *trans-cis* reaction occurs with a loss of absorbance near 360 nm and the emergence of $\pi-\pi^*$ and $n-\pi^*$ bands, at 290 and 460 nm respectively. Isomerisation in the solid state typically leads to a photostationary state in which 30–50% of the switch adopts a *cis* configuration, but higher yields are possible if the product becomes kinetically trapped. Moriyama *et al.* achieved such an effect in a bis(amide) gelator by irradiating a dichloromethane solution of the *trans* form with UV light whilst rapidly evaporating the solvent.²⁵⁶ In the recovered solid, UV-vis spectra displayed a 3:1 excess of the *cis* form, significantly exceeding the yield achieved in a comparable closed system.

Cis-trans isomerisations may also affect the structure or stability of a gel. Given that most azobenzene-based systems strongly favour a *trans* configuration under ambient conditions, it is perhaps unsurprising that the majority of gelators discovered produce gels in this form. Conversion to a *cis* configuration dramatically alters the shape of a molecule, which can be accommodated in the solid state only through substantial rearrangement of surrounding molecules. Such changes leave some aggregates morphologically unaltered, but their effect in a gel is often to induce dissolution of the material. Fibrous DMSO gels of tripodal azobenzene **12**, for example, were found to undergo gel-sol transitions when irradiated with UV light, even though the spherical structures formed in aqueous THF remain intact following isomerisation (Fig. 18).²⁵⁷ The breakdown of aggregates may result in a simple solution of the constituent compounds. However, it is also possible for new, smaller assemblies to be generated, as illustrated by Yagai *et al.* in a study of the melamine derivative **13**.²⁵⁵ In cyclohexane solutions, the molecule in its *trans* form co-assembles with a substituted barbiturate to form columnar stacks of rosette-like structures, but UV irradiation causes these to decompose into single rosettes, with *trans-to-cis* conversions of just 16% giving rise to a 50% decrease in aggregate size (Fig. 19). Light-induced gel-sol transitions may be exploited, like their thermal

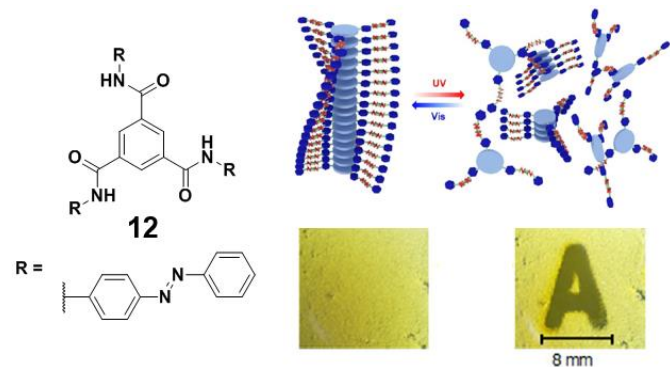


Fig. 18 Gels of **12** in DMSO consist of stacked assemblies of the tripodal gelator. The schematic diagram illustrates disassembly of the fibrils upon *trans-cis* isomerisation of the azobenzene groups. Localised UV illumination allows for well-resolved and reversible photolithography of a gel sample (bottom). Image adapted with permission from ref. 257. Copyright 2013 American Chemical Society.

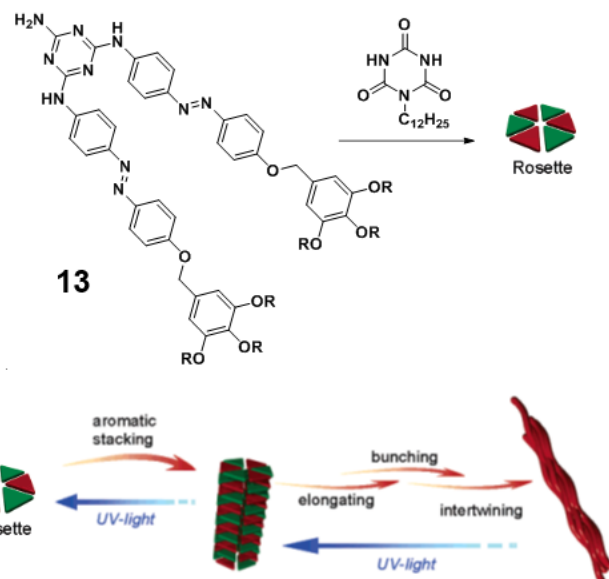


Fig. 19 Hierarchical self-assembly of **13** with a substituted barbiturate. Hydrogen bonding gives rise to rosette structures, but $\pi-\pi$ stacking into elongated columns is possible only in the *trans* configuration. Image adapted with permission from ref. 255. Copyright 2005 American Chemical Society.

counterparts, for the controlled release of drugs and other encapsulated species,²⁵⁸ and are uniquely suited to applications requiring remote or localised degelation, or where changes in temperature are difficult to accomplish.

In addition to altering the conformation of a molecule, a *cis-trans* isomerisation may strongly alter its polarity. The C-shaped *cis* form of an azobenzene compound tends to be more polar than the S-shaped *trans*,²⁵⁹ so a gel-sol transition may lead to precipitation if the material incorporates a non-polar solvent.²⁶⁰ In some cases, the kinetic stability of the precipitate may even prevent regeneration of the original aggregates by a *cis-trans* reaction.²⁶¹ Where the *trans* form is soluble in a non-polar solvent, however, conversion to the *cis* form may provide the reduction in solubility necessary for gelation to occur. Delbecq *et al.* illustrated this principle in solutions of a salt derived from 12-hydroxystearic acid and an azobenzene-containing primary amine.²⁶² A gel forms readily in toluene and undergoes a typical gel-sol transition upon UV irradiation, but in chloroform the compound exhibits the opposite behaviour, converting from a solution to a gel as the concentration of the *cis* structure increases. It is interesting to note that the chloroform gel is short-lived, since the azobenzene gelator reverts to its more stable *trans* configuration over time. The formation of materials that dissociate if not sustained by a continuous supply of energy is referred to as dynamic or dissipative self-assembly.²⁶³ Gels that form in this manner could be utilised as temporary catalyst supports and crystallisation media, and have also attracted interest as analogues for biological polymers that form under similar non-equilibrium conditions.²⁶⁴

Changes in polarity can be harnessed to effect sol-gel and gel-sol transitions, but they may also be utilised at the surface of an aggregate to modulate its interactions with the surrounding solvent. Such changes may induce swelling or contraction of the gel, as the capacity to encapsulate bulk liquid depends strongly on the energy of the solvent-gel interface. The

greater ability of *cis*-azobenzene groups to interact with polar solvents was beautifully demonstrated by Seki, who found that Langmuir monolayers of an azobenzene-based polymer can be made to expand reversibly across an air-water interface by exposure to UV light.²⁶⁵ Conversely, Borré *et al.* reported that zinc(II) metalloids of an azobenzene-functionalised terpyridyl ligand undergo deswelling of 85% upon isomerisation and, due to the limited solubility of the product, fail to return to their swollen state.²⁶⁶ It is worth noting that whilst light-induced volume transitions may resemble those achieved through heating, the microstructural changes involved in these processes can greatly differ. Xie *et al.* reported that mixed hydrogels of the dendron gelator **14** and azobenzene derivative **15** undergo thermally reversible deswelling when stored at 20 °C, but return to a swollen state upon isomerisation of the photoreactive species (Fig. 20).²⁶⁷ Although heating and irradiation produce swollen gels that are comparable in appearance, the latter affords fibres that are significantly wider and more twisted, and greatly diminishes the supramolecular chirality of the parent material.

Altering the local interactions of azobenzene groups can be a useful strategy for controlling other self-assembly processes. A detailed review by Sangeetha and Maitra explores the effects of LMWGs on the behaviour of molecules in the liquid phase, with a particular focus on how gelator isomerisation can influence the phase transitions of liquid-crystalline species.²⁶⁸ Gels of mesogens can exhibit electrical conductivities equal to or greater than those of the pure liquid crystals, and may accelerate alignment of the molecules under an applied electric field.^{269, 270} The mesh size of the gel network dictates the size of the liquid-crystal domains and thus the opacity of the material before an electro-optical response. Liquid-crystalline ordering, meanwhile, can template self-assembly of the gelator to produce fibrous aggregates with a more anisotropic arrangement. In one remarkable study, Moriyama *et al.* showed that photoisomerisation of a bis(amide) azobenzene gelator induces conversion of the nematic mesogen 4-cyano-4'-(pentyl)-biphenyl to a cholesteric phase, whilst also inducing a

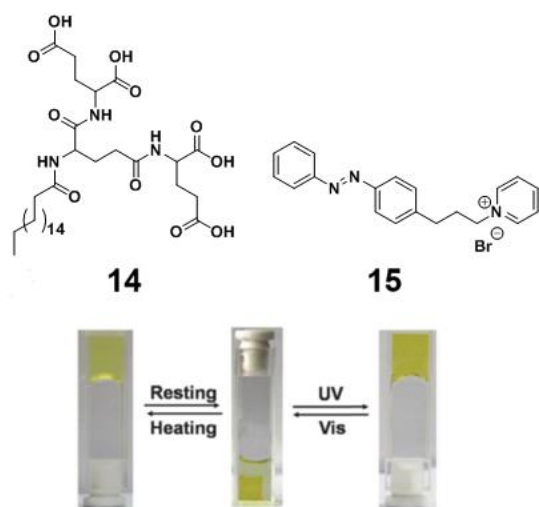


Fig. 20 Reversible deswelling and swelling transitions of a mixed hydrogel of **14** and **15**, on resting and after exposure to UV light. Image reproduced from ref. 267 with permission from The Royal Society of Chemistry.

gel-sol transition.²⁷¹ Reversion of the gelator to the *trans* form leads to regeneration of the gel state, but the resulting gel fibres are now aligned with the fingerprint texture of the cholesteric liquid crystal. Irradiation of the nematic gel through a photomask can thus produce a well-defined pattern of cholesteric gel domains, providing an effective non-electronic method for information storage over extended periods of time (Fig. 21).

To design a gel in which azobenzene isomerisation occurs readily, the environment of the switchable groups within the aggregate must be considered. Since the azobenzene moiety is small and only a weak hydrogen bond acceptor, its direct interactions are only occasionally important for stability,²⁷² but it may facilitate π - π stacking by providing a conjugated bridge between planar aromatic functionalities. It is therefore common for azobenzene-based gelators to assemble into H-aggregates, in which molecules are closely packed and, due to strong coupling between the aligned dipoles, non-emissive.²⁰⁹ The lack of vacant space in such materials strongly disfavours transformations that involve large conformational changes. Consequently, reaction of an azobenzene group in the gel state may be far slower than in solution, or require initiation by light of relatively high intensity.^{273, 274} To avoid these limitations, gelators have been constructed wherein hydrogen-bonding groups and non-planar, aliphatic frameworks favour the self-assembly of aggregates without π - π stacking.²⁶¹ A molecule with these properties was shown by de Loos *et al.* to promote thermal *cis-trans* switching of an azobenzene-containing bis(urea) in co-gels containing *n*-butanol.²⁷⁵ Indeed, the rate of isomerisation in gels was found to exceed that in solution, and could be further enhanced by using enantiomers of matching chirality in the self-assembly process.

When used as molecular switches, azobenzene groups exhibit a number of drawbacks. Conversion of the *trans* form to the *cis* cannot reach completion, and usually proceeds with quantum yields below 30%. Furthermore, unless thermal relaxation is disfavoured by particularly strong interactions in the product aggregate,²⁷³ reversion to the *trans* form tends to occur within hours of irradiation. These problems cannot be addressed easily whilst retaining the azobenzene moiety, but they may largely be resolved by the use of an alternative molecular switch, the stilbene group. Like azobenzene compounds, stilbenes undergo photoisomerisation between *cis* and *trans* configurations. However, the reactions display relatively high conversions and quantum yields, and a large

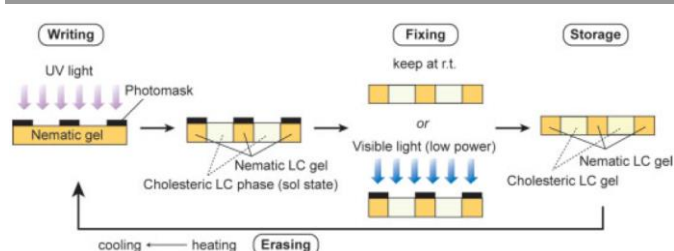


Fig. 21 Scheme for a non-electronic information storage device in which the ordering of a liquid crystal is controlled by photoisomerisation of a bis(amide) azobenzene gelator. Image reproduced with permission from ref. 271. Copyright 2003 John Wiley and Sons.

activation barrier precludes thermal relaxation at room temperature, allowing the two isomers to be stored and characterised without risk of compositional change.²⁷⁶

A good example of aggregation controlled by stilbene switching was provided by Xu *et al.*²⁷⁶ Irradiation by light at 387 nm induces quantitative conversion of **16** from the *E* form to the *Z*, while light at 360 nm triggers the reverse reaction. The compound can form fibrous aggregates in either form, but the mechanism of self-assembly is different for the two configurations (Fig. 22). A linear correlation between viscosity and concentration in solutions of the *E* form suggests that fibre growth occurs by isodesmic polymerisation, in which monomers are added to the end of a chain at a rate independent of its current length. The *Z* form, meanwhile, displays a discontinuity in the slope of its viscosity-concentration profile, indicating that linear fibres develop from cyclic intermediates via a ring-chain polymerisation pathway. Interestingly, only fibres of the *E* form are found to give rise to a stable gel. It is proposed that the extended conformation of the *E* form promotes the propagation of a one-dimensional supramolecular polymer, and the planarity of the molecules enables π - π stacking to give a three-dimensional network. By contrast, the C-shape of the *Z* form favours the formation of cyclic structures, and unidirectional π - π stacking is hindered by the proximity of the molecule's bulky side-chains, which prohibits the aromatic moieties from adopting a co-planar arrangement.

Another instance of stilbene isomerisation delivering a useful gel-sol transition was reported by Draper *et al.*²⁷⁷ A conjugate of stilbene 4,4'-dicarboxylic acid and phenylalanine, **17**, was shown to form hydrogels both on its own and in the presence of another dipeptide-based carboxylic acid gelator **18**. Due to their differing pK_a values, and the sensitivity of peptide gels to protonation equilibria,⁹⁸ the molecules can be induced

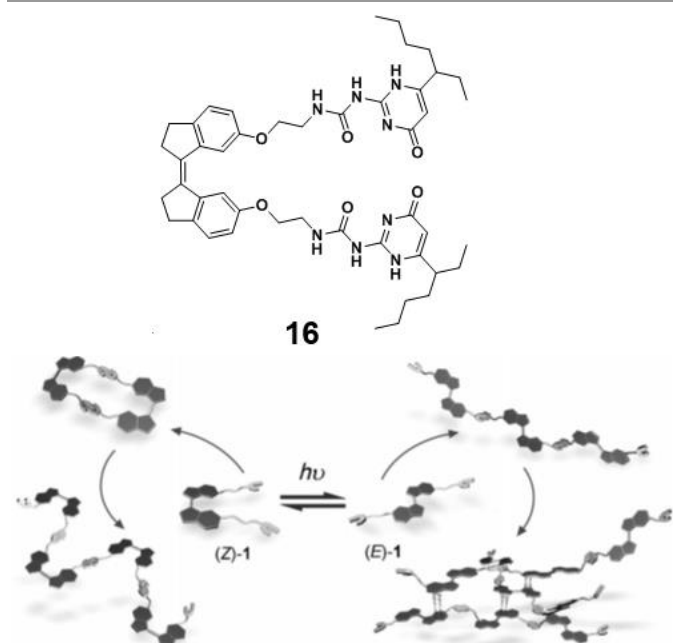


Fig. 22 Schematic representation of the self-assembly mechanism of stilbene **16**. The compound in its *E* form undergoes isodesmic polymerisation to give a fibrous gel network. The *Z* form, however, aggregates via a two-stage ring-chain pathway

and cannot form gels, due to a lack of π - π stacking between fibres. Image adapted with permission from ref. 276. Copyright 2013 John Wiley and Sons.

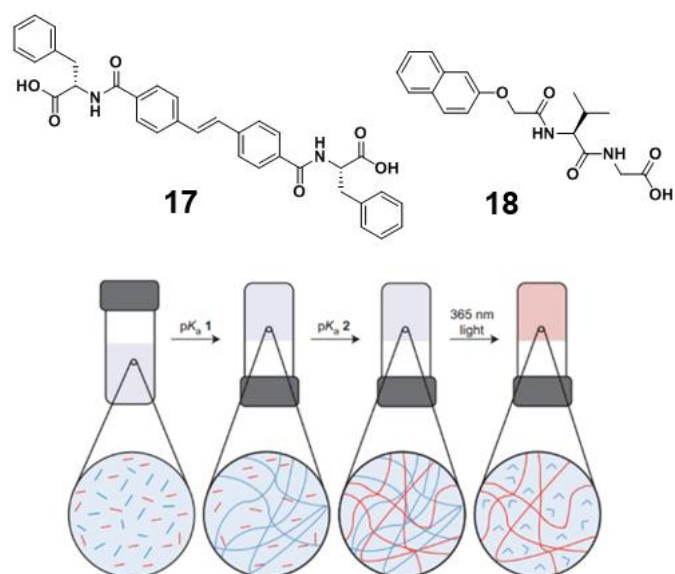


Fig. 23 Schematic representation of self-assembly in a mixed aqueous solution of **17** and **18**. Acidification produces self-sorted gel networks of **17** and **18**, whilst subsequent UV-irradiation causes the fibrous aggregates of stilbene **17** (shown in blue) to disassemble. Image adapted with permission from ref. 277, correcting stereochemistry of **17** in original diagram. Copyright 2015 Nature Publishing Group.

to self-sort into separate fibrous aggregates by gradually lowering the pH of the mixed sol (Fig. 23). Photoisomerisation of the stilbene causes the assemblies of **17** to revert to sols, while leaving those of the non-photoreactive gelator **18** unaffected. Through the use of a photomask, selected regions of the mixed gel may be converted to the single-component system, allowing the optical and rheological properties of the material to be altered in a spatially controllable fashion.

As in azobenzene-based systems, the effect of molecular switching in a stilbene gelator depends on how the rest of the molecule interacts before and after the conformational change. Miljanić *et al.* reported that solutions of a stilbene oxamide derivative in its *Z* form undergo gelation upon irradiation with 250–520 nm light, due to the lower solubility of the compound in its *E* configuration.²⁷⁸ A similar effect was observed by Chen *et al.* in a study of a dibenzosuberane-based helicene, but in this case the compound forms a sol if the concentrations of the *M* and *P* configurations are comparable, and acts as a gelator if either isomer is present in significant excess.²⁷⁹ Conversion of the *M* isomer to the *P* transforms one fibrous assembly to another via an intermediate vesicular phase, and can be controlled by adjusting the irradiation wavelength within the range 270–335 nm. It is suspected that linear aggregates form through complementary interactions between molecules of like chirality, whereas the competitive pairing of opposite enantiomers favours more cyclic supramolecular motifs, leading to discrete structures that are unsuited to the development of an extended gel network.

The stability of the stilbene moiety in its two configurations permits its use in situations that demand a predictable and long-lived response. For example, Matsumoto *et al.* utilised an alkene switch similar to a stilbene to achieve rapid and

controlled release of nanobeads, bacteria and large molecules from a glycolipid-based hydrogel.²⁸⁰ In the absence of UV irradiation, the gel fibres were found to act as a barrier to diffusion, limiting the efflux of one model compound, vitamin B₁₂, to 7.8% over three hours. Remarkably, switching of the alkene was also harnessed to reactivate an ATPase motor immobilised in the gel. Microbeads tethered to the enzyme in a buffered solution of magnesium-ATP were observed to cease rotating following gel formation, but returned immediately to their original rate of motion if the material was irradiated with 266 nm laser light.

Switching of stilbenes may additionally deliver changes in fluorescence to provide tuneable contrast in bio-imaging applications. Zhu *et al.* demonstrated that irradiation of a naphthalimide-functionalised cyanostilbene with UV light can shift fluorescence from yellow to blue, even when using cervical cancer (HeLa) cells as a medium for the dye.²⁸¹ The initial colour is attributed to emissions from the naphthalimide moiety, while the increase in wavelength results from an enhancement of the cyanostilbene fluorescence during the photo-induced *Z-E* isomerisation. Computational studies suggest that the *E* form is more emissive because steric hindrance prevents the formation of a stable excited species, known as a twisted intramolecular charge transfer (TICT) state, in which radiative relaxation is disfavoured. Prevention of TICT states is a common mechanism for the amplification of fluorescence during switching reactions,^{281, 282} and can occur more generally through aggregation, contributing to the AIEE phenomena outlined in section 2.3.²³

Notwithstanding their useful characteristics, stilbene-based molecular switches exhibit a number of significant limitations. In some cases, neighbouring functionalities may inhibit isomerisation of the alkene group, or promote the irreversible formation of cyclic species. Overlap in the absorption bands of the *E* and *Z* forms may render selective interconversion impossible, with mixtures of products arising even under monochromatic irradiation.^{281, 283} Furthermore, the reaction necessitates a large conformational change which may be strongly disfavoured in the solid state. Problems of this nature arise frequently in materials that deliver switchable behaviour by means of a *cis-trans* isomerisation. Indeed, to achieve a response that is rapid, reversible and high-yielding, it might be preferable to trigger changes in the connectivity of a molecule, whilst only moderately altering its overall conformation.

3.2 Coupling reactions

By conducting a reaction in the solid state, many of the limitations of solution-based chemistry may be avoided. Aggregation offers access to reactant concentrations far exceeding those in solution and may thus enable significant rate enhancements, particularly in reactions involving poorly soluble reagents. Molecules in an aggregate exhibit fixed conformations and relative orientations, so may react more selectively and at a reduced entropic cost. Furthermore, steric constraints and intermolecular forces often serve to stabilise products, allowing for the isolation and analysis of species that

could not persist in solution. Unfortunately, for such benefits to be realised, it is generally necessary for molecules to assemble in a reactive configuration and undergo transformations in a cooperative fashion. As a result, a reaction in the solid state is most effective when the reactants are pre-organised, by means of covalent or strong intermolecular bonds, to closely resemble the target transition state.

As illustrated in Table 1, a wide variety of LMWGs containing photoreactive functionalities have been developed. Irreversible processes that have been carried out in the gel state include pinacol reactions,²⁸⁴ polymerisations of diacetylenes,²⁸⁵ dimerizations of tyrosine residues in peptides and cascade reactions involving 1,3,4-oxadiazoles with styrenes.²⁸⁶ The formation of covalent crosslinks between gelator molecules can lead to an increase in gel stiffness and stability, as demonstrated by de Loos *et al.* in a study of *trans*-1,2-bis(ureido)cyclohexanes with pendant methacrylate moieties.²⁸⁷ Whilst gels in butyl acetate convert to precipitates within ten days and are readily thermoreversible, those irradiated with a 200 W high-pressure mercury lamp for two hours in the presence of a photoinitiator are remarkably stable: the materials can be heated to 135 °C or stored for several months with no significant changes in volume or turbidity. Moreover, photopolymerisation preserves the structure of the fibrous network upon removal of the solvent through freeze drying, allowing the materials to be solvated with liquids not normally amenable to gel formation.

The preservation of self-assembled structures through post-polymerisation, and the range of applications in which such processes might be exploited, have been discussed in detail by Sada *et al.*²⁸⁸ Although coupling within a gel may yield products similar to those of a solid-state reaction, the prevalence of gelator-solvent interactions serves to amplify the sensitivity of reacting aggregates to their external environment. Of particular note are organogels with cavities that are templated by strongly interacting solutes, and can thus selectively adsorb such molecules following fixture of the fibrous network by polymerisation. In a study by Zhang *et al.*, mixtures of methacrylates were gelled by the polymerisable compound *N*-octadecyl maleamic acid in the presence of an *L*-phenylalanine derivative.²⁸⁹ Crosslinking of the solvent and gelator molecules afforded robust porous frameworks which, after washing and drying to remove the template and excess solvent, were found to extract *L*-phenylalanine from a buffered aqueous solution with remarkable efficiency. Interestingly, the materials adsorbed less than half as much of the *D* isomer under the same conditions, although saturation of the pores took place after a similar length of time. Adsorption efficiencies and selectivities could be tuned by varying the ratio of components in the polymerised gel, and were significantly enhanced if crosslinks were induced by light rather than thermal treatment, owing to the formation of more ordered self-assembled structures at ambient temperatures.

Another popular application of gel-based polymerisation is to generate conductive arrays of conjugated π bonds. Shirakawa *et al.* demonstrated that copper(II) porphyrins decorated with butadiyne moieties can self-assemble in decalin to form columnar fibrils, facilitating photopolymerisation into

isolated nanowires.²⁹⁰ The reaction can be completed within hours using a high-pressure mercury lamp, and is marked by conversion from a red thixotropic gel to a highly insoluble purple precipitate. Néabo *et al.* achieved similar topochemical coupling in toluene gels comprising columnar stacks of **19**, although removal of the solvent was necessary before the reaction could take place.²⁹¹ Since the gelator is tripodal, and the alkyne moieties connected via a central aryl ring, polymerisation affords a rigid and highly extended π network, displaying an optical band gap 0.1 eV (5%) narrower than that of the linear analogue **20** (Fig. 24).

In some cases, illumination may serve to induce both the self-assembly and post-polymerisation of a reactive small molecule. Kim *et al.* describe a triphenylamine comprising amide and diacetylene functionalities that undergoes π - π stacking to form fibrillar assemblies under visible light.²⁹² Self-assembly of **21** is thought to be triggered by radical formation at the central nitrogen atom, and involves twisting of the phenyl rings to form a propeller-like arrangement around the C3 axis (Fig. 25). Surprisingly, the use of circularly polarised light can produce a bias in the twist direction, marked by an intense signal in the circular dichroism (CD) spectrum. Exposing the self-assembled aggregates to light of opposite polarisation causes a reversal in their net chirality, whereas non-polarised light, such as that from a ceiling lamp, results in total loss of CD activity. These changes may be driven to completion in just one hour, and are thus only slightly outpaced by the initial self-assembly, for which ten minutes of illumination is typically required. To eliminate this responsive behaviour, the structures can be fixed by polymerisation of the diacetylene units under UV light of the correct polarisation. It is worth noting that illumination of the non-polymerised assemblies can deliver a substantial increase

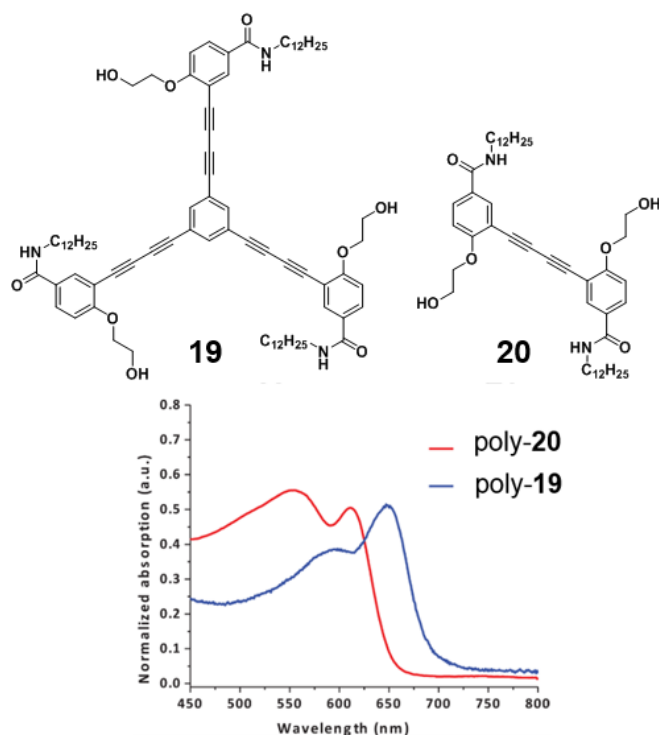


Fig. 24 Absorption spectra of tripodal gelator **19** and linear analogue **20** after photopolymerisation of the butadiyne moieties. The absorption maxima of the

two materials are separated by roughly 35 nm, corresponding to a difference in band gap of 0.1 eV. Image adapted with permission from ref. 291. Copyright 2013 American Chemical Society.

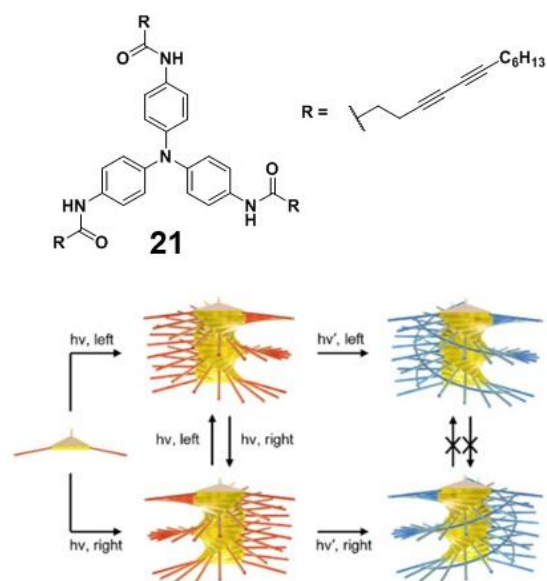


Fig. 25 Circularly polarised visible light (hv) induces **21** in 1,2-dichloroethane to self-assemble into helical structures with a chirality that matches the optical polarisation. The helix chirality may be switched by exposure to oppositely polarised light induces, but remains fixed after polymerisation with appropriately polarised UV light (hv'). Image adapted with permission from ref. 292. Copyright 2015 Nature Publishing Group.

in conductivity, and that this property is preserved when polymerisation is induced. This suggests that electron mobility in the aggregates depends primarily on the generation of stable radicals, and is only weakly influenced by the presence of covalent crosslinks between the side chains.

When designing a compound to undergo coupling in the solid state, it is common to incorporate structural motifs, such as a multipodal hydrogen-bonding core, which will induce molecules to self-assemble in an eclipsed configuration.^{45, 292, 293} However, it is important to note that even apparently minor structural changes can dramatically influence topochemical reactivity. In the diacetylene gelator **22** reported by Aoki *et al.*, the ability to polymerise was shown to depend on both diastereomeric purity and the number of carbon atoms, n , in the central chain (Fig. 26).²⁹⁴ If n is odd and a single chiral diastereomer is present, coupling in the gel state affords a more thermally stable gel with colour ranging from orange ($n = 3$) to

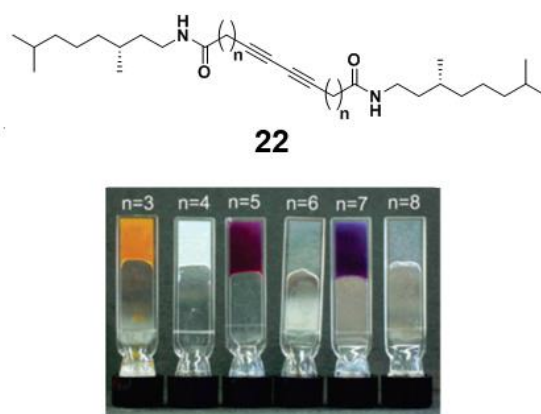


Fig. 26 Cyclohexane gels of bis(amide) gelator **22** at concentrations of 0.3% (w/w), after exposure to UV light from a high-pressure mercury lamp. The formation of coloured polymers occurs only if the number of methylene spacers between the alkyne and amide groups, n , is odd. Image adapted with permission from ref. 294. Copyright 2004 American Chemical Society.

blue-purple ($n = 7$). By contrast, gels of analogues with even n are non-photoreactive, and racemic mixtures of diastereomers do not form gels at all. Simple gas-phase modelling suggests that self-assembly of the smallest polymerisable gelator ($n = 3$) positions alkynes 0.46 nm apart and at an angle of 55° to the packing axis, approaching the values of 0.35–0.4 nm and 45° which are optimal for reactivity. Alkyne groups in the gelator with $n = 4$, meanwhile, are calculated to exhibit separations of 0.66 nm and inclinations of 72° , a configuration with limited potential for photopolymerisation.

All of the coupling reactions so far discussed are irreversible. Such a reaction may, however, lead to reversible stimuli-responsive behaviour provided the product is incorporated into a labile non-covalent assembly. Polymerisation of diacetylenes, for example, can deliver coloured aggregates that undergo reversible chromic transitions in response to heat or pH. In a study by Weiss *et al.*, a chiral amide-containing poly(diacetylene) was found to form blue left-handed quadruple helices in solution, which convert to red right-handed double helices and yellow isolated fibrils upon the addition of trifluoroacetic acid.²⁹⁵ Similarly, Dautel *et al.* reported that a polymer derived from a urea-functionalised butadiyne forms a blue gel in cyclohexane but converts to a red gel when heated to 130°C , with a purple intermediate observed at 40°C .²⁹⁶ Whilst the blue-to-purple transition is irreversible and associated with a thermodynamic relaxation of the hydrogen bonded network, the purple-to-red transition is reversible until the temperature reaches 120°C , whereupon the molecules adopt a non-hydrogen-bonded packing arrangement. Effects of this nature arise due to changes in the spacing and relative orientations of π systems and are thus strongly influenced by molecular geometry. This fact was highlighted by Ampornpun *et al.*, who found that thermochromic polymers derived from bis(amide) diacetylenes undergo reversible colour changes in solution only if the terminal alkyl chains are relatively long, and the amides linked by an even number of methylene spacers.²⁸⁵

More diverse and reliable switchable behaviour can be achieved if the coupling of gelator molecules is itself reversible. Takizawa *et al.* reported a paracyclophane-bridged imidazole dimer which is cleaved into imidazolyl radicals by UV light, causing the material to change from colourless to green.²⁹⁷ Performing the reaction in the gel state dramatically reduces its yield, since the limited transparency of a gel precludes effective illumination beyond the surface of the material. Loss of the photoproduct may, however, occur more readily in solution, where interactions between neighbouring radicals are not obstructed by large-scale packing effects. In particular, thermal bleaching of a $100\ \mu\text{M}$ cyclohexane gel proceeds with a half-life of 1.4 seconds, roughly five times longer than a benzene solution of equal concentration. The stabilising effect of gelator-gelator interactions is further marked by an increase in

cooperativity, which leads to a deviation from the first-order rate profile of the liquid-state recombination.

A more general strategy for achieving reversible coupling in gels is to make use of pericyclic reactions, especially cycloadditions. Reactions of this type can drastically alter the properties of a self-assembled material by reducing the planarity of the component molecules, and introduce new bonds which are relatively stable under ambient conditions.¹⁵³ As in diacetylene polymerisations, the yield and applicability of gel-phase cycloadditions is limited by the need for pre-organisation of the coupling partners. A compensatory benefit is that the fixed positions and orientations of reactants can lead to selectivity that would not be achievable by other means. Dawn *et al.* demonstrated such an effect in the photo-induced dimerisation of 2-anthracenecarboxylic acid, which can interact non-covalently with amine-functionalised bis(amide)s to gel a variety of solvents.²⁹⁸ Conducting the reaction in a gel can deliver the normally minor head-to-head product with high or even complete selectivity, in yields sometimes exceeding 70%. Moreover, the physical state of the product can be controlled by the choice of solvent. Although T_{gel} is usually increased by dimerization, gel-sol transitions may occur in non-polar solvents such as cyclohexane, or in chiral solvents displaying a sufficiently large enantiomeric excess.

Cycloadditions can dramatically alter the interactions between gelators and are thus often associated with gel-sol transitions. For example, dimerisation under 365 nm light was found by Kuang *et al.* to convert an acetone gel of **23** to a clear sol, but the nitrocinnamate moiety can be regenerated and the gel reformed by subsequent illumination at 254 nm (Fig. 27).²⁹⁹ Conversely, gels of amide-containing coumarin derivatives reported by Yu *et al.* remain stable when irradiated with UV light, despite undergoing a microstructural transition from helical fibres to interconnected globules.³⁰⁰ Reaction in the gel state affords the *syn* head-to-head dimer instead of the mixture of products observed in solution, but it is unclear whether this selectivity – reflecting the structure of the initial self-assembled aggregate – is preserved through multiple cycles of dimerization. Although treatment with light below 280 nm restores most of the fluorescence of the coumarin groups, the texture of the new material is markedly different, comprising sponge-like aggregates rather than the fibrous network of the original gel.

Like all photoreactions in the gel state, cycloadditions may deliver limited yields due to an internal filter effect, wherein

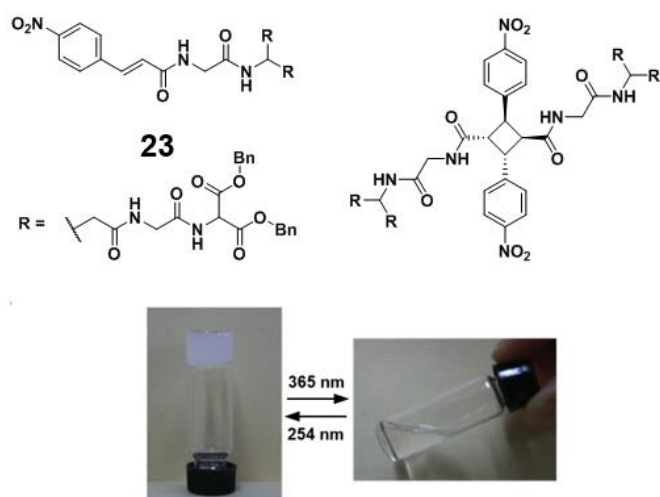


Fig. 27 Reversible gel-sol transition of nitrocinnamate **23** in acetone, resulting from dimerisation under a high-pressure UV lamp. Image adapted with permission from ref. 299. Copyright 2009 Elsevier.

products of the reaction prevent light of the required wavelength from reaching unreacted molecules. Conversions are further limited, however, by the statistical certainty that random dimerisation of neighbouring molecules will leave a fraction of the population isolated from coupling partners. Yields of less than 50% are not uncommon, and separation of the target adduct from unspent monomer can prove challenging. In addition, the presence of unreacted species may affect the physical properties of the resulting material. A remarkable study by Wang *et al.* demonstrated that non-uniformity in the product distribution can cause a fibrous gel aggregate to fragment into various intricately defined toroidal structures.³⁰¹ The reaction involves the [2+2] cycloaddition of a naphthylacryl-functionalised dialkylglutamide, and is thought to produce hollow architectures due to expansion of the material as the coupling proceeds. The monomer may be recovered through thermal dissolution of the product aggregate, and is rendered unreactive if self-assembly occurs in a solvent other than methanol or ethanol, due to slight differences in the packing of naphthylacryl moieties.

The large conformational changes involved in cycloadditions may at first seem incompatible with applications demanding a fully reversible and fatigue-resistant photoresponse. However, a suitable system may be obtained by attaching the light-responsive moieties to a structurally invariant covalent or supramolecular scaffold. This principle was successfully demonstrated by He *et al.* in a study of aqueous micelles composed of a diblock copolymer with coumarin side chains.³⁰² Aggregation of the micelles below a critical temperature affords a thermoreversible nanogel, which deswells when irradiated above 310 nm due to crosslinking of polymers in the micellar core. UV light below 260 nm induces the reverse reaction, causing the gel to swell by as much as 90% as the volume of encapsulated water increases. Conversion of coumarin groups to photodimers can be switched repeatedly from 85 to 25% over several hours, with each cycle inducing a change in micelle diameter from 39 to 48 nm. The stability of the coumarin dimer allows nanogels to be designed to release guests at a

predetermined rate, while the rapid and near-quantitative photocleavage reaction can be harnessed to control desorption *in situ*, in a non-invasive and spatially resolved fashion.

Cycloadditions, though popular, represent just one of the many reversible bond-forming processes that may be carried out in the gel state. Where it is necessary to induce a weaker, more rapid or shorter lived photoresponse, reactions involving more labile bonds and smaller changes in connectivity are often of greater utility. Such reactions may also prove achievable in species that cannot form assemblies suitable for bimolecular coupling, or be derivatised to incorporate reactive π systems, without the loss of gelation behaviour and other desirable properties.

3.3 Intramolecular proton transfer

A major obstacle to forming new covalent bonds in the gel state is the need for pre-organisation of the species to be coupled. To alleviate this problem, switching may be achieved by means of an intramolecular process, in which a suitable conformation is established through tethering of the reactive moieties. One possibility is the transfer of a proton between two basic functionalities involved in a cyclic hydrogen bonding motif. Such reactions are appealing for their reversibility, relatively weak impact on molecular conformation and, in many instances, reliable responsiveness to pH control.

A common mechanism for tautomerisation in gels is excited-state intramolecular proton transfer, or ESIPT.³⁰³ Reactions of this type arise when the most stable tautomer of a molecule in its ground state can relax to another form following excitation by light. ESIPT is frequently characterised by a large Stokes shift, since some of the energy gained by absorption is dissipated non-radiatively when proton transfer takes place. For example, although **24** emits strongly in DMF at wavelengths close to the absorption maximum at 360 nm, a second emission maximum occurs at the much higher wavelength of 541 nm (Fig. 28).³⁰⁴ The red-shifted fluorescence is attributable to the keto form of the compound, generated by proton transfer from the phenolic oxygen to the nitrogen of the benzoxazole group. Interestingly, gelation in DMF-toluene mixtures produces a hypsochromic shift and substantially enhances both the intensity and lifetime of the fluorescence, with emissions due to the keto form most strongly affected. These observations are consistent with a structure comprising π - π stacked planar molecules, in which the stages of ESIPT – excitation, proton transfer and radiative relaxation – can readily take place (Fig. 29).

In general, ESIPT in the solid state demands that tautomerisation occur without prohibitive changes in conformation. Hydrogen bonding groups, such as the amide moieties in **25a**, may promote ESIPT by stabilising close intramolecular arrangements of base and acid functionalities. Indeed, crystal structure predictions by Qian *et al.* suggest that amide-amide and π - π stacking interactions in **25a** are aligned, favouring tape-like assemblies of close-packed planar molecules

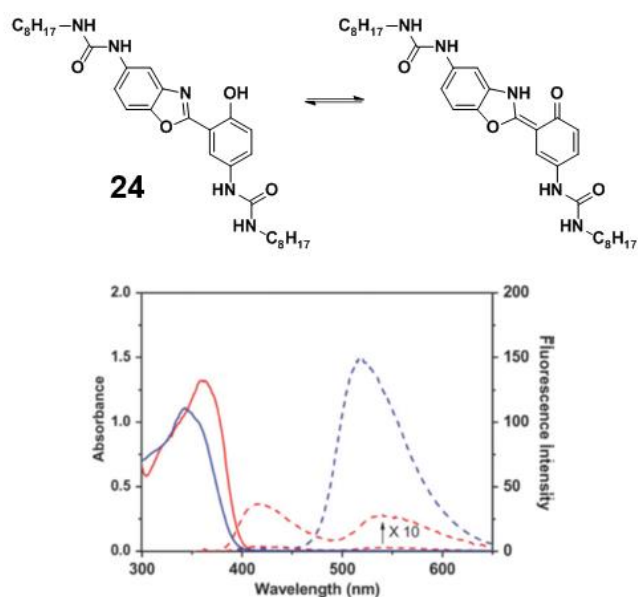


Fig. 28 Absorbance (solid lines) and fluorescence (dashed lines) spectra of **24** in DMF solution (red lines) and after aggregation in 1:58 (v/v) DMF-toluene (blue lines). Image adapted from ref. 304 with permission from The Royal Society of Chemistry.

with strong intramolecular hydrogen bonding motifs.³⁰⁵ In practice, the compound is weakly emissive in solution but forms highly fluorescent fibrous gels in mixtures of THF and cyclohexane. A large Stokes shift of 137 nm, and lack of emission bands closer to the absorption maximum, indicate the materials are strongly ESIPT-active, as expected.

When designing a gelator with ESIPT properties, it is important to note that even small changes in the substituents, including the tautomerising moieties themselves, may strongly influence the mode of self-assembly. By methylating the phenol group of gelator **26a**, Nayak sought to generate an analogue incapable of ESIPT activity.³⁰⁶ The fluorescence spectrum of the product **26b** consists of a single strong resonance between 360 and 410 nm, and is indeed simpler than that of **26a**, which displays signals from the enol and keto species at 390–450 and 500–575 nm respectively. However, whilst **26a** forms gels in dodecane and cyclohexane at concentrations as low as 0.25 wt.%, **26b** gives rise to needle-shaped crystals, suggesting that the intramolecular hydrogen bond of **26a** is crucial for the growth of an extended fibrous network. By contrast, replacing the naphthanilide moiety of **26a** with a salicylanilide end group does not greatly alter either the CGC or range of solvents gelled. The salicylanilide analogue **27a** also produces similar absorption spectra in its solutions and gels, but is notably emissive only at wavelengths ascribable to the keto tautomer, since the energy barrier for ESIPT is relatively low.³⁰⁷

Although derivatisation of a gelator can lead to drastic changes in its aggregation properties, it is not uncommon for its ESIPT responsiveness to be preserved. For instance, powder X-ray diffraction studies indicate that dodecane gels of **27a** and its dimethoxylated derivative **27b** are structurally dissimilar:

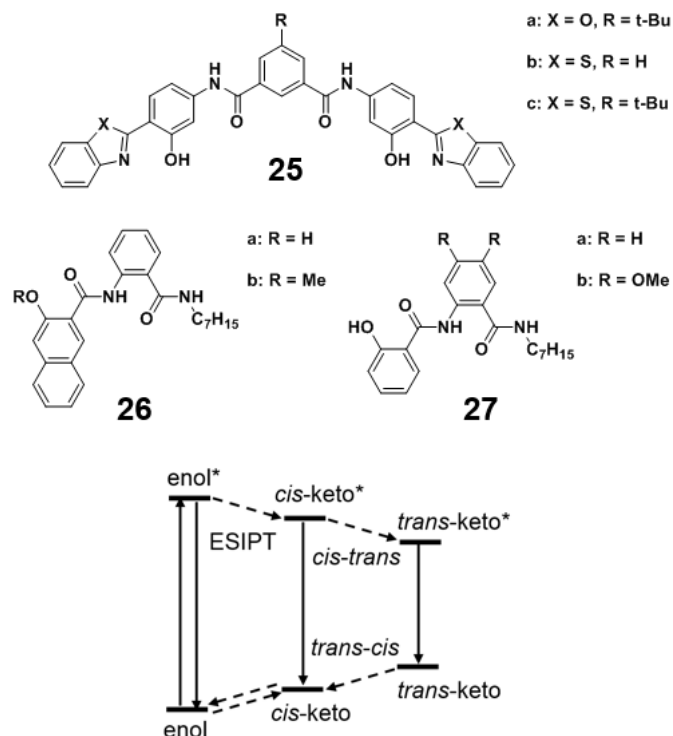


Fig. 29 Schematic energy level diagram for a general anil-like compound, of which **26a**, **27a** and **27b** are examples. Dashed and solid arrows indicate non-radiative and potentially radiative transitions respectively.

whereas the former displays the (*h* 0 0) reflections and short cell axis typical of interdigitated lamellae, the latter is best characterised as a hexagonal columnar assembly, with reciprocal *d*-spacings in the ratio 1:√3:2.³⁰⁷ Both compounds are effective gelators at concentrations of 0.2 wt.%, but while gels of **27a** are opaque due to the presence of rod-like aggregates several micrometres thick, those of **27b** are transparent and consist of entangled, flexible fibres only 100 nm in diameter. Despite these differences, the two systems give rise to similar unimodal emission spectra, signifying complete enol-keto conversion in their excited states.

The robustness of ESIPT behaviour illustrates the stability of intramolecular hydrogen bonding motifs in the presence of varying intermolecular interactions. Nonetheless, it is worth noting that the features of ESIPT are seldom wholly independent of the mode of self-assembly. The importance of supramolecular effects was strikingly demonstrated by Qian *et al.*, in a study of two benzothiazole-containing compounds with ESIPT activity.³⁰⁸ Aggregation in THF-water mixtures gives rise to AIEE effects in both **25b** and **25c**, but the quantum efficiency of proton transfer is increased only in the *t*-butylated system. It was proposed that **25b** forms an H-aggregate in which net excitation of the enol is reduced, though overall fluorescence is enhanced due to tilt in the aryl groups along the π - π stacking axis. Molecules of **25c**, meanwhile, are forced by steric constraints to adopt a head-to-tail arrangement, delivering a highly emissive J-aggregate that suppresses relaxation of the excited enol back to its ground state.

Evidently, control of ESIPT in a gel can be accomplished by adjusting either the structures of the gelator molecules or the interactions between them. Since intramolecular proton

transfer tends to alter the shape of a molecule only slightly, molecular packing within a self-assembled material is rarely affected by the ESIPT process itself. However, switching between gels with different ESIPT capabilities can occur if the gelator contains a molecular switch capable of larger conformational changes. *N*-salicylidene-anilines, or anils, are well suited to such applications, as they can typically undergo a *cis-trans* isomerisation in addition to tautomerisation.³⁰⁹ ESIPT involves the thermally interconvertible enol and *cis*-keto isomers, but irradiation of either form with UV light results in a short-lived *trans*-keto compound, in which proton transfer between the basic nitrogen and oxygen atoms can no longer take place.

One advantage of the switching responses in anils is their orthogonality: by stimulating the enol form with heat or light, it is possible to separately target the *cis*- or *trans*-keto products.³⁰⁹ Another useful feature is that the reactions proceed via excited states with energies largely determined by the environment of the molecule. Ziótek *et al.* reported that the lifetime of the *trans*-keto isomer of the anil-like compound salicylaldehyde azine can be increased from 65 to 500 μ s by the use of more viscous solvents, and may even reach 700 μ s if the compound is entrapped in a polyethylene film.³¹⁰ Viscosity is thought to inhibit thermal relaxation by providing friction to oppose the *trans-cis* isomerisation, whereas a polymer matrix is likely to restrict the space around the molecule such that more energy is needed to induce a conformational change. These effects are clearly of particular importance in gels, where – in contrast to bulk solids – interactions with solvent play a significant role.

The lifetimes of excited states may also be influenced by the intermolecular forces between anils. While dissolved anils can complete a cycle of switching within microseconds, those in the solid state may persist in high-energy states for hours or even days due to inhibition of interconversion pathways.^{311, 312} Indeed, the concentration of the *cis*-keto tautomer in a crystalline anil is generally comparable to, and sometimes even greater than, that of the enol, despite the overwhelming favourability of the latter in isolated molecules.^{313, 314} Prediction of the dominant isomer is made difficult by the mechanistic complexity of isomerisation, which may proceed via twisted intermediate states^{314, 315} or deliver a product that is long-lived despite its relative high energy.³¹⁶ In addition, competing reaction pathways may arise if the anil can interact with other functionalities in the molecule. For example, Robert *et al.* reported that a cyclic isomer of the anil-like **28** may act as a non-photoreactive reservoir for the *trans*-keto compound, allowing its concentration to rebound after light-driven conversion to the enol appears to have reached completion (Fig. 30).³¹⁷

Each step in the switching response of anils is associated with a different chromic response. Heating a solid anil typically results in yellow or orange coloration, owing to increased diffuse reflectance in the range 400–500 nm.^{311, 318, 319} This transition is usually attributable to a rise in the concentration of the *cis*-keto tautomer, but it may also occur in the absence of tautomerisation through thermally induced broadening of

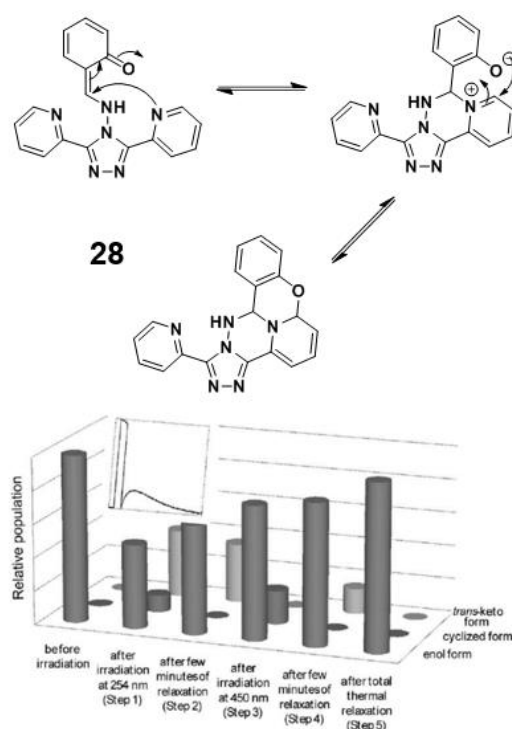


Fig. 30 Proposed mechanism for the cyclisation of anil-like compound **28** and the changes in the concentrations of the enol starting material and cyclic and *trans*-keto photoproducts following consecutive 254 and 450 nm light pulses. Inset right is a schematic plot illustrating the changes in the *trans*-keto population over time. Image adapted with permission from ref. 317. Copyright 2010 John Wiley and Sons.

absorption bands.³²⁰ In the *trans*-keto system, diffuse reflectance is augmented at higher wavelengths still, producing materials with a dark orange or red appearance. Fluorescence is possible in all states, but is generally dominated by contributions from the *cis*-keto isomer, which is by far the least susceptible to non-radiative $\pi^* \rightarrow \pi$ transitions.³¹⁸ The emissions of solid anils are often amplified due to the increased stability of the *cis*-keto structure, alongside more general AIEE effects such as J-aggregation, restricted conformational freedom and the prevention of TICT states.³²¹

A further notable characteristic of anils in the solid state, and crystals in particular, is their variable susceptibility to isomerisation. Anils prone to tautomerisation upon heating are more likely to adopt planar conformations, which localise electron density on the nitrogen atom by minimising π - π overlap with the adjacent aniline ring.³⁰⁹ Light-reactive anils, conversely, are typically non-planar and loosely packed, to accommodate the pedal-like motion of molecules undergoing *cis-trans* transformations.³²² These opposing structural trends underlie the oft-cited rule that thermo- and photochromic responses of solid anils are mutually exclusive. It has been noted, however, that the behaviour of anils in disordered materials such as gels is sometimes less strongly constrained. For example, Hadjoudis *et al.* found that an anil derived from 1-adamantylamine, which is purely thermochromic when crystalline, can undergo photochromic switching after forming a supramolecular inclusion complex with β -cyclodextrin.³²³ The cavity of the macrocycle is sufficiently large for the *cis-trans* isomerisation to occur, and also prolongs the lifetimes of the

two most stable *cis*-keto conformers, producing a bimodal resonance in the compound's emission spectrum.

A variety of anils and similar moieties, such as 2-(2'-hydroxyphenyl)benzothiazoles,³⁰⁸ 3-hydroxy-2-naphthanilides³⁰⁶ and 2-hydroxynaphthylidene acetohydrazides³²⁴ have been successfully incorporated into LMWGs. Gelation has been found to amplify fluorescence by as much as three orders of magnitude, whilst still allowing chromic transitions to take place.³²⁵⁻³²⁷ Furthermore, thermal disassembly of a gel provides an additional mechanism through which the optical properties of the system may be controlled. The interplay between aggregation and stimuli-responsiveness was demonstrated in a study by Chen *et al.*, which found that the intense yellow colour of **29** in cyclohexane gels can be turned off by either a decrease in temperature or a heat-induced gel-sol transition (Fig. 31).³²⁶ Similarly, Zang *et al.* reported that gels of **30** display greater fluorescence at 77 K than under ambient conditions, even though the yellow colour of the *cis*-keto isomer is greatly diminished by cooling (Fig. 32).³²⁸

Owing to their basicity, the responsiveness of many ESIPT-active groups may be tuned by the addition of metal ions. The use of coordination to control supramolecular interactions in anil-based gels is particularly effective, as the hydroxyl and imine substituents of the salicylidene group are well placed to form chelated complexes. In the aforementioned study by Zang *et al.*, gels of **30** were found to dissolve when treated with solutions of first-row transition metals, and could also be

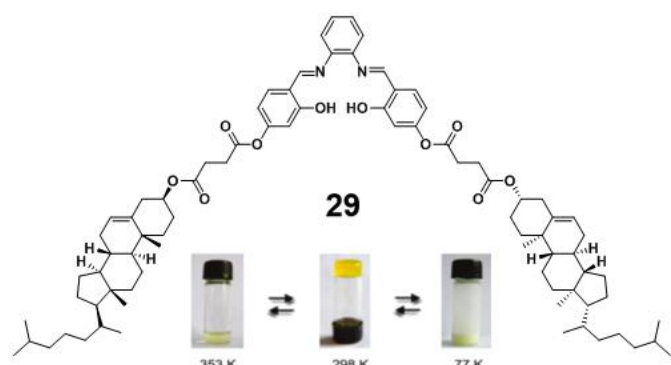


Fig. 31 The yellow colour of **29** in cyclohexane gels can be diminished by cooling, or heating to induce a gel-sol transition. Image adapted with permission from ref. 326. Copyright 2009 American Chemical Society.

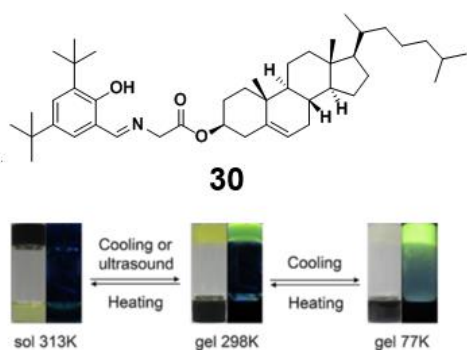


Fig. 32 Cooling an ethanol gel of **30** leads to a loss of yellow colour accompanied by a large increase in emissivity. Heated solutions of the gelator are non-emissive and less strongly coloured than the parent gel. Image adapted with permission from ref. 328. Copyright 2013 Elsevier.

disrupted by fluoride ions due to the abundance of hydrogen bonds in the self-assembled network.³²⁸ All gel-sol transitions were accompanied by an increase in absorption at higher wavelengths, and zinc(II) ions further produced an intense emission band in the region 400–650 nm. In other systems, the formation of complexes has been shown to facilitate gelation. For instance, Jin *et al.* found that copper(II) can interact with a non-gelating anil to form gels, while inducing a gelating analogue to form twisted, chiral fibres rather than the usual linear aggregates.³²⁹

It is clear that functionalities capable of intramolecular proton transfer may confer responsiveness to a range of chemical and physical stimuli. However, where switching must substantially alter the mechanical properties of a material, groups that can undergo larger structural changes are usually better suited to the task. A popular strategy is to employ intramolecular reactions that alter the connectivity and hybridisation of atoms within the backbone of the molecule, without greatly affecting their relative positions. Of the reactions that satisfy these criteria, the most versatile and widely utilised are electrocyclic processes, in which two sites in a conjugated system are linked to generate a new cyclic moiety.

3.4 Electrocyclic reactions

Electrocyclic processes are among the most commonly reported intramolecular photoreactions in small-molecule gels. As in ESIPT-active materials, pre-organisation is assured, since reactions proceed from either a closed ring or a rigid, extended π system.³³⁰ However, due to the changes in planarity associated with the loss or gain of sp^2 centres, the macroscopic effects of ring closing and opening are often more pronounced than those of tautomerisations. For example, Ahmed *et al.* showed that an LMWG containing a dihydroindolizine group can form a gel in polar solvents but undergoes a reversible ring opening under UV irradiation, yielding the betaine isomer in the form of a red-coloured sol.³³¹

Other molecular motifs that display light-induced electrocyclic reactions include spiroopyrans, spirooxazines, naphthopyrans and benzopyrans, otherwise known as chromenes. All of these compounds undergo ring opening within a six-membered heterocycle to generate a new double bond and a ketone, enol or phenol moiety.³³⁰ The products contain fewer sp^3 sites than the reactants so tend to adopt a more planar conformation, allowing for increased conjugation and the emergence of new optical absorption bands in the range 570–750 nm. A sol-gel transition may occur due to the possibility of increased π - π stacking,^{332, 333} and other effects requiring close interactions between conjugated systems, such as Förster transfer³³⁴ or the formation of donor-acceptor complexes,³³² may also be observed. The sensitivity of supramolecular assemblies to such changes in packing was illustrated by Qiu *et al.* in a study of a spiroopyran linked to a di-D-alanine moiety.³³² While the closed-form spiroopyran **31** is non-gelating, UV irradiation of this compound in aqueous solution generates a merocyanine species, which can form dark red fibrous gels at low pH (Fig. 33). In addition to visible light,

which induces regeneration of the closed-ring system, the gels may be disrupted by one equivalent of vancomycin, a large chiral molecule capable of strong hydrogen bonding interactions. Intriguingly, however, this ligand-guest response does not occur if the gelator is based on the L enantiomer of alanine rather than the D. It is evident that binding of the guest demands a particular combination of hydrogen bonds and π - π stacking interactions, which can compete with those in the gel assembly only if the merocyanine gelator exhibits a complementary structure.

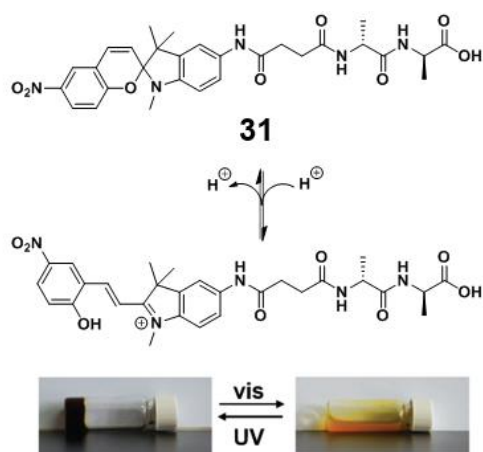


Fig. 33 Acidic aqueous sols of **31** undergo sol-gel transition on exposure to UV light, and assume a dark red colour due to increased absorbance between 450 and 550 nm. Irradiating the gel with visible light (> 400 nm) reverses the transition. Image adapted from ref. 332 with permission from The Royal Society of Chemistry.

A notable feature of the gels reported by Qiu *et al.* is that they form only from acidic solutions. This pH sensitivity is common among gelators formed by electrocyclic reactions, since the products of ring opening are often sufficiently basic to be significantly protonated at moderately low pH. Consequently, incorporating such species into supramolecular systems may enable multiaddressable behaviour that would be difficult to achieve by other means. Ethanol solutions of a spironaphthoxazine gelator were found by Li *et al.* to change from colourless to blue on exposure to UV light, but underwent gelation only in the presence of paratoluenesulfonic acid.³³⁵ Maity *et al.*, meanwhile, obtained photoreactive gels by utilising the electrocyclic reaction itself as a proton source, catalysing the reversible formation of a tris(hydrazone) hydrogelator via the ring closure of a non-gelating spiropyran.³³⁶ Although gels are formed even in the absence of the photoacid, its use results in stiffer materials comprising more branched and interconnected fibres, and allows for spatial control of the gelation process by localised illumination of the precursor sol.

A drawback of many electrocyclic reactions is that their products are short-lived under ambient conditions. Although the lifetime of a photoresponse in the gel state may exceed that in solution by as much as two orders of magnitude, significant loss of product typically occurs within minutes, making such systems unsuitable for information storage over extended periods of time.^{337, 338} An electrocyclic switch exhibiting more stable photo-induced transitions is the dithienylethene (DTE) moiety. DTE groups convert to a closed-ring structure upon exposure to UV light, and can persist in this form for months and

even years at room temperature.³³⁹ Ring closure is usually reversible by visible light, but one or both parts of this reaction cycle may be inhibited depending on the nature of the groups around the DTE core.³⁴⁰ In a comparison of DTEs based on cyclopentenes and maleimides, Herder *et al.* found the latter to be highly resistant to photo-induced ring closure, and were able to attribute this effect to stable TICT states and small LUMO coefficients on the atoms to be coupled.²⁸² By contrast, dithiocyclopentenes and fluorinated derivatives deliver reliable and reversible photochemical reactions, and are thus a popular target for investigations of molecular switches in the gel state.

Ring closure of a DTE reduces the flexibility of the molecule, so may favour gelation by lowering the entropic cost of aggregation. However, the reaction also generates two sp^3 sites and forces the substituents at these sites to be oriented out of the plane of the molecule. The effects of such changes were demonstrated by Yagai *et al.* in a study of the DTE gelator **32**.³⁴¹ In its closed form, the compound gives rise to non-fluorescent solutions in methylcyclohexane, but ring opening under 600 nm light produces a highly fluorescent gel within one minute. Molecular modelling suggests that the photoproduct can self-assemble into ordered π - π stacked aggregates, with efficient migration of excitation energy leading to strong emissivity (Fig. 34). The closed species, however, forms only disordered structures, as the steric hindrance of methyl groups prevents close π - π interactions between DTE moieties. Indeed, aggregation of the open form is so favourable that ring opening in the gel-sol system is only partially reversible, unless the

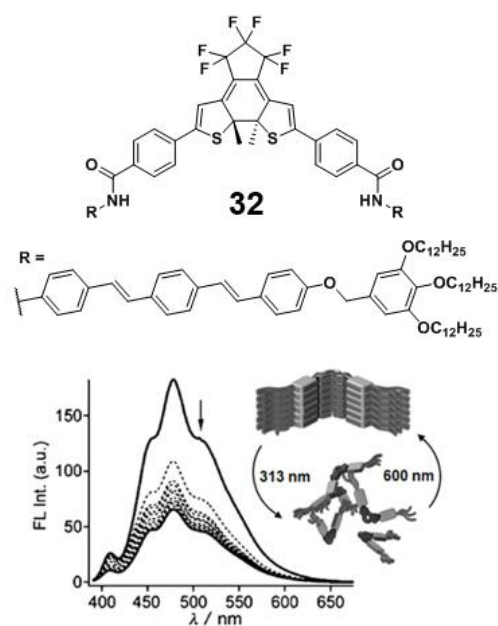


Fig. 34 Closed form of DTE-OPV conjugate **32**, schematic representations of the molecular packing in the open (top) and closed (bottom) forms, and changes in fluorescence upon ring closing in methylcyclohexane. Due to the strong π - π interactions within aggregates of the open isomer, conversion to the closed form is limited to 6%, but even this yield is sufficient to reduce the intensity of emissions by 36%. Image adapted with permission from ref. 341. Copyright 2013 John Wiley and Sons.

reaction is conducted within a thin film to prevent molecules from accessing their optimum packing arrangement.

Changes in aggregation induced by closure of a DTE system were also identified by Hotta *et al.*³⁴² The open isomer of a DTE-

containing bis(urea) was found to be soluble in chloroform but form fibrous H-aggregates upon gradual dilution with hexane. The suspended assemblies undergo over 90% conversion to the closed form when treated with UV light, producing a purple solution of needle-like nanofibres with a 60% enlargement in mean hydrodynamic radius. Irradiation of the chloroform solution, however, delivers a slightly lower yield of the isomerised species, and subsequent self-assembly gives rise to nanoparticles instead of fibrous aggregates. It is proposed that the close-packed molecular arrangement in assemblies of the open isomer forces ring closure to proceed in a cooperative fashion, such that each resulting nanofibre comprises only one enantiomer of the closed molecule. In solution, meanwhile, the (*R,R*) and (*S,S*) enantiomers are formed in equal quantities and remain mixed on aggregation, forming disordered assemblies with no preferred axis of growth. As in most DTE systems, the aggregates are stable under ambient conditions, but may be interconverted through cycles of UV and visible light with no significant degradation of their responsive behaviour.

The stability of the DTE group in both its open and closed forms means that it is well suited to applications involving the release of an entrapped species. One strategy is to incorporate a DTE into a ditopic ligand for the construction of porous metallocages with gel-forming capability. Wei *et al.* found that four molecules of a pyridyl-functionalised DTE may coordinate a pair of palladium(II) ions to form a cage enclosing a central cavity.³⁴³ Heating and cooling of the complex in DMSO and DMSO-acetonitrile mixtures affords brown gels that are both thermoreversible and thixotropic, but this self-assembly process is possible only if the ligand adopts its more flexible, open form. Thus, inducing closure of the DTE through UV irradiation causes the gels to disassemble into blue solutions, which persist until the reverse reaction is triggered by exposure to visible light. Although guest encapsulation was not attempted, cavities of this nature have been shown elsewhere to bind and release molecules in response to photonic stimulation. Work by Foster *et al.* further demonstrated that hydrogels comprising a metal-organic cage can selectively bind benzene in the presence of the similarly sized anisole, and release this guest upon the addition of furan, a competitive binding agent.³⁴⁴ It is noted that since non-encapsulated guests may leave the extrinsic pores of a gel by ambient diffusion, gels with intrinsic porosity enable the controlled delivery of multiple reagents at differing rates, with potential applications in catalysis, drug delivery and chemical purification.⁵⁶

In spite of their stability, DTEs frequently boast a high rate of isomerisation when illuminated, even in the solid state. Rapid switching of a DTE was strikingly demonstrated by de Jong *et al.*, in work aimed at achieving sol-gel switching in a spatially controlled manner.³⁴⁵ Photolithography utilising gel-gel and gel-sol transitions is frequently reported,^{257, 271, 280, 346-349} but similarly localised formation of a gel from a solution is difficult, since aggregation must outpace the transport of material away from the irradiated area. Nonetheless, UV irradiation of **33** in toluene produces bands of material that closely reproduce the shape of the photomask, with spacings as small as 5 μm capable of being resolved (Fig. 35). Optical density measurements

indicate that the gelator concentration in the aggregated regions can exceed that of the non-irradiated solution by a factor of 20, owing to entrapment of the compound following the ring-closing reaction. It can be seen that photo-induced aggregation serves to sequester the gelator within the irradiated regions, allowing concentration gradients to be established that mirror the variation in light intensity.

Additional studies by de Jong *et al.* highlight another advantage of DTEs: the generation of two chiral centres upon ring closure can, in molecules that are already chiral, result in diastereomeric products with differing optical and aggregation

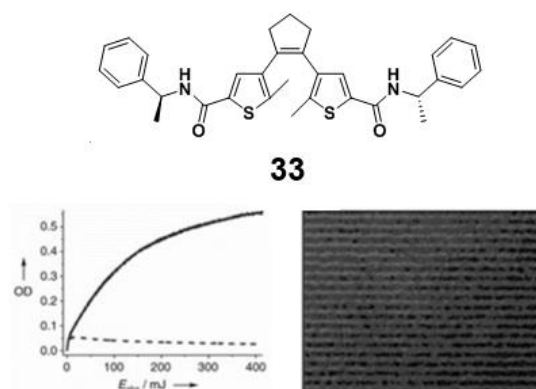


Fig. 35 Optical density of a toluene gel of **33** during ring closure with uniform (dashed line) and localised (solid line) UV illumination, as a function of total adsorbed energy E_{ads} . Bands of gel reproducing the shape of a photomask grating are shown. Images adapted with permission from ref. 345. Copyright 2005 John Wiley and Sons.

properties. Although the *M* and *P* atropisomers of **33** can interconvert in solution, selective self-assembly in toluene produces a gel of the pure *P* form following a heating-cooling cycle.³⁵⁰ UV irradiation of this gel yields the closed-ring (*S,S*) structure with 96% diastereomeric excess and 40% conversion, but the resulting gel is metastable: if the material is dissolved by heating and then cooled, a more stable gel of the closed (*R,R*) form arises. Finally, irradiating this material with visible light produces a metastable gel of the open *M* atropisomer, which is impossible to obtain directly from the original toluene sol. This method cannot be used to isolate the atropisomers and ring-closure products of a non-chiral DTE, but such resolution may be achieved via selective co-assembly of the isomers with a chiral DTE. For example, **33** was found to preferentially co-assemble with one atropisomer of a related achiral gelator, allowing the corresponding closed-ring structure to be obtained with up to 94% enantiomeric excess.³⁵¹

A notable property of the systems investigated by de Jong *et al.* is that each permutation of thermal and photonic inputs exerts a unique influence on the chirality, physical state and molecular configuration of the DTE switch. Given that the responses are well-defined, long-lasting and resistant to fatigue over several cycles, such materials could be of use in chemical information storage applications. Indeed, it is common for DTEs to satisfy an additional requirement of effective data storage: that the stimulus required for data readout have no effect on the system state.³⁵² In one study, Xiao *et al.* reported that fluorescence of a pyridyl DTE gelator can be excited by light at 470 nm, whereas isomerisation of the closed- and open-ring

structures demands irradiation near 365 and 620 nm respectively.³⁴⁷ The open form of the gelator emits only weakly above 500 nm, but ring closure results in a strong emission signal around 623 nm. Thus, the composition of the system may be determined rapidly, reliably and non-invasively, without risk of conversion to an alternative state.^{339, 353}

A related use for the DTE group is as a component of a molecular logic gate, or MLG. Like their electronic counterparts, MLGs deliver an output signal in the presence of a particular combination of inputs, in accordance with a predefined set of Boolean operations.³⁵⁴ A tetrakis(amide) gelator developed by Xue *et al.*, for instance, acts as an XNOR gate in DMSO-water mixtures, losing its fluorescence at 650 nm if fluoride ions are present without acid, or vice versa.³⁵⁵ Gel-sol transitions and absorbance at 450 nm, meanwhile, behave in the manner of an INHIBIT gate, in that they occur only in response to acid in the absence of fluoride. The ability of MLGs to deliver multiple outputs means that they may perform series of logical operations that would normally require a combination of logic gates, potentially allowing chemical systems to be modulated *in situ* without the use of invasive devices. Control of this nature was demonstrated by Komatsu *et al.*, in a study of a bis(amide) hydrogelator with a switchable alkene group.¹⁵⁸ Concentrated solutions of the compound in its *cis* form are converted to gels of the *trans* form by visible light, but at lower concentrations acid or calcium ions must also be present for gelation to occur. By varying the makeup of the gel and the input stimuli, sol-gel and gel-sol transitions may be induced in accordance with four different Boolean operations, allowing entrapped compounds to be released under specific environmental conditions.

Chemically addressable MLGs could be useful in applications requiring a single switching event, such as sensing and drug delivery. However, cycles of writing and erasing in data-storage systems necessitate repeatable responses, which may only be achieved through the use of MLGs with exclusively non-invasive inputs. An elegant solution is to incorporate two or more different remotely switchable groups into the same species. This approach is exemplified by compound **34**, reported by Andréasson *et al.*, which contains cyclisable DTE and fulgimide moieties and displays a remarkable array of logic-gating behaviour (Fig. 36).³⁵⁶ The two molecular switches in the molecule can be induced to undergo ring opening and closing in an orthogonal fashion, with each combination of isomers producing a characteristic pattern of absorption and fluorescence signals. In consequence, **34** can, as a single molecule, perform most of the basic Boolean operations, and may even function as a keypad lock, due to the dependency of certain outputs on the order in which photonic inputs are applied.

The majority of gels so far discussed are prepared by heating or cooling a gelator solution. Although such thermal methods are often effective, certain classes of gelator either cannot be dissolved by heating or form non-fibrous aggregates if the temperature is varied. Furthermore, even when gelation is successful, the resulting materials may exhibit suboptimal physical properties, such as strongly quenched fluorescence or a low yield stress. Photo-induced aggregation can offer access

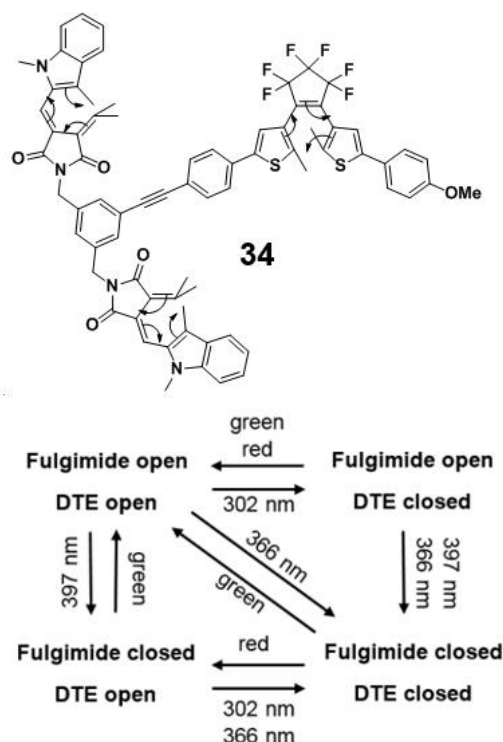


Fig. 36 Different wavelengths of UV light can induce ring closure of the DTE and fulgimide moieties in **34** either separately or in combination (curly arrow mechanisms shown). The reverse reactions are triggered by red and/or green light. Since the state of one switchable group affects the inputs needed to trigger switching of the other, the system can display a wide range of logic-gating behaviour.

to novel supramolecular systems with superior characteristics, but is not the only non-thermal route by which the self-assembly landscape may be explored. For example, Liu *et al.* succeeded in cyclically assembling and disassembling a gel of Fmoc-protected phenylalanine in a microfluidic channel, by applying voltages to alternately oxidise and reduce hydroquinone and thus generate an oscillating pH gradient.³⁵⁷ Gelation has also been achieved through frontal radical polymerisation driven by the local heating of iron oxide nanoparticles in a strong magnetic field,³⁵⁸ and the inclusion of ferromagnetic particles can enable the remote disruption of gels by similar means.³⁵⁹

A more common approach is to induce gelation by employing a physical trigger such as stirring, shaking, or ultrasound. Like heat and light, these mechanical stimuli can additionally be used to bring about gel-sol transitions, modify the texture of a material already formed, or drive switching responses at the molecular level. Indeed, the behaviour of a gel under stress may prove crucial to its functionality, delivering a method of control orthogonal to other inputs, and offering valuable structural insights over a range of lengthscales.

4. Gels that respond to sound

4.1 Mechanically induced gelation

Where self-assembly is kinetically disfavoured, a mechanical stimulus may be employed to overcome the activation barrier or offer access to more viable aggregation pathways. The product material may differ significantly from that of a thermal

or light-induced process, as neither the temperature of the system nor the structure of the gelator need be altered during self-assembly. Indeed, agitation may be the only method by which a gel can be obtained. Piepenbrock *et al.* found that bis(urea) **35** forms strong gels in the presence of copper(II) bromide if the solution is shaken, but otherwise affords only viscous solutions (Fig. 37).³⁶⁰ Cryo-SEM studies indicate that aggregates in the original sol consist mainly of straight, unbranched fibres. Upon shaking, however, the density of interconnections is increased, as shearing the coordination polymer fibres results in their rapid recombination into more

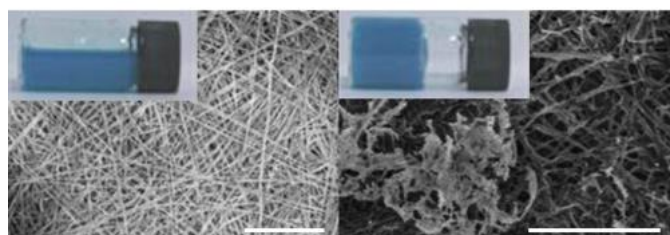
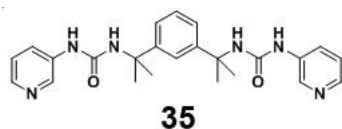


Fig. 37 Cryo-SEM images of **35** and 0.3 equivalents of copper(II) bromide in methanol, before (left) and after (right) shaking. Scale bars represent 1 and 2 μm respectively. Inset are images of the bulk materials, illustrating the shear-induced sol-gel transition. Images adapted from ref. 360 with permission from The Royal Society of Chemistry.

highly entangled configurations.⁵⁸

The use of a mechanical stimulus to induce a kinetically disfavoured self-assembly process does not preclude thermoresponsive behaviour in the resulting material. This principle was illustrated in a study by van Herpt *et al.*, profiling the gelation behaviour of a carbazole-based bis(urea).¹¹² Although gels in DMSO cannot be obtained by thermal cycling, they may be formed in less than a minute when solutions of the gelator are vigorously shaken. The gels are destroyed by heating but, intriguingly, reform upon cooling if the temperature remains below 75 °C. The presence of secondary aggregates in the heated sol is reflected in the NMR signals of the gelator, which are diminished by slow relaxation in the gel state and only fully recover above 80 °C. It is suspected that the dissolved structures are the initial products of self-assembly and serve as intermediates for the reversible formation of larger gel fibres. Agitation may initiate this process by fragmenting nascent fibres to create additional sites for secondary nucleation. Alternatively, the mechanical input may act as a driving force for convection, which has been shown in similar shear regimes to lead to self-accelerating particle coagulation.³⁶¹

Ultrasonication, or exposure to sound waves with frequencies of 1 MHz or higher, is another stimulus often employed in the preparation of supramolecular materials. Within a typical laboratory sonication bath,³⁶² propagation of ultrasound through a sample solution generates transient bubbles of vapour which undergo abrupt implosion, or cavitation, under the pressure of the surrounding liquid.^{363, 364} Kinetic³⁶⁵ and sonoluminescence³⁶⁶ studies suggest that the

short timescale of cavitation may lead to local temperatures of up to 5000 K and pressures of several hundred atmospheres. Energy from cavitation is released in the form of shockwaves and jets which may fragment nearby particles, or cause them to melt and fuse through high-speed collisions.³⁶⁷ Perhaps surprisingly, self-assembly can take place in such an environment,³⁶⁸⁻³⁷⁰ and may even proceed at a lower concentration, higher temperature or faster rate than would be possible under milder conditions.^{129, 371, 372} Moreover, the resulting aggregates may prove unusual, with structures or physical properties that would be difficult to achieve by other methods.

Many routine uses of ultrasound exploit its capacity to break up and dissolve materials that are resistant to thermal treatment. It is interesting to note that such solubilisation can, under certain circumstances, prove instrumental to gelation. In one study, Anderson *et al.* exploited sonication to partially dissolve the highly insoluble compounds uric acid and melamine in water, allowing the materials to re-aggregate as a stable co-gel.³⁷³ Similarly, Baddeley *et al.* attributed the sonication-induced gelation of one pyridine-cored bis(urea) in alcohols to the dissolution of “imperfect” assemblies, which may thereafter reassemble into a fibrous product.³⁷⁴ The application of ultrasound provides a driving force for equilibration, so that aggregates can evolve into the thermodynamic product in spite of kinetic competition from alternative pathways.

Sonication may further promote gelation through its effects on nucleation.^{129, 375, 376} Under ambient conditions, aggregation typically involves the development of a relatively small number of nuclei into dense, highly branched spherulites through gradual sequestration of the dissolved gelator. Exposure to ultrasound, however, fragments and disperses the initial aggregates to create a much larger population of nuclei, resulting in vastly accelerated fibre growth. Because separate assemblies propagate independently, they experience a less supersaturated environment on average and mature into smaller, less branched and more interpenetrated spherulites that are better suited to gel formation (Fig. 38). Wang *et al.* exploited this phenomenon in gels of **36** to reduce the CGC from 2.0 to 0.5% (w/v) and increase gel strength by up to three orders of magnitude relative to thermally generated materials.³⁷⁶ The degree of branching, average fibre diameter and thermodynamic stability of the sonogels could be tuned via the temperature or concentration, or by varying the duration or power of the mechanical stimulus.^{112, 145, 371}

The microstructures of sonogels are often markedly different from those of aggregates generated by other mechanical processes. As a result of the more extreme conditions experienced by the material, a gel produced by sonication typically exhibits particles with clearer signs of fragmentation. For example, Bardelang *et al.* found that sonicated crystals of a TEMPO-based compound are smaller and more effectively gelating than those subjected to shaking or stirring.³⁷⁷ Likewise, metallogels reported by Weng *et al.* are strengthened by vigorous shaking or sonication, due to the progressive breakup and fusion of globular particles upon exposure to shear forces.³⁷⁸ By contrast, Teunissen *et al.*

describe gels of a urethane-functionalized ditopic ureidopyrimidinone, which become stronger only after stirring the system for several hours.³⁷⁹ Infrared and NOESY NMR experiments suggest that lateral stacking of the initial linear assemblies is obstructed by urethane-ureidopyrimidinone interactions, but prolonged agitation causes these kinetically trapped structures to dissociate, allowing for the formation of larger aggregates linked by a continuous network of urethane-

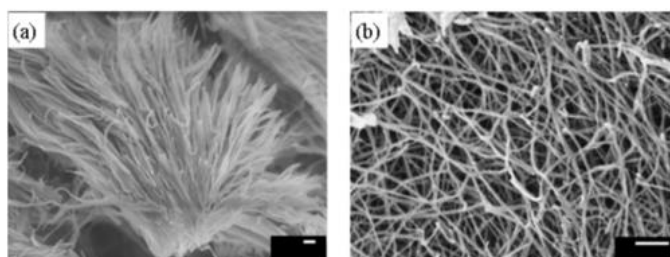
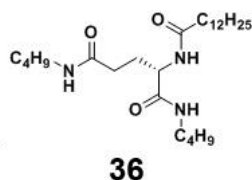


Fig. 38 SEM micrographs (scale bars 500 nm) of propylene glycol gels of **36** after a heating-cooling cycle (a) and with additional ultrasound treatment (b). An increase in gel strength after sonication is associated with a conversion from highly branched spherulites to thicker and less interconnected fibres. Image reproduced with permission from ref. 376. Copyright 2009 American Chemical Society.

urethane motifs.

Unlike more gentle mechanical stimuli, sonication may induce changes in the local environment of a molecule sufficient to dramatically alter its structure. One possible outcome is a conformational change, which might influence the ability of the molecule to engage in supramolecular interactions. In one of the earliest reports of sonogelation by an LMWG, Naota and Koori showed that the chiral palladium(II) complex **37** converts from a clothes-peg-like conformation to a more open structure, permitting the self-assembly of continuous, π - π stacked chains (Fig. 39).³⁸⁰ Gelator **38**, similarly, was found by Liu *et al.* to twist under sonication, forcing the central naphthalimide ring into the plane of the platinum(II)-terpyridyl head group (Fig. 40).³⁸¹ While the original molecules form vesicles bounded by hydrophilic head groups, aggregates of the new conformer consist of extended bilayers, with outwardly oriented cholesteryl groups creating a hydrophobic interface. Such particle-to-fibre transitions have been demonstrated in a wide range of supramolecular materials, and are of particular interest in peptide-based systems, where unfolding can give rise to the cross- β sheet assemblies implicated in amyloid aggregation.^{382, 383}

In addition to driving conformational changes, ultrasound may facilitate the breaking and rearrangement of labile bonds. Interactions involving metals are often relatively weak and thus particularly susceptible to scission. Paulusse *et al.* have studied the effects of sonication on a number of coordination polymer systems, and describe the generation of reactive fragments which can exchange ligands, cyclise or recombine to create

mixtures of new species.^{384, 385} A report by Zhang *et al.* similarly linked the sheet-to-fibre transformation of a coordination polymer to a rearrangement of the constituent zinc(II) complexes, from tetrahedral to see-saw configurations.³⁸⁶ Paradoxically, sonication may also result in the strengthening of interactions. Work by Komiya *et al.* exemplifies this phenomenon: the platinum-based analogue of complex **37** forms weakly associated and non-emissive vesicular assemblies in solution, but exposure to ultrasound results in

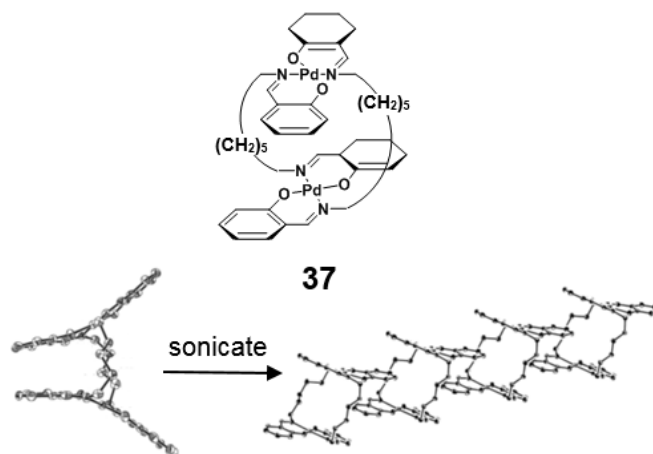


Fig. 39 Sonication of **37** in a range of organic solvents induces conversion from a clothes-peg conformation to a more open structure, which can undergo π - π stacking to form extended assemblies. The packing arrangement shown is part of the X-ray crystal structure of an analogous complex, in which imine nitrogen atoms are linked by chains of six methylene groups. Image adapted with permission from ref. 380. Copyright 2005 American Chemical Society.

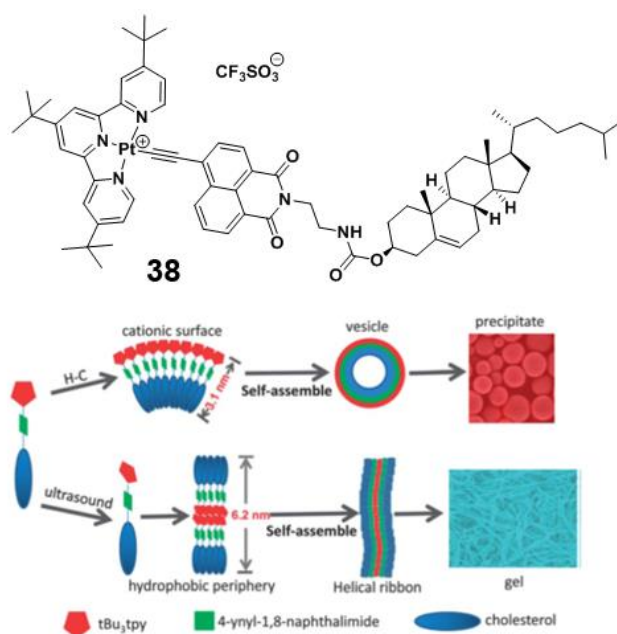


Fig. 40 Schematic representation of the self-assembly mechanism of platinum(II) complex **38**. Heating and cooling (H-C in diagram) produces a vesicular precipitate, but a conformational change induced by sonication allows for closer interactions between cationic head-groups to give ribbon-like fibres. Image reproduced from ref. 381 with permission from The Royal Society of Chemistry.

phosphorescent fibrous gels, due to conversion of the parent aggregates into structures with strong π - π and metal-metal interactions.²²²

Other changes in aggregate morphology are often attributable to the disruption of hydrogen bonds. An increase in the propensity for non-covalent bonding may facilitate a transition from discrete self-assembled systems to more continuous architectures. For example, Wang *et al.* found that sonication-induced gelation of cyclohexane by (*R*)-*N*-Fmoc-octylglycine occurs alongside an increase in fibre branching and shifts in the FT-IR spectrum of the system, which could reflect a switch from $R_1^1(7)$ and $C(5)$ interactions to $C(4)$ motifs.³⁸⁷ Similarly, Deng *et al.* reported that tripodal tris(urea)s form dimeric aggregates in acetonitrile solutions, but reassemble under ultrasound to give gels comprising α -tape motifs.³⁸⁸ Sonication may also influence binding to solvent molecules, leading to changes in gelator solubility or the solvation capacity of an aggregate.^{145, 360} In a study by Park and Kim, concerning the gelation of a 2'-deoxyadenosine derivative in water, an effect of this nature was cited to explain the conversion of needle-like precipitates to interconnected fibres upon sonication.³⁸⁹ It is proposed that hydroxyl radicals solubilise the gelator by converting it to a more hydrophilic oxidised species, but subsequent reduction causes the solution to become supersaturated, leading to the rapid formation of an amorphous gel.

Although the molecular effects of ultrasound may serve to initiate self-assembly, the morphologies of the final aggregates more typically reflect the large-scale physical impacts of cavitation events. Constructive processes, such as the fusion of discrete particles into sheets and fibres, are sometimes observed (Fig. 41),³⁷¹ but these are frequently accompanied by signs of exposure to extreme conditions, such as a decrease in

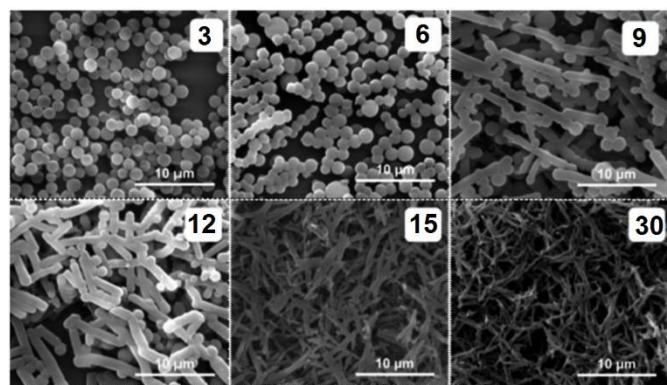


Fig. 41 SEM images (after drying) of a cholesteryl calix[4]arene in isopropanol, illustrating the changes in morphology during sonication to form a fibrous gel. Numbers (inset) indicate the number of minutes for which samples were agitated. Fusion of vesicles appears to reach completion after 15 minutes. Image adapted from ref. 371 with permission from The Royal Society of Chemistry.

particle size^{145, 390, 391} or loss of crystallinity. More generally, the application of stress to a gel often induces a transition between solid- and liquid-like properties, culminating in fracture, plastic deformation and near-total liquefaction. This strain behaviour may be associated with other, non-mechanical responses such as AIE effects, and can be tuned, like many gel properties, through careful optimisation of the gelator structure and its aggregation environment.

4.2 Gels under stress

In many applications, the usefulness of a gel is dictated by its behaviour on exposure to a mechanical stimulus. Changes in bulk properties are commonly probed by means of an oscillatory shear experiment, in which a sample is sandwiched between two plates and subjected to a periodic rotational stress.³⁹² The shear modulus G , defined as the ratio of shear strain to shear stress, can be resolved into an in-phase component G' and out-of-phase component G'' , corresponding to elastic and dissipative deformations respectively. In a typical gel, the storage modulus G' exceeds the loss modulus G'' by an order of magnitude and remains roughly constant up to the yield stress, δ , at which the material begins to flow. The behaviour in the vicinity of δ may be indicative of the mechanism by which gel disruption arises. Hyun *et al.* suggest that an increase in G' could be due to the formation of close-packed aggregates, while an increase in G'' signifies the breakup of such structures as they align with the direction of shear.³⁹³ The latter effect, termed weak strain overshoot, is common among gels containing crystals and other discrete particles, and frequently implicated in complex mechanoresponsive behaviours.³⁹⁴ For example, Piepenbrock *et al.* observed that weak strain overshoots in silver(I) metallo gels of a pyridyl-functionalised bis(urea) correlate with larger G' values, lower yield stresses and higher densities of silver nanoparticles, and may be enhanced by UV irradiation or increased silver loadings.³⁹⁵ Yu *et al.*, meanwhile, noted that a rise in G'' during the shear-induced collapse of a toluene gel of **39** coincides with the fragmentation of nano-ring structures, which can reassemble on resting to restore the original gel network (Fig. 42).³⁹⁶

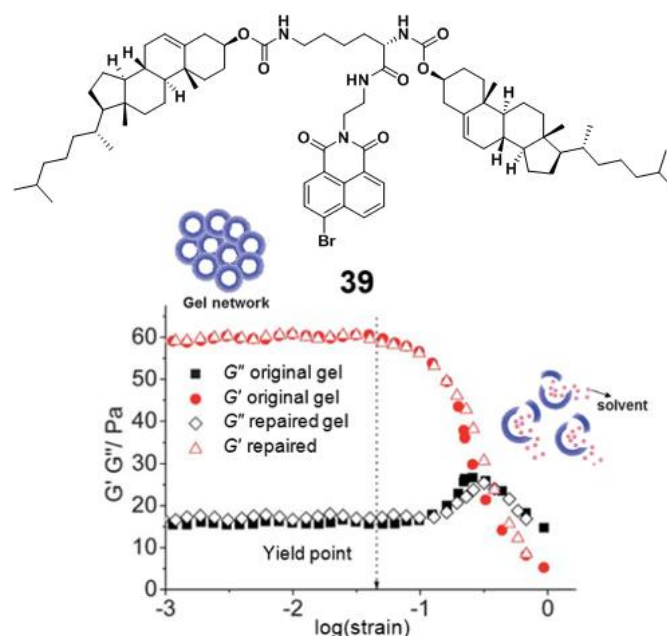


Fig. 42 Strain-sweep plots for a 0.86 wt.% gel of **39** in toluene at 25 °C, before and after self-repair. Resting of the gel after disruption leads to complete restoration of its original rheological properties. As represented schematically, the increase in G' near the yield point of the gel coincides with fragmentation of nano-ring structures under the imposed stress. Image adapted from ref. 396 with permission from The Royal Society of Chemistry.

The dependency of rheological parameters on the gelator concentration, c , may also be instructive. Between the CGC, c_0 ,

and the point of saturation, pre-shear G' and δ usually change in accordance with the power law expression $(c - c_0)^n$, or c^n if $c \gg c_0$. Shih *et al.* propose that the exponent n in colloidal gels will depend on whether the interactions between aggregate flocs are weaker than, or comparable to, those of the floc interior.³⁹⁷ In the former case, termed the weak-link regime, n is dictated solely by the fractal dimension of the floc network and is typically greater than unity. In the strong-link regime, meanwhile, an additional dependency on the fractal dimension of the internal floc structure causes δ and c to become negatively correlated, whilst G' scales with powers of c higher than those of the weak-link regime. Sangeetha *et al.* applied this theory to gels of a cationic bile acid derivative in aqueous sodium chloride, and found that the system undergoes a transition from weak-link to strong-link behaviour as the gelator concentration rises.³⁹⁸ The value of δ reaches a maximum at the transition point, as expected, but the rate of change in G' undergoes a surprising increase, due to a substantial reduction in the fractal dimension. Such marked rheological variation can result from dramatic changes in the size or connectivity of a gel's constituent particles. For example, Xu *et al.* observed that gels of a nitrobenzoxadiazole-containing cholesteryl derivative in THF-methanol and pyridine-methanol mixtures become stronger with increasing concentration of the gelator or methanol antisolvent, due to a transition from narrow fibrous aggregates to dense spheroidal particles several micrometres in diameter.³⁹⁹

Not all gels are well described by the model of colloidal aggregation. Whereas G' in floc-based networks commonly conforms to a power law with $n > 3$, particularly in the strong-link regime, many small-molecule gels exhibit G' vs. c plots that are almost exactly quadratic.¹⁰ Values of δ also increase with c but at somewhat lower rates, with exponents n in the vicinity of 1.5. Such behaviour is characteristic of a cellular network made up of stiff rods with fixed points of interconnection, wherein G' scales linearly with the Young's modulus, E_s , of the load-bearing struts.⁴⁰⁰ By fitting this model to the rheological profiles of chiral bis(urea) organogels, and assuming the gel fibres to be equal in density to the corresponding single crystals, Lloyd *et al.* were able to estimate values for E_s in the range 1–2 GPa.⁴⁰¹ Helical nanofibres of a tripodal tris(urea) were found by Stanley *et al.* to exhibit similar mechanical properties, but in this system the mechanism of gel collapse in the region of δ was also considered.⁴⁰² Noting that the observed values of δ are an order of magnitude lower than expected if failure occurs through elastic buckling, it was proposed that fibre networks collapse via plastic deformation, with individual fibres displaying a plastic yield stress on the order of 1 MPa. Plastic failure in gels is generally marked by a large increase in strain deviating from the linear elastic stress-strain relationship, and involves non-recoverable processes such as the fracturing of crystallites and breakage of permanent fibre junctions. Strain is concentrated in the mostly weakly connected regions of the fibres and may be accompanied by twisting or untwisting of the affected fibrils, weakening of the intermolecular bonds between fibrils and an increasing abundance of solvent-aggregate interactions.^{403, 404} In consequence, the value of the plastic yield stress is usually

dependent on the solvent, level of crystallinity and dimensions of fibres and their constituent fibrils.

Both floc-based and cellular materials can be described by a spherulitic model of aggregate growth. Continuous fibre networks arise if fibre branching by secondary nucleation vastly outpaces the primary nucleation of additional spherulites, whereas flocs are observed if the rates of the two processes are similar in magnitude. In both cases, the strength of the resulting material may be controlled via adjustments to the fibre dimensions and connectivities. By simulating spherulitic networks of interconnected rigid rods, Shi *et al.* derived a power law relationship between G' and the ratio L/R , where L is the length of a rod between branch points and R its cross-sectional radius.⁵⁹ The exponent of this relationship was estimated as -1.7, indicating that G' may be dramatically enhanced by increasing either the density of network junctions or the thickness of the component rods. In floc-based networks, an increase in the number of weak interparticle junctions offsets increasing spherulite density to produce a more gradual scaling of G' , but changing the aggregation environment to favour more frequent branching remains an effective strategy for maximising gel strength.⁷² A promising approach is to add surfactants to the gelator solution to modify the surface energies of growing fibres. Chen *et al.* found that gels of 2,3-di-*n*-decyloxyanthracene in DMSO display smaller and more highly branched spherulites in the presence of the non-ionic surfactant polyethylene glycol *t*-octyl-phenyl ether (Triton X-100), whilst another non-ionic surfactant sorbitan monolaurate (Span 20) produces larger, more weakly branched spherulites comparable to a continuous fibrous network.⁴⁰⁵ NMR studies suggest that the alkyl chains of Span 20 associate with those on the sides of gel fibres to promote branching along their length, whereas Triton X-100 interacts with fibre tips and primary nucleation sites to facilitate the initiation and peripheral branching of isolated flocs. Both surfactants serve to enhance G' at low concentrations, but addition of Span 20 in larger quantities may produce the opposite result, due to excessive loss of the extended branches needed for effective interpenetration of the fibre networks.

The presence of surfactants is just one of a number of factors that can be harnessed to modify gel strength. Tang *et al.* showed that floc-based propylene glycol gels of **36** can be weakened by Span 20, which suppresses spherulitic growth by confining branch points to the periphery of primary fibres (Fig. 43).⁴⁰⁶ At high concentrations, however, the surfactant additive forms spherical micelles, which act as nucleation sites for spherulites to produce an increase in G' . In the same system, Yuan *et al.* increased spherulite size by raising the temperature, but were also able to limit the number of spherulites along one axis by inducing gelation within a narrow glass cell.⁶² While G' initially scales with average spherulite separation, ζ , to the power of just 0.12, imposing a gap of 0.85 mm leads to a fourfold increase beyond 70 °C, the temperature at which ζ and the gap width become comparable in size. G' rises until 80 °C but falls at higher temperatures due to an increasing dependency on the branch separation L , which varies in inverse proportion to the supersaturation.⁴⁰⁷

Deformation of a soft material under stress does not occur instantaneously, but over a finite timescale linked to its viscosity, μ .⁴⁰⁸ Viscosity under steady shear is defined as the ratio of shear stress σ to shear strain $\dot{\gamma}$. In oscillatory shear experiments, meanwhile, it is customary to define a complex viscosity, μ^* , equal to the magnitude of G divided by the

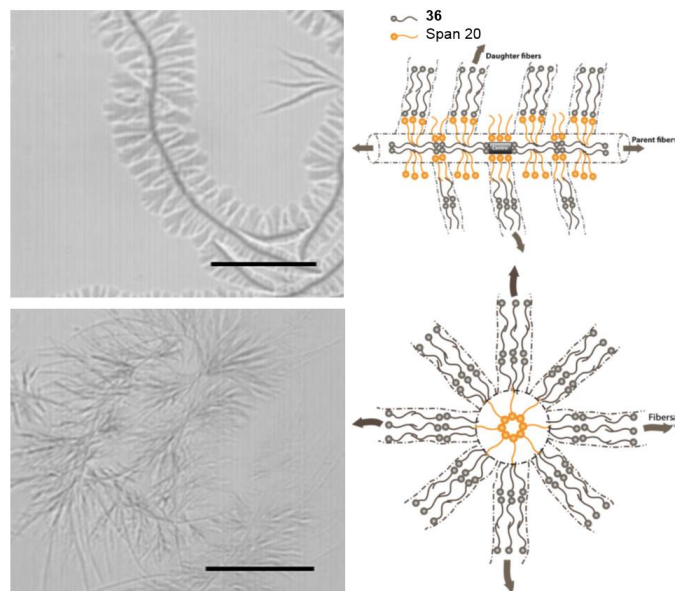


Fig. 43 Optical microscope images (scale bar 100 μm) and schematic diagrams illustrating the effect of the surfactant Span 20 on the aggregation of gelator **36** in propylene glycol. Below the critical micelle concentration (CMC) of Span 20, the surfactant promotes branching of the gel fibres to produce a comb-like topology (upper images). Micelles of Span 20, meanwhile, act as nucleation sites for fibre growth, producing spherulitic aggregates (lower images). Images adapted with permission from ref. 406. Copyright 2009 John Wiley and Sons.

frequency ω . The viscosity of a Newtonian fluid is constant with respect to both $\dot{\gamma}$ and ω and obeys the Cox-Merz rule, adopting the same value irrespective of the stress regime. In non-Newtonian fluids such as gels, however, μ and μ^* are variable and may therefore violate the Cox-Merz rule under certain conditions. It is generally true for gels below their yield point δ that $G'' \ll G'$, and the Kramers-Kronig relation further asserts that G'' scales as the rate of change of G' with ω .⁴⁰⁹ Thus, G' should remain almost constant over a wide range of ω , resulting in a roughly inverse relationship between μ^* and ω . A more accurate analysis reveals that G' increases with ω in an approximate power law relationship, with an exponent equal to the ratio G''/G' .⁴¹⁰ Classically cellular gels of 12-hydroxystearic acid in toluene, dodecane and nitrobenzene were shown by Terech *et al.* to conform to this trend, exhibiting exponents in the range 0.02–0.09.¹⁰ The associated negative correlation between μ^* and ω is termed shear-thinning behaviour and may be ascribed to alignment of fibres along the axis of stress. It is important to note that increased flow at higher rates of shear need not correspond to yielding of the material: provided the stress does not exceed δ , the magnitude of strain remains almost unaltered and deformation of the material is predominantly elastic and reversible. The greater-than-linear reduction in viscosity with increasing flow rate is particularly useful in materials such as lubricants and dyes for inkjet printing, which are required to flow under temporary high-shear conditions but otherwise display solid-like properties.

Following mechanical disruption, the aggregates in a gel may reassemble into a new solid or viscoelastic material. Reconstruction of a gel in response to macroscale fracturing is often referred to as self-healing, and is fairly common among metallogels and other materials supported by labile covalent bonds and/or dynamic supramolecular motifs.^{266, 411} Shi *et al.* prepared self-healing hybrid gel films with conductivities up to 12 S m^{-1} by freeze-drying phytic acid hydrogels and impregnating the resulting aerogels with acetonitrile solutions of a gelating zinc(II)-terpyridyl coordination cage.⁴¹² The gels become more resistive if cut or stretched but rapidly return to their original state on resting, allowing a circuit to be broken and reconnected in less than one minute. Likewise, Sahoo *et al.* found that the dicyclohexylammonium salt of Boc-protected L-glycine forms a robust double-stranded hydrogen bonded network in nitrobenzene, affording a fibrous gel that can be cut and fused together with limited loss of tensile strength.⁴¹³ Interestingly, any change in the gelator composition results in a marked reduction in both the strength of the gel and its self-healing ability, as other amino acids and ammonium cations favour an alternative tape-like supramolecular network that is less well suited to gel formation.

Recovery of a gel can also occur in response to shaking, shearing or sonication, which lead to microscale fracturing in the bulk of the material. Self-healing of this nature may partly result from surface tension and buoyancy forces, especially if the gel is surrounded by an immiscible liquid phase. For example, Yan *et al.* found that heptane gels of the ferrocene-containing cholesteryl compound **41**, dispersed in an aqueous iodine solution with shaking, efficiently absorb and entrap the

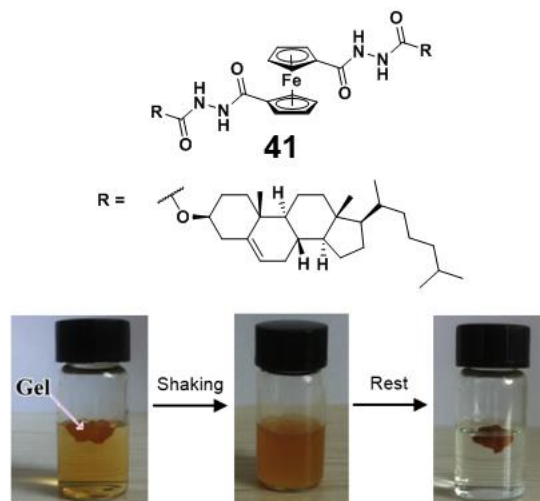


Fig. 44 Heptane gels of **41** are disrupted by shaking but reform on resting, providing an effective method for extracting iodine from an aqueous solution. The gels are thermoreversible and may also be disrupted irreversibly through oxidation with ceric ammonium nitrate, producing a colour change from orange-brown to green. Image adapted with permission from ref. 414. Copyright 2015 Elsevier.

iodine before reforming an easily isolable gel at the air-solvent interface (Fig. 44).⁴¹⁴ More generally, the bulk regeneration of a gel can be attributed to the renewal of junctions between fibres, and may be observed following an oscillatory shear experiment as a gradual increase in G' and reduction in strain. Gels that respond to stresses in excess of δ by undergoing

progressive shear-thinning over time, but tend towards their initial solid-like state after removal of the stress, may be referred to as thixotropic materials.⁴¹⁵⁻⁴¹⁷ The magnitude of a thixotropic response may be modified with the use of additives that interact strongly with the gelator,⁴¹⁷ or by altering the aggregation environment or type of stress applied. In one notable study, co-gels of a pyridyl bis(urea) with dicarboxylic acids were found by Liu and Steed to reform after mechanical disruption, but become non-thixotropic upon exposure to heating, high pH or prolonged sonication.⁴¹⁸

A further complication in the design of thixotropic gels is the possibility of material fatigue. Non-recoverable strain increases with the magnitude of the applied stress and can be attributed to the loss or weakening of fibre junctions or large-scale changes in aggregate morphology. For instance, Lloyd *et al.* observed that interconnections between fibres in a chiral bis(urea) gel become thinned after shearing and self-repair, resulting in a G' value 45% lower than that of the parent material.⁴⁰¹ It is worth noting that the self-healing capacity of a gel may not be correlated with its initial resistance to mechanical disruption. In one study, Terech *et al.* showed that a decane gel of 12-hydroxystearic acid deforms ten times more slowly than a DMF gel of terpyridyl ligand **42** and nickel(II) chloride but exhibits strain recovery of just 32%, compared with 72% in the metal-containing system (Fig. 45).⁴¹⁹ The thermodynamic stability of a gel is of particular importance since fragmented assemblies may be sequestered by competitive modes of aggregation, preventing the reestablishment of lost transient junctions under dynamic conditions.⁴²⁰

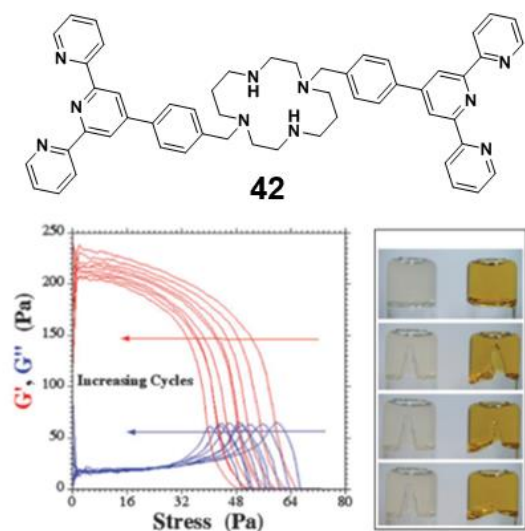


Fig. 45 Stress-sweep plots for a DMF gel of **42** (40 mM) and two equivalents of nickel(II) chloride over multiple cycles of disruption and recovery. The gel recovers after fracturing within 48 hours (right) but a decane gel of 12-hydroxystearic acid with the same storage modulus does not exhibit self-healing behaviour (centre). Images adapted from ref. 419 with permission from the PCCP Owner Societies.

The strength of a gel does not always decrease upon the application of stress. Stiffening may arise at stresses less than δ if these lead to increased jamming, close packing or crosslinking of aggregates.⁴²¹ Compression stiffening is implicated in the behaviour of certain biological tissues,⁴²² and could be reproduced synthetically by exploiting feedback between the

density of crosslinks and their rate of formation. A computational study by Yashin *et al.* showed that coupling the BZ reaction with a gel-based ruthenium(II)-terpyridyl catalyst might be a promising strategy, since the proportion of metal sites undergoing reduction and crosslinking would increase upon compression of the material.⁴²³ The magnitude of the effect would largely be dictated by the concentration of fibres and could thus be usefully modulated by triggering a deswelling response. Such rheological sensitivity to particle density mirrors that of biological materials such as blood clots, which consist of a fibrous fibrin network with entrapped cells and platelets. Materials of this type soften under compression in the manner of a classical polymer network⁴²⁴ but exhibit stiffening behaviour if water is lost, increasing the density of the fibre network.⁴²⁵ Stiffness perturbations are thought to play an important role in cellular development, signalling and disease processes, as changes to the characteristic rheological properties of tissues can strongly influence the shapes, motilities, growth rates and differentiation pathways of constituent cells.⁴²⁶⁻⁴²⁸

Gels of fibrous biological macromolecules such as fibrin, actin and collagen may also display stiffening behaviour if subjected to extensional stresses exceeding a critical value, σ_c .^{429, 430} Stress stiffening can be attributed to a transition between entropic and enthalpic stretching and is typically characterised by a power-law scaling of G with σ , tending towards a maximum exponent of 1.5.⁴³¹ Though common in biomaterials, stress stiffening is rarely observed in synthetic gels as the requirement for semi-flexible fibres, or a persistence length comparable to the distance between junctions, is difficult to satisfy.⁴³² Nonetheless, biomimetic stiffening behaviour was realised by Jaspers *et al.* in a range of hydrogels comprising polyisocyanopeptides with peripheral tri(ethylene glycol) substituents.⁴³³ The materials display dimensions comparable to those of neurofilaments but can access substantially higher G values with stiffening over a wider range of stresses. Furthermore, the gels are heat-set and display unprecedented marginal properties close to T_{gel} , transitioning from viscous fluids to solid-like elastic networks in response to extremely small applied forces. Stress stiffening may be tuned, like other rheological properties, through variation of the gelation conditions. Both pre-shear G and σ_c scale roughly quadratically with concentration and exponentially with temperature, whilst the rate of change of G with σ increases slowly and linearly as the material is heated.

Stiffening of a gel under a directional mechanical stimulus may be partly due to alignment of fibres with the applied force. Indeed, shear may induce gelation by converting coiled fibres into extended bundles suitable for incorporation into a three-dimensional network. Pappas *et al.* demonstrated that short, curved nanofibres of the tripeptides ^DFFD and ^DFFI can be converted to bundles of parallel nanofibres through directional sonication, resulting in strong gels with pronounced supramolecular chirality.⁴³⁴ Alignment of nanofibres in solution may also be induced by audible (20 Hz to 20 kHz) sound waves, or within the high-shear flows of a printing nozzle or liquid vortex. The susceptibility of an aggregate to alignment and the

magnitude of the resulting optical effects can in some cases be controlled by exploiting other stimuli-induced responses, such as the isomerisation of a photoreactive switch. Velocity gradients generated by 120 Hz sound at an amplitude of 13.5 Pa were found by Hotta *et al.* to orient nanofibres of a DTE-containing bis(urea) in *n*-hexane, but the resulting linear dichroism (LD) signal spans UV and visible frequencies only if the closed DTE isomer is used.³⁴² More strikingly, the azobenzene derivative **43** produces a strong sound-induced LD signal in cyclohexane solutions of its *trans* form but becomes LD silent when isomerised, due to fragmentation of the fibrous aggregates into non-orientable spheroidal particles (Fig. 46).⁴³⁵

The symmetry of fibres can be similarly influenced by anisotropic stress. Net chirality in assemblies of achiral or racemic molecules commonly results from chiral impurities, trace enantiomeric enrichment of the parent solution⁴³⁶⁻⁴³⁸ or the aggregation phenomenon known as the Adam effect,⁴³⁹ in which heating or mechanical disturbance causes a chiral material to evolve from a small, non-statistical population of primary nuclei.⁴⁴⁰⁻⁴⁴² However, there is some evidence to suggest that stirring can itself template the assembly of helical fibres, producing a bias in handedness dependent on the sense of rotation of the liquid medium.^{443, 444} For example, Escudero *et al.* showed that J-aggregated bilayers of a sulfonated porphyrin can undergo folding above a critical width, producing different CD signals depending on the stirring direction.⁴⁴⁵ Ultrasound, meanwhile, was utilised by Azeroual *et al.* to disrupt helical stacks of an achiral foldamer, allowing it to reassemble into homochiral fibres in the presence of the chiral template diethyl tartrate.⁴⁴⁶ It is important to note that the

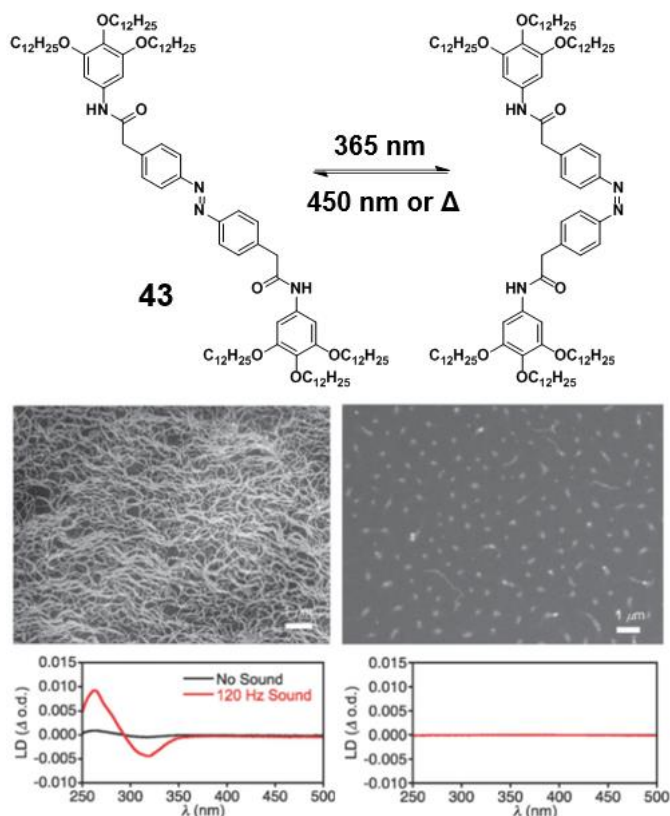


Fig. 46 SEM micrographs of air-dried samples of *trans*-**43** (left) and *cis*-**43** (right) from cyclohexane, and LD spectra with and without 120 Hz sound (amplitude 13.5 Pa). Image adapted from ref. 435 with permission from The Royal Society of Chemistry.

spectroscopic methods used to identify supramolecular chirality are subject to experimental artefacts which may exaggerate or invert the apparent anisotropy.⁴⁴⁷ In addition, deflection of liquid by the vessel walls produces vortical flows in opposing directions, so the resulting mechanoresponsive behaviour may prove container-dependent and difficult to control.⁴⁴⁸

Microstructural and rheological transitions are not the only stress-induced responses that a gel may exhibit. Mechanical stimuli can affect the wettability of an aggregate post-drying, as well as optical properties such as colour, opacity and emissivity. For example, Dou *et al.* found that ultrasound-induced gelation of **44** in DMF is associated with a shift in fluorescence wavelength from green to yellow (Fig. 47), while grinding of the dry material triggers a piezochromic transition from orange to yellow.³⁷⁵ Like changes in aggregate morphology, optical effects

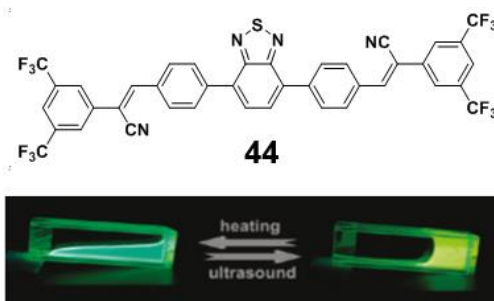


Fig. 47 Fluorescence of **44** in DMF under 365 nm light, after treatment with heat (left) and ultrasound (right). Image reproduced with permission from ref. 375. Copyright 2011 American Chemical Society.

can vary with the nature and duration of the applied stimulus. In a study of cholesterol-appended ferrocene gelator, Liu *et al.* found that sonication of a transparent cyclohexane gel results in a viscous opaque suspension, whereas shaking or heating the material produces a transparent solution.⁴⁴⁹ Komiya *et al.*, meanwhile, observed that sonicating the platinum analogue of complex **37** for three seconds in cyclohexane affords weakly phosphorescent gels, which exhibit stronger emissions and more intense metal-ligand charge-transfer absorption bands after prolonged exposure to ultrasound.²²² Although NMR spectra indicate that complete aggregation occurs regardless of sonication time, the extended treatment appears to produce thicker bundles of fibres, in which increased ordering and rigidity of molecules diminishes the rate of non-radiative relaxation.

The ability to undergo multiple reversible transformations in response to external stimuli is crucial if gels are to function as smart devices, with properties that can be adjusted *in situ* to suit a range of operating environments. Of particular interest are multiresponsive gels that are also multiaddressable, in that they exhibit a range of responses that can be separately initiated by different stimulus combinations. Given the ubiquity of mechanical triggers in real-world processes, multiaddressable systems based on stress-induced responses clearly hold much promise. Such systems would benefit from

the rheological tuneability of supramolecular gels, the variety of mechanical inputs available for use, and the ease of controlling the amplitude, frequency and duration of the forces applied.

4.3 Multiaddressable systems

The most frequently encountered multiaddressable gels are those that respond to both thermal and mechanical stimuli. The strength of a gel and its thermal stability are both dictated by interactions between gelator molecules, but effects which serve to increase G' do not always influence T_{gel} in a similar fashion. For example, Roy *et al.* showed that sonogels of thymine and a diaminated triazine in water exhibit lower CGCs and higher G' values than thermal gels, but consist of narrower, less crystalline fibres which undergo melting and gel-to-crystal transitions more readily.⁹⁹ More commonly, T_{gel} and G' are positively correlated but display different patterns of variation as the gelation conditions are altered. Brinksma *et al.* examined the gelation behaviour of a cyclohexyl bis(urea) in primary alcohols and noted that T_{gel} is inversely proportional to the negative logarithm of the gelator concentration, c , in accordance with the van't Hoff equation.⁴⁵⁰ By contrast, pre-shear G' obeys the usual power-law relationship for cellular networks, with exponent n in the range 1.6–2.1. Estimates of the CGC from T_{gel} and rheological measurements differ in magnitude by as much as a factor of two, but the studies reveal a consistent rise in CGC with increasing chain length of the alcohol solvent. Gels of the heavier alcohols also exhibit lower melting enthalpies and T_{gel} values and are less mechanically robust, producing smaller G' values that increase less rapidly with gelator concentration.

Differences in the effects of thermal and mechanical stimuli can sometimes be attributed to well-defined supramolecular phenomena. Wu *et al.* found that one series of naphthalimide functionalised cholesteryl derivatives display different powder X-ray diffraction patterns in gels generated thermally and through sonication.⁴⁵¹ The sonogels typically comprise smaller and more highly connected aggregates with lower G' values, less pronounced weak strain overshoots and higher wettabilities after drying. Zhang *et al.* similarly observed that whereas thermal gels of the dihydrazide derivative **45** consist of fibrous aggregates with a triclinic structure, exposing the hot gelator solution to ultrasound during cooling leads to the emergence of a more particulate and less thermally stable monoclinic material (Fig. 48).⁴⁵² In this case, however, differences in microstructure and molecular packing may be eliminated by conducting the sonication treatment at higher temperatures or for shorter periods of time. Sonication at 35 °C gave rise to a 37% monoclinic sonogel with a contact angle of 146.7° in the xerogel state, whilst treatment at 60 °C produced no detectable monoclinic component and a contact angle of 111.2°, approaching the value of 122.1° measured in the absence of ultrasound.

More quantitative comparisons of the self-assembly outcome may be made by considering the kinetics of the gelation process. A popular approach is to monitor the degree of aggregation over time, using an appropriate spectroscopic

signal or rheological property as a proxy for aggregate concentration. According to the modified Avrami equation,⁸⁹ the fraction of gelator remaining in solution is related to the fractal dimension of the aggregate, D_f , and the time since gelation. Liu and Sawant successfully applied this theory to gels of **36** in isopropanol, finding that light scattering and shear modulus measurements yield near-identical estimates for D_f in the vicinity of 2.15.⁴⁵³ Adopting a fluorescence-based approach,

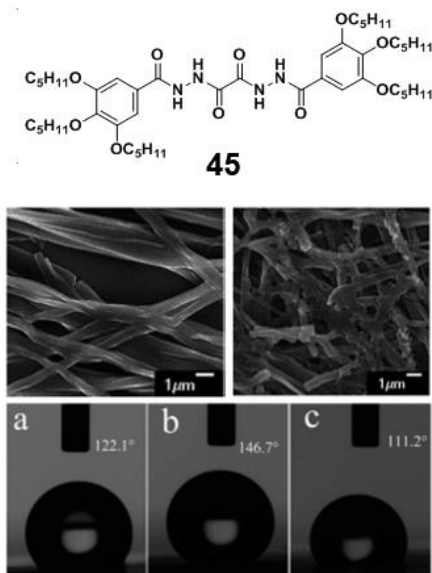


Fig. 48 SEM micrographs of gels of **45** in ethanol prepared by cooling a heated solution in a 3 °C water bath (top left) and sonicating a heated solution at 35 °C for five minutes (top right). Sonication appears to produce more fragmented fibres with some particulate material. The contact angle of the thermal gel (a) is less than that of the sonogel prepared at 35 °C (b) but greater than that of a sonogel prepared at 60 °C (c). Image adapted from ref. 452 with permission from The Royal Society of Chemistry.

Zhang *et al.* likewise demonstrated that an ethanol sonogel of **45**, with a typical D_f of 1.88, is more highly branched than a comparable thermal material, with D_f in the range 0.99–1.15.⁴⁵² Interestingly, despite their superior connectivity, the sonogels are significantly less stable to both heat and mechanical stress, displaying lower values of G' and T_{gel} than the materials.

A difficulty often encountered when inducing thermal and mechanical responses in gels is that the stimuli employed may damage or alter encapsulated guests, such as single crystals or living cells. To surmount this obstacle, it is often beneficial for the system to respond to additives which have little impact on the materials to be preserved. Depending on their size, charge and solvation energy,⁴⁵⁴ anions may serve to disrupt hydrogen bonds between LMWGs by introducing competitive supramolecular motifs. In one notable study, Foster *et al.* used bis(urea) gels as chemically tuneable media for the crystallisation of carbamazepine, and were able to isolate undamaged single crystals of the drug by adding acetate ions to induce a gel-sol transition.¹²³ Also commonly employed in LMWGs are redox-active groups, such as ferrocenes, tetrathiafulvenes, disulfides, chains of pyrroles and thiophenes and electroactive transition metal complexes.⁴⁵⁵ These groups can behave as chemically triggered molecular switches, and may sometimes be linked to photoreactive groups to deliver a multiaddressable system. For example, Wang *et al.* constructed

a gelator with both azobenzene and tetrathiafulvene groups, to allow for the interconversion of gel and sol phases by cycles of UV and visible light, an applied voltage alternating between +0.75 and -0.2 V, or successive additions of iron(III) perchlorate and ascorbic acid (Fig. 49).⁴⁵⁶ As well as being multiaddressable, gelator **46** may be considered multiresponsive, since the reaction of each molecular switch produces a different sol state. Whilst *trans-cis* isomerisation of the azobenzene group delivers an orange sol that converts back to the original orange gel even at 5 °C, oxidation of the tetrathiafulvene group leads to a green

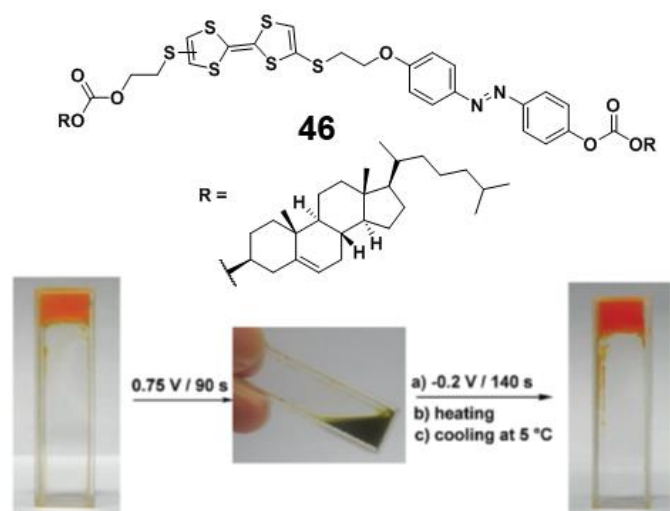


Fig. 49 Compound **46** forms orange gels in 3:1 (v/v) mixtures of chloroform and methanol, but is converted to a green sol upon reduction of the tetrathiafulvene group. The orange gel may be regenerated by oxidation of the sol followed by thermal cycling. A reversible gel-sol transition may also be induced by isomerisation of the azobenzene group under UV illumination, but in this case the sol generated is orange in colour. Image adapted from ref. 456 with permission, correcting stereochemistry of **46** in original diagram. Copyright 2010 American Chemical Society.

sol which can reform a gel on reduction only if thermal cycling takes place.

A small number of reactive groups are inherently multiaddressable. Anils may respond to both heat and light, and metal complexes can sometimes undergo both redox reactions and stress-induced recombination processes. In many cases, however, the effects of different stimuli are difficult to differentiate. Liu *et al.* found that *trans-cis* isomerisation of one azobenzene-functionalised dendritic gelator converts fibrous sonogels to particulate sols, which in some solvents are also observed after a heating-cooling cycle.⁴⁵ Similarly, Duan *et al.* noted that both heating and UV irradiation of **47** in toluene produce a weakening of its CD signals, due to breakup of the chiral helical assemblies responsible for gelation (Fig. 50).⁴⁵⁷ Molecular switches that produce different physical responses on exposure to multiple environmental triggers are relatively rare. A good example was reported by Liu *et al.*, in ethanol-water co-gels of an alkylated spiropyran and cationic amphiphile.⁴⁵⁸ Reversible ring opening of the spiropyran under UV light produces a colour change from pale pink to red, while acidification of the merocyanine product generates a yellow material. Remarkably, the system can also act as a chiroptical switch, due to chirality transfer between the chiral amphiphile and achiral chromophore. Photoisomerisation reverses the

direction of the CD signal and induces a red shift from 390 to 550 nm, while protonation of the merocyanine reduces the signal wavelength by 120 nm without a change in sign.

In order to enhance the responsive properties of a gel, it is sometimes feasible to introduce a guest aggregate with complementary stimuli-induced behaviours.⁴⁵⁹ A simple approach is to employ a gel as a matrix to encapsulate useful particulate materials. By sonicating an ionogel of an amide-containing cholesteryl gelator with iron(III) oxide nanoparticles and then heating and cooling the mixture, Yan *et al.* obtained a composite gel that collapses on exposure to a magnetic field.⁴⁶⁰ The gel reforms upon repetition of the original preparative treatment and, unlike many other magnetorheological materials, retains its responsive behaviour over multiple cycles of disruption and regeneration. It is unclear whether nanoparticles affect the rheology of the gel in the absence of

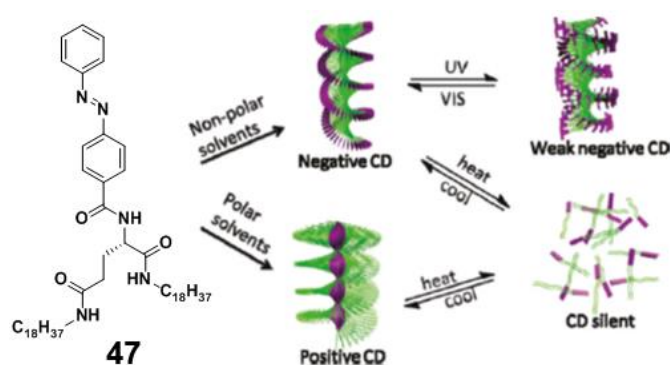


Fig. 50 Self-assembly of **47** in non-polar solvents leads to a helical aggregate with peripheral azobenzene residues (shown in purple) and a handedness opposite to that of aggregates in polar solvents. Disassembly on heating is marked by a loss of CD activity. UV irradiation triggers a *trans-cis* isomerisation in non-polar solvents to produce a weakening of the CD signal, but has no effect on aggregates in polar solvents, due to close packing of the azobenzene groups in the helix core. Image adapted with permission from ref. 457. Copyright 2011 American Chemical Society.

the magnetic stimulus, but such synergistic interplay between the host and guest properties is not uncommon. In one notable investigation, Cayuela *et al.* found that encapsulating luminescent quantum dots in an aqueous bis(urea) sonogel serves to strengthen the gel, reduce the gelation time from ten days to a few minutes, and enhance the emission intensities of the guest particles by at least one order of magnitude.¹¹⁹

An alternative method for producing multiaddressable or multiresponsive gels is to target aggregates based on two or more functional molecules. Blending of gelators can afford material properties that would not be achievable in a single-component system.⁴⁶¹ Foster *et al.* showed that whilst gels of an achiral bis(urea) and a chiral pyrene-functionalised analogue consist of flat ribbons and cylindrical fibres respectively, co-assembly in a toluene 9:1 co-gel leads to ribbons with a pronounced helical twist and suppresses excimer emissions from the pyrenyl species.⁴⁶² Likewise, Miyamoto *et al.* found that gels obtained by mixing pairs of pyrenyl gelators may prove more strongly fluorescent than the single-component gels or exhibit CD signals of the opposite sign.⁴⁶³ Optical effects enhanced by donor-acceptor interactions are a common illustration of how co-assembly in a mixed gel can usefully modulate a stimuli-induced response. To achieve comparable

coupling of non-optical behaviours, co-gelators may be chosen such that the responses of one species serve to stimulate those of another. Wang *et al.* recognised that thermal deswelling of an elastomeric peptide based on a repeating five-residue sequence can be induced through irradiation of reduced graphene oxide sheets, which produce heat on exposure to near-infrared light.⁴⁶⁴ Hybrid nanoparticles of the two materials retained the hydrogelation properties of the peptide and could be successfully incorporated into a flexible anisotropic sheet, capable of reversible bending in response to localised heating or infrared illumination via a laser source.

An advantage of mixed gels is that the components of the aggregate framework need not show gelation behaviour when utilised separately. Indeed, such materials are frequently designed by identifying molecules that interact weakly when pure, but form more robust supramolecular motifs in combination with a different species. For example, Okumura and Ito developed remarkably superabsorbent hydrogels based on topologically bound rotaxanes of poly(ethylene glycol) and cross-linked cyclodextrins,⁴⁶⁵ while Liu and Steed enhanced the strength of pyridyl-functionalised bis(urea) hydrogels by adding dicarboxylic acids in a 1:1 molar ratio.⁴¹⁸ Unlike particles suspended in the cavities of a gel, species incorporated into the supramolecular network must deviate from their usual mode of aggregation and associated physical properties. Xue *et al.* demonstrated that gelator **48**, which forms emissive H-aggregated gels in *o*-dichlorobenzene, can co-assemble with the non-gelating fullerene derivative **49** to produce a hybrid gel system (Fig. 51).⁴⁶⁶ Photo-induced electron transfer serves to quench the fluorescence of the gelator around 500 nm and may, in xerogels, give rise to appreciable photocurrents, with calculated and measured band gaps in the region of 406 nm.

Mixed gelator systems represent a promising route to more functional gel-based materials, but their usefulness is limited by

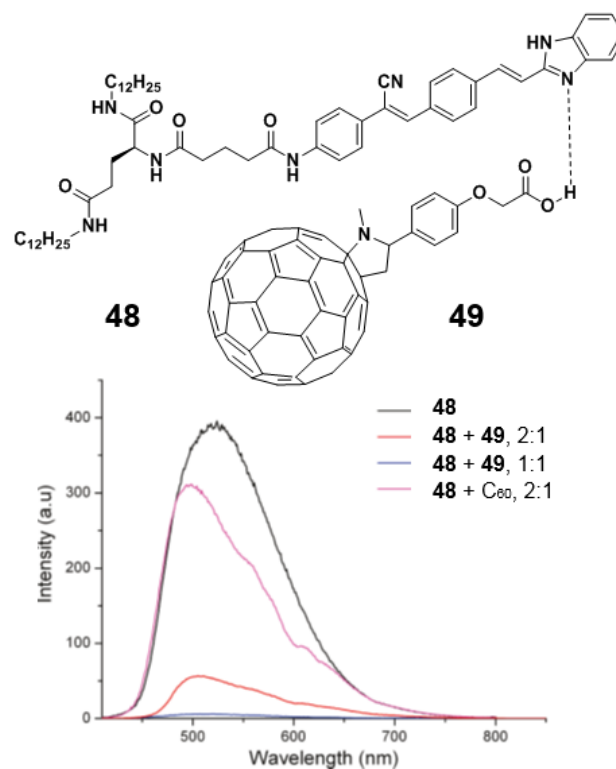


Fig. 51 Fluorescence spectra of *o*-dichlorobenzene gels of **48** with fullerene additives. Compound **49** quenches emissions from **48** more effectively than unsubstituted C₆₀ (pink line). Image adapted with permission from ref. 466. Copyright 2010 American Chemical Society.

difficulties in predicting and optimising the aggregation outcome. A more practical strategy would be to combine self-assembled systems that develop in an orthogonal fashion, such that desirable properties of the single-component gels are preserved in the multicomponent material. Self-sorting may arise due to the selective formation of supramolecular motifs involving like gelator molecules, or through the sequential self-assembly of different species in a varying aggregation environment. The latter possibility was illustrated by Morris *et al.* in a study of naphthalene-functionalised dipeptide hydrogelators (Fig. 52).⁴⁶⁷ Due to their differing pK_a values, **50a** self-assembles prior to **50b** upon gradual acidification of the mixed system, with the result that small-angle neutron scattering and fibre diffraction experiments reveal a combination of single-component aggregates. The hydrolysis of glucono- δ -lactone to gluconic acid can be exploited to gradually lower the pH of the bulk solution, while the electrochemical oxidation of hydroquinone produces a local decrease in pH to induce gelation on the surface of the driving electrode.⁴⁶⁸ Building on this work, Colquhoun *et al.* found that lowering the pH of an aqueous solution of **50c** and **50d** produces an initial fibrous network composed solely of **50c**.⁴⁶⁹ In this case, however, the second component is deposited as a crystalline material which reduces the strength of the composite material. Thus, gels of **50c** and **50d** attain a maximum *G'* at pH 5.5–6.0, close to the pK_a of **50d**, whereas mixed hydrogels of **50a** and **50b** become stronger with decreasing pH and exhibit higher *G'* values than their single-component counterparts.

Self-sorting of gelators can give rise to interpenetrated

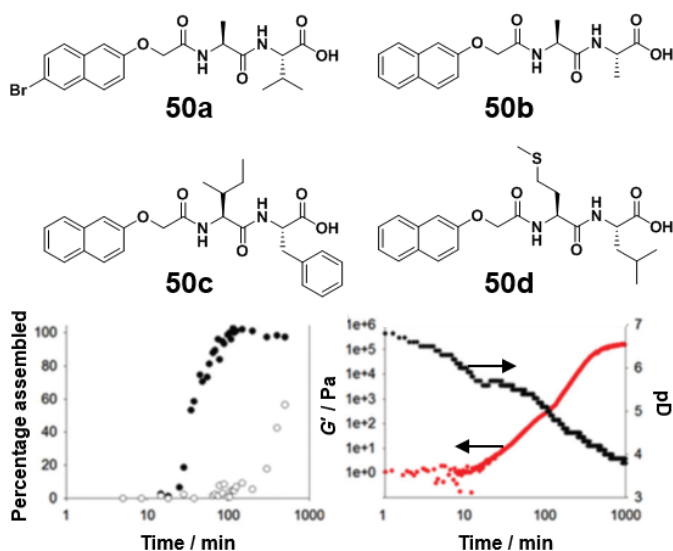


Fig. 52 As the pD of a mixed D₂O solution of **50a** and **50b** decreases, the two gelators self-assemble in isolation (left plot). Aggregation of **50a** (filled circles, pK_a 5.9) takes place before that of **50b** (empty circles, pK_a 5.1), as gauged by the fractional disappearance of characteristic NMR signals. Decreasing the concentration of glucono- δ -lactone increases the time difference between the self-assembly processes, but the concentration must exceed a threshold value for aggregation of **5b** to take place. G' increases with pD (right plot) since the two gel networks both contribute to the strength of the gel. Images adapted from ref. 467 with permission from The Royal Society of Chemistry.

networks with vastly different rheological properties. Gels with unprecedented strength and yield characteristics may be achieved by constructing a double network, in which a small concentration of rigid, brittle fibres spans a softer, more ductile fibrous matrix. Materials of this type are typically prepared by swelling a rigid, highly crosslinked polymer in an aqueous solution of the second monomer, which is polymerised with low crosslink density in the pores of the resulting gel. As outlined in reviews by Gong⁴⁷⁰ and Haque *et al.*,⁴⁷¹ double networks may exceed the tensile, compressive and strain moduli of the corresponding single-component gels by as much as two orders of magnitude, and withstand significantly larger strains prior to the point of failure. Substantial hysteresis in the stress-strain response, atypical of polymer hydrogels, provides evidence as to the cause of this dramatic strengthening: the scission of bonds in the brittle fibres, which releases energy that would otherwise be stored as strain in the flexible fibrous network. This mechanism may be likened to the reinforcement of bone, wherein a calcium-rich glue provides sacrificial bonds to oppose the separation and elongation of collagen fibres.⁴⁷² Indeed, double-network gels are under investigation as artificial replacements for a number of biomaterials, including cartilage and cornea tissue.¹⁵³ Shear-induced alignment of rigid polymers may also offer access to anisotropic networks with complex motile responses to stress or swelling, mimicking the morphological transformations of biological membranes.⁴⁷³

Alongside the mechanical properties of a gel, self-sorting may influence how the aggregated gelators interact with heat or light. In a simple system, gelation may involve the sequestration of one switchable molecule from a library of alternatives, producing a supramolecular material dominated by the reactive properties of that component alone. For example, Li *et al.* used HPLC-MS to show that solutions of **51** and **52** in an aqueous borate buffer contain a variety of structures,

including dimers of **51**, interlocked trimers of **52** and mixed dimers and tetramers of the two molecules (Fig. 53).⁴⁷⁴ Addition of magnesium chloride, however, produces hydrogels in which supramolecular polymers of **51** linked by carboxylate-amide hydrogen bonds, disulfide bridges and networks of hydrated magnesium ions are the only aggregated species. The gels may be disrupted by heat, shaking or photoisomerisation of the azobenzene group, and are able to reform over several days. Furthermore, the assemblies may be disrupted chemically by reducing the disulfide groups with dithiothreitol, and are found to crystallise if calcium chloride is used in place of the magnesium salt. The solutions afforded by reduction return to the gel state upon gradual oxidation by air, whereas calcium complexes of **51** can be converted to gels in the presence of the charged additive glycine, which provides electrostatic repulsion between the linear polymers to prevent their lateral association.

If gelation involves the self-assembly of two or more species, self-sorting may lead to highly compartmentalised aggregates with structures closely tied to their stimuli-responsive properties. Pham *et al.* designed a triblock polymer with one cationic and one collagen-like block, which can surround an anionic homopolymer to form micellar assemblies.⁴⁷⁵ Whilst the triblock polymer alone forms non-gelating triple helical structures in solution, the micelles produce strong, thermoreversible hydrogels that may be weakened or disassembled by competitive ions. On a larger scale, Woodward *et al.* employed a branched co-polymer surfactant to encapsulate polymer-decorated iron(III) oxide nanoparticles within emulsified droplets of dodecane.⁴⁷⁶ Immersing a magnet in the emulsion to generate a localised magnetic field induced aggregation of the droplets at the air-water interface. Likewise, a gel monolith prepared by creaming of the emulsion at low pH was found to bend in the direction of a nearby magnet, and could be floated on water to act as a surficial stirring bar

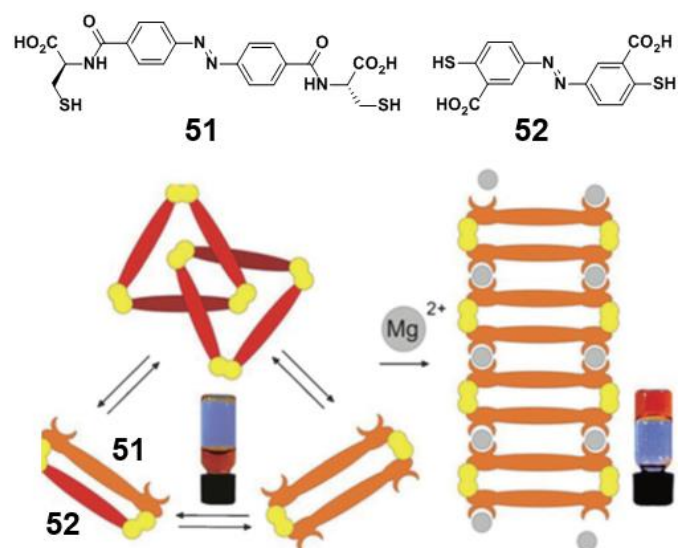


Fig. 53 Azobenzene derivatives **51** (shown schematically in orange) and **52** (shown in red) form a mixture of assemblies in buffered aqueous solutions, linked by disulfide bridges (shown in yellow) and hydrogen bonds. However, the addition of magnesium ions (shown as grey circles) leads to self-sorting of **51** into single-component gel fibres. Image adapted with permission from ref. 474, correcting stereochemistry of **51** in original diagram. Copyright 2014 John Wiley and Sons.

controllable by a rotating magnetic field.

Exposing a gel to a different stimulus may provide access to a wider range of physical properties, but even greater variation is possible if stimuli are applied in combination. Systems in which one stimulus modifies the effects of another are said to exhibit logic gating behaviour, and commonly described in terms of the Boolean operations they perform. Whilst photoreactive groups are the most popular tool in the development of gel-based logic gates, useful coupling between chemically induced responses has also been reported. Gelator **48** was shown by Xue *et al.* to function as an INHIBIT logic gate in DMSO solutions, turning red with the addition of fluoride or hydroxide ions but reverting to yellow in the presence of trifluoroacetic acid.³⁵⁵ The compound gels a 1:4 mixture of water and DMSO and behaves thereafter as a combination logic gate, fluorescing at 470 nm in response to 400 nm light if the gel is untreated or both acid and fluoride ions are present. Of course, it is possible to design a molecular logic gate that exhibits light-induced transitions in addition to chemical sensitivity. Yang *et al.* integrated an azobenzene group into a gelator with a terminal acyl chloride, allowing gel-sol transitions to be induced by UV light, in addition to heat and sonication.⁴⁷⁷ Conversion of the acyl chloride to an ester, however, leads to a dramatic reduction in solubility, altering the range of solvents in which gelation can take place and, potentially, the behaviour of the compound under UV illumination.

Alternative permutations of stimuli can sometimes produce similar effects. For example, Wei *et al.* observed that ring closing in aluminium complexes of a dicarboxylated DTE species in alcohols produces a colour change from yellow to red, but affects neither the heat-setting of gels at 80 °C nor the dissolution of these materials on cooling to room temperature.⁴⁸ In other cases, the behaviour of the gel depends on the order in which stimuli are applied. Chen *et al.* demonstrated that gels of a spiropyran-functionalised fibrous dendron can cycle between red emissive and yellow non-emissive states by alternating treatments with visible and UV light.³⁴⁶ Heated solutions of the gelator, however, form particulate merocyanine aggregates when cooled under UV irradiation, and cannot revert to their original state unless redissolved by heating above 80 °C. A comparable effect was observed by Pham *et al.* in gels of a triblock polymer with elastin-like and silk-like regions, which aggregate under high-temperature and low-pH conditions respectively.⁴⁷⁸ If the system is heated to 35 °C and subsequently acidified to pH 2, the elastin-like region of the polymer is first to self-assemble, and the resulting material consists of fibrous, weakly gelating micellar aggregates that can be resolubilised by the addition of base. Lowering the pH before heating, meanwhile, leads to stacking of the silk-like segment to afford fibrous gels with relatively high G' values. Interestingly, whereas heating a freshly prepared pH 2 solution produces an opaque gel, incubating the acidified system at 5 °C for ten hours before heating results in a transparent gel that becomes weaker with additional thermal cycling. AFM images indicate that heating causes the initial fibrous aggregates to form bundled structures, and these only

partially dissociate when the polymer is cooled below its critical micelle temperature.

Much of the versatility of LMWGs stems from their ability to access a range of molecular arrangements with diverse chemical and physical properties. Precise navigation of this self-assembly landscape is crucial to the development of complex hierarchical structures in biological systems. In order to realise this level of control in synthetic materials, it is necessary to circumvent thermodynamic aggregation by adjusting the self-assembly environment to favour alternative kinetic pathways. Many of the successes so far have relied on chemical strategies, such as varying the pH, altering the composition of a solvent mixture or adding a reactive species to continuously replenish kinetically unstable structures. The advent of smart gelators with multiaddressable behaviour will greatly expand this toolkit, allowing materials to adapt autonomously to changing demands, or assemble piecewise into intricate heterogeneous nanostructures with useful biomimetic functionalities.

5. Conclusions

Gels that undergo physical changes on exposure to external stimuli are not uncommon. Indeed, cycles of heating and cooling are a typical method for preparing such materials, and they are frequently identified and categorised based on their characteristic rheological responses to mechanical stress. What distinguishes a smart gel from a generic viscoelastic material is the variety, specificity and reversibility of its reactive behaviour. By exploiting these properties, systems may be engineered to deliver drugs, bind pollutants or catalyse reactions, and even mimic the complex dynamic properties of biological machinery, such as intracellular filaments, muscle tissue and sensory receptors.

Although a wide variety of smart gels have been examined to date, many opportunities remain unexplored. The potential for chemical variation among LMWGs is practically unlimited, and the use of co-gelators, additives or solvent mixtures allows the physical properties of gels to be adjusted for a range of applications. Designers of small-molecule gels enjoy access to well-defined scaffolds and reactive groups which can be combined in a modular fashion to deliver supramolecular systems with the desired responsive characteristics. However, a small number of structural motifs account for the vast majority of reported gelators, whilst a number of potentially useful moieties have yet to be utilised. Moreover, there is scope to develop smart gels comprising both smart LMWGs and non-gelating functional materials, including polymers, nanoparticles and metal-organic frameworks. Such hybrid systems could be imbued with properties difficult to achieve in pure small-molecule gels, and thus provide access to more varied and practically useful switchable behaviour.

A further limitation of current gelator design is that it relies on an incomplete model of gel formation. Self-assembly of small groups of molecules has been thoroughly investigated, and the microstructures of gel systems are also well documented. More poorly defined are the processes via which idealised supramolecular assemblies - which can be likened to the

primary structure of a peptide - evolve into the fibres, lamellae and vesicles constituting its tertiary structure. Nucleation, growth and folding of aggregates are often governed by environmental factors such as temperature, pH and solvent, and thus represent the earliest manifestation of stimuli-responsive behaviour in any gel system. The ability to computationally predict the dominant aggregation pathway would lead to more robust methods of gelator design, free of the empiricism and serendipity necessitated by our current level of understanding.

There is much to be gained from the emergence of smart gels with rationally designed characteristics. An obvious advantage of such materials is that they may be controlled remotely and non-invasively, to minimise unwanted effects on supported materials such as cells, crystals or catalytic particles. When used as reaction vessels and growth media, smart gels could provide a confined environment with tuneable interactions to influence transport, adhesion and coalescence of the guest. However, in contrast to biological matrices and even other synthetic porous materials, small-molecule gels are often uniform in composition and constructed from disordered networks of polydisperse aggregates. To produce more specific binding and more strongly influence guest behaviour, gels must be designed with surfaces that are chemically or microstructurally complementary to the target adsorbent. In gel-phase crystallisations, modified crystal habits have been generated through the use of gelators tailored to form supramolecular synthons with the crystallising molecule. Enhanced control of the gel-crystal interface might be achieved in mixed-gelator systems by orchestrating the sequential self-assembly of components with orthogonal stimuli. Alternatively, swelling or dissolution of the gel, induced by heat or illumination, could generate surface patterns of ridges and channels, to modulate the area available for binding or the speed and directionality of guest diffusion.

New avenues of research are made possible by the advent of gels responsive to multiple stimuli. Of particular note are systems that act as logic gates, with switchable behaviour that varies depending on the combination of thermal, optical and mechanical inputs. The more sophisticated examples of multiaddressable materials also deliver temporal information, responding differently to permutations of the same inputs or exploiting long-lived transformations to retain a memory of past treatments. Switchable small-molecule gels could record the changing conditions of a reaction mixture or deliver drugs *in vivo* at selected locations, by undergoing programmed dissolution at the target site. In addition, the logic gating capabilities of such systems may be viewed as conceptual analogues of natural feedback loops, which govern a range of complex phenomena such as bacterial quorum sensing, nerve signal propagation and microtubule growth through dynamic self-assembly.

It is clear that smart gels will continue to play an important role in the development of novel multifunctional nanomaterials. Innovations based on stimuli-sensitive LMWGs promise to revolutionise existing technologies and enable a new generation of exciting applications, in which the properties of a

gel can be tuned in response to varying real-time conditions. As archetypal examples of self-assembled systems, small-molecule gels will serve to inspire and inform new models of supramolecular aggregation and provide a test bed for bottom-up approaches to material design. Furthermore, improved mechanistic understanding of stimuli-induced behaviour will create the foundation for more intelligent gel-based devices, and offer insight into the complex and interdependent responses of their biological counterparts.

Acknowledgements

We are grateful to Stephen Jones (pineta.co.uk) for assistance in the preparation of the graphical abstract, and to the Engineering and Physical Sciences Research Council for funding via a Doctoral Scholarship (grant 1374655).

Notes and references

1. Y. Osada and K. Kajiwara, *Gels Handbook: Applications*, Academic Press, 2001.
2. K. Nishinari, *Prog. Colloid Polym. Sci.*, 2009, **136**, 87-94.
3. J. Alemán, A. V. Chadwick, J. He, M. Hess, K. Horie, R. G. Jones, P. Kratochvíl, I. Meisel, I. Mita, G. Moad, S. Penczek and R. F. T. Stepto, *Pure Appl. Chem.*, 2007, **79**, 1801-1827.
4. L. A. Estroff and A. D. Hamilton, *Chem. Rev.*, 2004, **104**, 1201-1217.
5. P. Terech and R. G. Weiss, *Chem. Rev.*, 1997, **97**, 3133-3159.
6. J. Le Bideau, L. Viau and A. Vioux, *Chem. Soc. Rev.*, 2011, **40**, 907-925.
7. M. Suzuki and K. Hanabusa, *Chem. Soc. Rev.*, 2010, **39**, 455-463.
8. J. W. Steed, *Chem. Commun.*, 2011, **47**, 1379-1383.
9. S. R. Raghavan and B. H. Cipriano, *Molecular Gels*, Springer, 2006.
10. P. Terech, D. Pasquier, V. Bordas and C. Rossat, *Langmuir*, 2000, **16**, 4485-4494.
11. J. H. van Esch, *Langmuir*, 2009, **25**, 8392-8394.
12. P. Dastidar, *Chem. Soc. Rev.*, 2008, **37**, 2699-2715.
13. J. G. Hardy, A. R. Hirst, I. Ashworth, C. Brennan and D. K. Smith, *Tetrahedron*, 2007, **63**, 7397-7406.
14. T. Rossow, S. Hackelbusch, P. van Assenbergh and S. Seiffert, *Polym. Chem.*, 2013, **4**, 2515-2527.
15. N. Zweep, A. Hopkinson, A. Meetsma, W. R. Browne, B. L. Feringa and J. H. van Esch, *Langmuir*, 2009, **25**, 8802-8809.
16. M. de Loos, B. L. Feringa and J. H. van Esch, *Eur. J. Org. Chem.*, 2005, 3615-3631.
17. J. Nanda, A. Biswas and A. Banerjee, *Soft Matter*, 2013, **9**, 4198-4208.
18. S. Ray, A. K. Das and A. Banerjee, *Chem. Mater.*, 2007, **19**, 1633-1639.
19. D. Schmaljohann, *Adv. Drug Deliv. Rev.*, 2006, **58**, 1655-1670.
20. K. Sugiyasu, N. Fujita, M. Takeuchi, S. Yamada and S. Shinkai, *Org. Biomol. Chem.*, 2003, **1**, 895-899.
21. P. Rajamalli and E. Prasad, *Org. Lett.*, 2011, **13**, 3714-3717.
22. P. Xie and R. B. Zhang, *J. Mater. Chem.*, 2005, **15**, 2529-2550.

23. Z. J. Zhao, J. W. Y. Lam and B. Z. Tang, *Soft Matter*, 2013, **9**, 4564-4579.
24. J. M. J. Paulusse and R. P. Sijbesma, *Angew. Chem. Int. Edit.*, 2006, **45**, 2334-2337.
25. A. Heller, *Curr. Opin. Chem. Biol.*, 2006, **10**, 664-672.
26. Y. Wu, Y. Hirai, Y. Tsunobuchi, H. Tokoro, H. Eimura, M. Yoshio, S. Ohkoshi and T. Kato, *Chem. Sci.*, 2012, **3**, 3007-3010.
27. P. Grondin, O. Roubeau, M. Castro, H. Saadaoui, A. Colin and R. Clérac, *Langmuir*, 2010, **26**, 5184-5195.
28. A. Das, M. R. Molla, B. Maity, D. Koley and S. Ghosh, *Chem. Eur. J.*, 2012, **18**, 9849-9859.
29. Y. H. Hou, F. F. Xin, M. J. Yin, L. Kong, H. C. Zhang, T. Sun, P. Y. Xing and A. Y. Hao, *Colloids Surf., A*, 2012, **414**, 160-167.
30. X. Y. Yang, G. X. Zhang and D. Q. Zhang, *J. Mater. Chem.*, 2012, **22**, 38-50.
31. Y. Qiao, Y. Y. Lin, Z. Y. Yang, H. F. Chen, S. F. Zhang, Y. Yan and J. B. Huang, *J. Phys. Chem. B*, 2010, **114**, 11725-11730.
32. L. W. Yan, Y. Xue, G. Gao, J. B. Lan, F. Yang, X. Y. Su and J. S. You, *Chem. Eur. J.*, 2010, **16**, 2250-2257.
33. X. D. Yu, Q. A. Liu, J. C. Wu, M. M. Zhang, X. H. Cao, S. Zhang, Q. Wang, L. M. Chen and T. Yi, *Chem. Eur. J.*, 2010, **16**, 9099-9106.
34. C. Wang, D. Q. Zhang and D. B. Zhu, *J. Am. Chem. Soc.*, 2005, **127**, 16372-16373.
35. S. S. Song, R. H. Dong, D. Wang, A. X. Song and J. C. Hao, *Soft Matter*, 2013, **9**, 4209-4218.
36. D. M. Ke, C. L. Zhan, A. D. Q. Li and J. N. Yao, *Angew. Chem. Int. Edit.*, 2011, **50**, 3715-3719.
37. S. N. Qu, L. J. Wang, X. Y. Liu and M. Li, *Chem. Eur. J.*, 2011, **17**, 3512-3518.
38. P. Jana, S. Maity, S. K. Maity, P. K. Ghorai and D. Haldar, *Soft Matter*, 2012, **8**, 5621-5628.
39. D. Braga, S. d'Agostino, E. D'Amen and F. Grepioni, *Chem. Commun.*, 2011, **47**, 5154-5156.
40. P. Y. Xing, S. Y. Li, F. F. Xin, Y. H. Hou, A. Y. Hao, T. Sun and J. Su, *Carbohydr. Res.*, 2013, **367**, 18-24.
41. N. Yan, Z. Y. Xu, K. K. Diehn, S. R. Raghavan, Y. Fang and R. G. Weiss, *Langmuir*, 2013, **29**, 793-805.
42. C. D. Dou, D. Li, H. Z. Gao, C. Y. Wang, H. Y. Zhang and Y. Wang, *Langmuir*, 2010, **26**, 2113-2118.
43. S. Kiyonaka, K. Sugiyasu, S. Shinkai and I. Hamachi, *J. Am. Chem. Soc.*, 2002, **124**, 10954-10955.
44. M. O. M. Piepenbrock, G. O. Lloyd, N. Clarke and J. W. Steed, *Chem. Rev.*, 2010, **110**, 1960-2004.
45. Z. X. Liu, Y. Feng, Z. C. Yan, Y. M. He, C. Y. Liu and Q. H. Fan, *Chem. Mater.*, 2012, **24**, 3751-3757.
46. L. Feng and K. A. Cavicchi, *Soft Matter*, 2012, **8**, 6483-6492.
47. A. R. Hirst, I. A. Coates, T. R. Boucheteau, J. F. Miravet, B. Escuder, V. Castelletto, I. W. Hamley and D. K. Smith, *J. Am. Chem. Soc.*, 2008, **130**, 9113-9121.
48. S. C. Wei, M. Pan, K. Li, S. J. Wang, J. Y. Zhang and C. Y. Su, *Adv. Mater.*, 2014, **26**, 2072-2077.
49. P. Y. Xing, T. Sun, S. Y. Li, A. Y. Hao, J. Su and Y. H. Hou, *Colloids Surf., A*, 2013, **421**, 44-50.
50. M. H. Yan, S. K. P. Velu, M. Marechal, G. Royal, J. Galvez and P. Terech, *Soft Matter*, 2013, **9**, 4428-4436.
51. J. J. Wu, M. L. Cao, J. Y. Zhang and B. H. Ye, *RSC Adv.*, 2012, **2**, 12718-12723.
52. F. F. Xin, H. C. Zhang, B. X. Hao, T. Sun, L. Kong, Y. M. Li, Y. H. Hou, S. Y. Li, Y. Zhang and A. Y. Hao, *Colloids Surf., A*, 2012, **410**, 18-22.
53. X. de Hatten, N. Bell, N. Yufa, G. Christmann and J. R. Nitschke, *J. Am. Chem. Soc.*, 2011, **133**, 3158-3164.
54. Y. Y. Li, J. A. Liu, G. Y. Du, H. Yan, H. Y. Wang, H. C. Zhang, W. An, W. J. Zhao, T. Sun, F. E. Xin, L. Kong, Y. M. Li, A. Y. Hao and J. C. Hao, *J. Phys. Chem. B*, 2010, **114**, 10321-10326.
55. K. Kuroiwa, T. Shibata, A. Takada, N. Nemoto and N. Kimizuka, *J. Am. Chem. Soc.*, 2004, **126**, 2016-2021.
56. J. A. Foster and J. W. Steed, *Angew. Chem. Int. Edit.*, 2010, **49**, 6718-6724.
57. D. J. Pochan, J. P. Schneider, J. Kretsinger, B. Ozbas, K. Rajagopal and L. Haines, *J. Am. Chem. Soc.*, 2003, **125**, 11802-11803.
58. J. L. Li and X. Y. Liu, *Adv. Funct. Mater.*, 2010, **20**, 3196-3216.
59. J. H. Shi, X. Y. Liu, J. L. Li, C. S. Strom and H. Y. Xu, *J. Phys. Chem. B*, 2009, **113**, 4549-4554.
60. W. T. Xu, H. W. Tang, H. Y. Lv, J. Li, X. L. Zhao, H. Li, N. Wang and X. N. Yang, *Soft Matter*, 2012, **8**, 726-733.
61. X. Y. Liu, P. D. Sawant, W. B. Tan, I. B. M. Noor, C. Pramesti and B. H. Chen, *J. Am. Chem. Soc.*, 2002, **124**, 15055-15063.
62. B. Yuan, X. Y. Liu, J. L. Li and H. Y. Xu, *Soft Matter*, 2011, **7**, 1708-1713.
63. M. Lescanne, A. Colin, O. Mondain-Monval, F. Fages and J. L. Pozzo, *Langmuir*, 2003, **19**, 2013-2020.
64. G. Schramm and G. Haake, *A practical approach to rheology and rheometry*, Haake Karlsruhe, 1994.
65. J. R. Moffat, I. A. Coates, F. J. Leng and D. K. Smith, *Langmuir*, 2009, **25**, 8786-8793.
66. G. M. Newbloom, K. M. Weigandt and D. C. Pozzo, *Macromolecules*, 2012, **45**, 3452-3462.
67. X. J. Wang, L. B. Xing, W. N. Cao, X. B. Li, B. Chen, C. H. Tung and L. Z. Wu, *Langmuir*, 2011, **27**, 774-781.
68. G. Tan, V. T. John and G. L. McPherson, *Langmuir*, 2006, **22**, 7416-7420.
69. R. Y. Wang, X. Y. Liu, J. Narayanan, J. Y. Xiong and J. L. Li, *J. Phys. Chem. B*, 2006, **110**, 25797-25802.
70. X. Y. Liu, *J. Phys. Chem. B*, 2001, **105**, 11550-11558.
71. J. L. Li, B. Yuan, X. Y. Liu and H. Y. Xu, *Cryst. Growth Des.*, 2010, **10**, 2699-2706.
72. J. L. Li, B. Yuan, X. Y. Liu, R.-Y. Wang and X. G. Wang, *Soft Matter*, 2013, **9**, 435-442.
73. M. A. Rogers and A. G. Marangoni, *Langmuir*, 2009, **25**, 8556-8566.
74. R. Lam, L. Quaroni, T. Pederson and M. A. Rogers, *Soft Matter*, 2010, **6**, 404-408.
75. D. H. Zhao and J. S. Moore, *Org. Biomol. Chem.*, 2003, **1**, 3471-3491.
76. P. Jonkheijm, P. van der Schoot, A. Schenning and E. W. Meijer, *Science*, 2006, **313**, 80-83.
77. S. Malik, S. K. Maji, A. Banerjee and A. K. Nandi, *J. Chem. Soc., Perkin Trans. 2*, 2002, 1177-1186.
78. T. Nakagawa, M. Amakatsu, K. Munenobu, H. Fujii and M. Yamanaka, *Chem. Lett.*, 2013, **42**, 229-231.
79. D. A. S. Grahame, C. Olafson, R. S. H. Lam, T. Pedersen, F. Borondics, S. Abraham, R. G. Weiss and M. A. Rogers, *Soft Matter*, 2011, **7**, 7359-7365.
80. A. Pal and J. Dey, *Langmuir*, 2013, **29**, 2120-2127.
81. M. O. M. Piepenbrock, G. O. Lloyd, N. Clarke and J. W. Steed, *Chem. Commun.*, 2008, **23**, 2644-2646.

82. S. Abraham, Y. Q. Lan, R. S. H. Lam, D. A. S. Grahame, J. J. H. Kim, R. G. Weiss and M. A. Rogers, *Langmuir*, 2012, **28**, 4955-4964.
83. M. A. Rogers, S. Abraham, F. Bodondics and R. G. Weiss, *Cryst. Growth Des.*, 2012, **12**, 5497-5504.
84. V. Čaplar, L. Frkanec, N. S. Vujičić and M. Žinić, *Chem. Eur. J.*, 2010, **16**, 3066-3082.
85. V. J. Nebot, J. J. Ojeda-Flores, J. Smets, S. Fernández-Prieto, B. Escuder and J. F. Miravet, *Chem. Eur. J.*, 2014, **20**, 14465-14472.
86. C. X. Zhang, T. R. Zhang, N. Ji, Y. Zhang, B. L. Bai, H. T. Wang and M. Li, *Soft Matter*, 2016, **12**, 1525-1533.
87. E. Dickinson, *J. Chem. Soc., Faraday Trans.*, 1997, **93**, 111-114.
88. J. Málek, *Thermochim. Acta*, 2000, **355**, 239-253.
89. M. Avrami, *J. Chem. Phys.*, 1939, **7**, 1103-1112.
90. M. M. Su, H. K. Yang, L. J. Ren, P. Zheng and W. Wang, *Soft Matter*, 2015, **11**, 741-748.
91. S. S. Rohner, J. Ruiz-Olles and D. K. Smith, *RSC Adv.*, 2015, **5**, 27190-27196.
92. H. Q. Xu, J. Song, T. Tian and R. X. Feng, *Soft Matter*, 2012, **8**, 3478-3486.
93. M. L. Muro-Small, J. Chen and A. J. McNeil, *Langmuir*, 2011, **27**, 13248-13253.
94. D. J. Adams, K. Morris, L. Chen, L. C. Serpell, J. Bacsá and G. M. Day, *Soft Matter*, 2010, **6**, 4144-4156.
95. J. L. Zhou, X. J. Chen and Y. S. Zheng, *Chem. Commun.*, 2007, 5200-5202.
96. J. H. Fuhrhop, P. Schnieder, J. Rosenberg and E. Boekema, *J. Am. Chem. Soc.*, 1987, **109**, 3387-3390.
97. K. Murata, M. Aoki, T. Suzuki, T. Harada, H. Kawabata, T. Komori, F. Ohseto, K. Ueda and S. Shinkai, *J. Am. Chem. Soc.*, 1994, **116**, 6664-6676.
98. K. A. Houton, K. L. Morris, L. Chen, M. Schmidtman, J. T. A. Jones, L. C. Serpell, G. O. Lloyd and D. J. Adams, *Langmuir*, 2012, **28**, 9797-9806.
99. B. Roy, P. Bairi and A. K. Nandi, *Soft Matter*, 2012, **8**, 2366-2369.
100. Y. J. Wang, L. M. Tang and J. Yu, *Cryst. Growth Des.*, 2008, **8**, 884-889.
101. I. Kapoor, E. M. Schön, J. Bachl, D. Kühbeck, C. Cativiela, S. Saha, R. Banerjee, S. Roelens, J. J. Marrero-Tellado and D. Díaz, *Soft Matter*, 2012, **8**, 3446-3456.
102. G. O. Lloyd and J. W. Steed, *Soft Matter*, 2011, **7**, 75-84.
103. G. H. Li, Y. Y. Hu, J. F. Sui, A. X. Song and J. C. Hao, *Langmuir*, 2016, **32**, 1502-1509.
104. C. D. Jones, J. C. Tan and G. O. Lloyd, *Chem. Commun.*, 2012, **48**, 2110-2112.
105. P. Byrne, G. O. Lloyd, L. Applegarth, K. M. Anderson, N. Clarke and J. W. Steed, *New J. Chem.*, 2010, **34**, 2261.
106. A. Vidyasagar and K. M. Sureshan, *Angew. Chem. Int. Edit.*, 2015, **54**, 12078-12082.
107. L. J. Teece, J. M. Hart, K. Y. N. Hsu, S. Gilligan, M. A. Faers and P. Bartlett, *Colloids Surf., A*, 2014, **458**, 126-133.
108. W. Li, Y. L. Guo, P. He, R. Yang, X. G. Li, Y. Chen, D. H. Liang, M. Kidowaki and K. Ito, *Polym. Chem.*, 2011, **2**, 1797-1802.
109. Y. L. Chen, Y. X. Lv, Y. Han, B. Zhu, F. Zhang, Z. S. Bo and C. Y. Liu, *Langmuir*, 2009, **25**, 8548-8555.
110. S. K. Samanta, A. Pal and S. Bhattacharya, *Langmuir*, 2009, **25**, 8567-8578.
111. P. Babu, N. M. Sangeetha, P. Vijaykumar, U. Maitra, K. Rissanen and A. R. Raju, *Chem. Eur. J.*, 2003, **9**, 1922-1932.
112. J. T. van Herpt, M. C. A. Stuart, W. R. Browne and B. L. Feringa, *Langmuir*, 2013, **29**, 8763-8767.
113. D. P. Penaloza, A. Shundo, K. Matsumoto, M. Ohno, K. Miyaji, M. Goto and K. Tanaka, *Soft Matter*, 2013, **9**, 5166-5172.
114. D. D. Díaz, D. Kühbeck and R. J. Koopmans, *Chem. Soc. Rev.*, 2011, **40**, 427-448.
115. B. Escuder, F. Rodríguez-Llansola and J. F. Miravet, *New J. Chem.*, 2010, **34**, 1044-1054.
116. F. Rodríguez-Llansola, B. Escuder and J. F. Miravet, *J. Am. Chem. Soc.*, 2009, **131**, 11478-11484.
117. J. Bachl, A. Hohenleutner, B. B. Dhar, C. Cativiela, U. Maitra, B. König and D. Díaz Díaz, *J. Mater. Chem. A*, 2013, **1**, 4577-4588.
118. C. Ruiz-Palomero, S. R. Kennedy, M. L. Soriano, C. D. Jones, M. Valcárcel and J. W. Steed, *Chem. Commun.*, 2016, **52**, 7782-7785.
119. A. Cayuela, S. R. Kennedy, M. L. Soriano, C. D. Jones, M. Valcárcel and J. W. Steed, *Chem. Sci.*, 2015, **6**, 6139-6146.
120. A. Dawn, K. S. Andrew, D. S. Yufit, Y. X. Hong, J. P. Reddy, C. D. Jones, J. A. Aguilar and J. W. Steed, *Cryst. Growth Des.*, 2015, **15**, 4591-4599.
121. D. K. Kumar and J. W. Steed, *Chem. Soc. Rev.*, 2014, **43**, 2080-2088.
122. D. B. Amabilino and J. Puigmarti-Luis, *Soft Matter*, 2010, **6**, 1605-1612.
123. J. A. Foster, M. O. M. Piepenbrock, G. O. Lloyd, N. Clarke, J. A. K. Howard and J. W. Steed, *Nat. Chem.*, 2010, **2**, 1037-1043.
124. L. A. Estroff, L. Addadi, S. Weiner and A. D. Hamilton, *Org. Biomol. Chem.*, 2004, **2**, 137-141.
125. H. J. Moon, D. Y. Ko, M. H. Park, M. K. Joo and B. Jeong, *Chem. Soc. Rev.*, 2012, **41**, 4860-4883.
126. A. R. Hirst, B. Escuder, J. F. Miravet and D. K. Smith, *Angew. Chem. Int. Edit.*, 2008, **47**, 8002-8018.
127. S. Armon, H. Aharoni, M. Moshe and E. Sharon, *Soft Matter*, 2014, **10**, 2733-2740.
128. M. Quesada-Pérez, J. Ramos, J. Forcada and A. Martín-Molina, *J. Chem. Phys.*, 2012, **136**, 244903.
129. M. M. Zhang, L. Y. Meng, X. H. Cao, M. J. Jiang and T. Yi, *Soft Matter*, 2012, **8**, 4494-4498.
130. C. Shi, Z. Huang, S. Kilic, J. Xu, R. M. Enick, E. J. Beckman, A. J. Carr, R. E. Melendez and A. D. Hamilton, *Science*, 1999, **286**, 1540-1543.
131. M. Quesada-Pérez, J. A. Maroto-Centeno, J. Forcada and R. Hidalgo-Alvarez, *Soft Matter*, 2011, **7**, 10536-10547.
132. T. Li, F. Nudelman, J. W. Tavecchi, H. Vass, D. J. Adams, A. Lips and P. S. Clegg, *Adv. Mater. Interfaces*, 2016, **3**, 8.
133. C. Liu, J. F. Yu, G. Q. Jiang, X. L. Liu, Z. Y. Li, G. Gao and F. Q. Liu, *J. Mater. Sci.*, 2013, **48**, 774-784.
134. S. L. Zhou, S. Matsumoto, H. D. Tian, H. Yamane, A. Ojida, S. Kiyonaka and I. Hamachi, *Chem. Eur. J.*, 2005, **11**, 1130-1136.
135. B. G. Xing, C. W. Yu, K. H. Chow, P. L. Ho, D. G. Fu and B. Xu, *J. Am. Chem. Soc.*, 2002, **124**, 14846-14847.
136. F. Ilmain, T. Tanaka and E. Kokufuta, *Nature*, 1991, **349**, 400-401.
137. M. Yemloul, E. Steiner, A. Robert, S. Bouguet-Bonnet, F. Allix, B. Jamart-Grégoire and D. Canet, *J. Phys. Chem. B*, 2011, **115**, 2511-2517.

138. E. Krieg, E. Shirman, H. Weissman, E. Shimoni, S. G. Wolf, I. Pinkas and B. Rybtchinski, *J. Am. Chem. Soc.*, 2009, **131**, 14365-14373.
139. G. D'Errico, L. Paduano, O. Ortona, G. Mangiapia, L. Coppola and F. Lo Celso, *J. Colloid Interface Sci.*, 2011, **359**, 179-188.
140. L. Bromberg, M. Temchenko, G. D. Moeser and T. A. Hatton, *Langmuir*, 2004, **20**, 5683-5692.
141. F. Rodríguez-Llansola, B. Escuder, I. W. Hamley, W. Hayes and J. F. Miravet, *Soft Matter*, 2012, **8**, 8865-8872.
142. M. M. Zhang, B. B. Wang, T. Jiang, M. J. Jiang and T. Yi, *CrystEngComm*, 2012, **14**, 8057-8062.
143. I. A. Coates and D. K. Smith, *Chem. Eur. J.*, 2009, **15**, 6340-6344.
144. D. Bardelang, F. Camerel, J. C. Margeson, D. M. Leek, M. Schmutz, M. B. Zaman, K. Yu, D. V. Soldatov, R. Ziessel, C. I. Ratcliffe and J. A. Ripmeester, *J. Am. Chem. Soc.*, 2008, **130**, 3313-3315.
145. Y. Cao, L. M. Tang, Y. J. Wang, B. Y. Zhang and L. K. Jia, *Chem. Lett.*, 2008, **37**, 554-555.
146. Y. Li and T. Tanaka, *J. Chem. Phys.*, 1990, **92**, 1365-1371.
147. Q. Huang, C. Y. Bao, W. Ji, Q. Y. Wang and L. Y. Zhu, *J. Mater. Chem.*, 2012, **22**, 18275-18282.
148. D. Klinger and K. Landfester, *Soft Matter*, 2011, **7**, 1426-1440.
149. M. Quesada-Pérez, J. A. Maroto-Centeno and A. Martín-Molina, *Macromolecules*, 2012, **45**, 8872-8879.
150. H. X. Yan and B. Jin, *Eur. Phys. J. E*, 2012, **35**, 36.
151. P. Hansson, *J. Phys. Chem. B*, 2009, **113**, 12903-12915.
152. E. Kokufuta, *Langmuir*, 2005, **21**, 10004-10015.
153. X. Bai, S. Y. Lu, Z. Cao, C. M. Gao, H. G. Duan, X. B. Xu, L. Sun, N. N. Gao, C. Feng and M. Z. Liu, *Chem. Eng. J.*, 2016, **288**, 546-556.
154. W. B. Liechty, D. R. Kryscio, B. V. Slaughter and N. A. Peppas, *Annu. Rev. Chem. Biomol. Eng.*, 2010, **1**, 149-173.
155. H. Omidian and K. Park, *J. Drug Deliv. Sci. Technol.*, 2008, **18**, 83-93.
156. L. C. Dong and A. S. Hoffman, *J. Control. Release*, 1991, **15**, 141-152.
157. H. Omidian, K. Park and J. G. Rocca, *J. Pharm. Pharmacol.*, 2007, **59**, 317-327.
158. H. Komatsu, S. Matsumoto, S. Tamaru, K. Kaneko, M. Ikeda and I. Hamachi, *J. Am. Chem. Soc.*, 2009, **131**, 5580-5585.
159. A. Shome, S. Debnath and P. K. Das, *Langmuir*, 2008, **24**, 4280-4288.
160. S. Dutta, T. Kar, D. Mandal and P. K. Das, *Langmuir*, 2013, **29**, 316-327.
161. C. Valenta, E. Nowack and A. Bernkop-Schnürch, *Int. J. Pharm.*, 1999, **185**, 103-111.
162. J. C. Tiller, *Angew. Chem. Int. Edit.*, 2003, **42**, 3072-3075.
163. A. Vintiloiu and J. C. Leroux, *J. Control. Release*, 2008, **125**, 179-192.
164. C. J. Yu, Z. Duan, P. X. Yuan, Y. H. Li, Y. W. Su, X. Zhang, Y. P. Pan, L. L. Dai, R. G. Nuzzo, Y. G. Huang, H. Q. Jiang and J. A. Rogers, *Adv. Mater.*, 2013, **25**, 1541-1546.
165. Y. Klein, E. Efrati and E. Sharon, *Science*, 2007, **315**, 1116-1120.
166. Z. L. Wu, M. Moshe, J. Greener, H. Therien-Aubin, Z. Nie, E. Sharon and E. Kumacheva, *Nat. Commun.*, 2013, **4**, 1586.
167. G. Stoychev, S. Zakharchenko, S. Turcaud, J. W. C. Dunlop and L. Ionov, *ACS Nano*, 2012, **6**, 3925-3934.
168. L. Ionov, *Adv. Funct. Mater.*, 2013, **23**, 4555-4570.
169. F. Pinaud, L. Russo, S. Pinet, I. Gosse, V. Ravaine and N. Sojic, *J. Am. Chem. Soc.*, 2013, **135**, 5517-5520.
170. G. Q. Wang, K. Kuroda, T. Enoki, A. Grosberg, S. Masamune, T. Oya, Y. Takeoka and T. Tanaka, *Proc. Natl. Acad. Sci. U.S.A.*, 2000, **97**, 9861-9864.
171. E. L. Cussler, *Diffusion: mass transfer in fluid systems*, Cambridge University Press, 2009.
172. P. C. Carman, *Chem. Eng. Res. Des.*, 1937, **75**, S32-S48.
173. T. Stylianopoulos, B. Diop-Frimpong, L. L. Munn and R. K. Jain, *Biophys. J.*, 2010, **99**, 3119-3128.
174. A. Erikson, H. N. Andersen, S. N. Naess, P. Sikorski and C. D. Davies, *Biopolymers*, 2008, **89**, 135-143.
175. M. Wallace, D. J. Adams and J. A. Iggo, *Soft Matter*, 2013, **9**, 5483-5491.
176. L. Petit, C. Barentin, J. Colombani, C. Ybert and L. Bocquet, *Langmuir*, 2009, **25**, 12048-12055.
177. S. Ramanujan, A. Pluen, T. D. McKee, E. B. Brown, Y. Boucher and R. K. Jain, *Biophys. J.*, 2002, **83**, 1650-1660.
178. E. M. Johnson, D. A. Berk, R. K. Jain and W. M. Deen, *Biophys. J.*, 1996, **70**, 1017-1023.
179. L. Lebrun and G. A. Junter, *Enzyme Microb. Technol.*, 1993, **15**, 1057-1062.
180. Y. E. Solomentsev and J. L. Anderson, *Phys. Fluids*, 1996, **8**, 1119-1121.
181. E. B. Schirmer and G. Carta, *Aiche J.*, 2009, **55**, 331-341.
182. D. Farnan, D. D. Frey and C. Horváth, *J. Chromatogr., A*, 2002, **959**, 65-73.
183. W. J. Musnicki, N. W. Lloyd, R. J. Phillips and S. R. Dungan, *J. Colloid Interface Sci.*, 2011, **356**, 165-175.
184. M. M. Tomadakis and D. Rupani, *Chem. Eng. J.*, 2007, **128**, 1-10.
185. J. M. Zalc, S. C. Reyes and E. Iglesia, *Chem. Eng. Sci.*, 2004, **59**, 2947-2960.
186. M. Golmohamadi, T. A. Davis and K. J. Wilkinson, *J. Phys. Chem. A*, 2012, **116**, 6505-6510.
187. R. J. Phillips, *J. Colloid Interface Sci.*, 2009, **338**, 250-260.
188. N. Lorén, L. Shtykova, S. Kidman, P. Jarvoll, M. Nydén and A. M. Hermansson, *Biomacromolecules*, 2009, **10**, 275-284.
189. K. B. Kostou and W. M. Deen, *Biophys. J.*, 2005, **88**, 277-286.
190. A. Pluen, P. A. Netti, R. K. Jain and D. A. Berk, *Biophys. J.*, 1999, **77**, 542-552.
191. M. Golmohamadi and K. J. Wilkinson, *Carbohydr. Polym.*, 2013, **94**, 82-87.
192. W. P. Krekelberg, V. K. Shen, J. R. Errington and T. M. Truskett, *J. Chem. Phys.*, 2011, **135**, 154502.
193. M. O. Coppens, *Catal. Today*, 1999, **53**, 225-243.
194. R. J. Phillips, *Biophys. J.*, 2000, **79**, 3350-3353.
195. J. Labille, N. Fatin-Rouge and J. Buffle, *Langmuir*, 2007, **23**, 2083-2090.
196. C. Nicholson and J. M. Phillips, *J. Physiol.*, 1981, **321**, 225-257.
197. J. Kowalczyk, A. Rachocki, M. Bielejewski and J. Tritt-Goc, *J. Colloid Interface Sci.*, 2016, **472**, 60-68.
198. W. M. Zhang, I. Gaberman and M. Ciszowska, *Anal. Chem.*, 2002, **74**, 1343-1348.
199. S. Poggendorf, G. A. Mba, D. Engel and G. Sadowski, *Colloid Polym. Sci.*, 2011, **289**, 545-559.
200. K. K. S. Buck, S. R. Dungan and R. J. Phillips, *J. Fluid Mech.*, 1999, **396**, 287-317.
201. J. Kowalczyk, M. Bielejewski, A. Łapiński, R. Luboradzki and J. Tritt-Goc, *J. Phys. Chem. B*, 2014, **118**, 4005-4015.

202. T. Oya, T. Enoki, A. Y. Grosberg, S. Masamune, T. Sakiyama, Y. Takeoka, K. Tanaka, G. Q. Wang, Y. Yilmaz, M. S. Feld, R. Dasari and T. Tanaka, *Science*, 1999, **286**, 1543-1545.
203. G. F. Elliott and S. A. Hodson, *Rep. Prog. Phys.*, 1998, **61**, 1325-1365.
204. R. Yoshida, T. Takahashi, T. Yamaguchi and H. Ichijo, *J. Am. Chem. Soc.*, 1996, **118**, 5134-5135.
205. Y. Shiraki and R. Yoshida, *Angew. Chem. Int. Edit.*, 2012, **51**, 6112-6116.
206. K. Miyakawa, F. Sakamoto, R. Yoshida, E. Kokufuta and T. Yamaguchi, *Phys. Rev. E*, 2000, **62**, 793-798.
207. B. Valeur, *Molecular fluorescence: principles and applications*, John Wiley & Sons, 2013.
208. E. J. Bowen and J. Sahu, *J. Phys. Chem.*, 1959, **63**, 4-5.
209. M. Kasha, *Radiat. Res.*, 1963, **20**, 55-70.
210. F. Würthner, T. E. Kaiser and C. R. Saha-Möller, *Angew. Chem. Int. Edit.*, 2011, **50**, 3376-3410.
211. S. Yao, U. Beginn, T. Gress, M. Lysetska and F. Würthner, *J. Am. Chem. Soc.*, 2004, **126**, 8336-8348.
212. V. K. Praveen, S. J. George, R. Varghese, C. Vijayakumar and A. Ajayaghosh, *J. Am. Chem. Soc.*, 2006, **128**, 7542-7550.
213. Y. N. Hong, J. W. Y. Lam and B. Z. Tang, *Chem. Soc. Rev.*, 2011, **40**, 5361-5388.
214. K. Char, C. W. Frank, A. P. Gast and W. T. Tang, *Macromolecules*, 1987, **20**, 1833-1838.
215. B. Chen, K. L. Liu, Z. X. Zhang, X. P. Ni, S. H. Goh and J. Li, *Chem. Commun.*, 2012, **48**, 5638-5640.
216. P. Rajamalli and E. Prasad, *Soft Matter*, 2012, **8**, 8896-8903.
217. X. D. Xu, J. Zhang, X. D. Yu, L. J. Chen, D. X. Wang, T. Yi, F. Y. Li and H. B. Yang, *Chem. Eur. J.*, 2012, **18**, 16000-16013.
218. Y. Kamikawa and T. Kato, *Langmuir*, 2007, **23**, 274-278.
219. T. Kato and K. Tanabe, *Chem. Lett.*, 2009, **38**, 634-639.
220. S. Yamane, Y. Sagara and T. Kato, *Chem. Commun.*, 2013, **49**, 3839-3841.
221. T. Cardolaccia, Y. J. Li and K. S. Schanze, *J. Am. Chem. Soc.*, 2008, **130**, 2535-2545.
222. N. Komiya, T. Muraoka, M. Iida, M. Miyanaga, K. Takahashi and T. Naota, *J. Am. Chem. Soc.*, 2011, **133**, 16054-16061.
223. S. Alex, M. C. Basheer, K. T. Arun, D. Ramaiah and S. Das, *J. Phys. Chem. A*, 2007, **111**, 3226-3230.
224. U. Rösch, S. Yao, R. Wortmann and F. Würthner, *Angew. Chem. Int. Edit.*, 2006, **45**, 7026-7030.
225. M. Cigáň, J. Donovalová, V. Szöcs, J. Gašpar, K. Jakusová and A. Gáplovský, *J. Phys. Chem. A*, 2013, **117**, 4870-4883.
226. A. Ajayaghosh and V. K. Praveen, *Acc. Chem. Res.*, 2007, **40**, 644-656.
227. Y. Cho, J. H. Lee, J. Jaworski, S. Park, S. S. Lee and J. H. Jung, *New J. Chem.*, 2012, **36**, 32-35.
228. C. Wang, C. J. Berg, C. C. Hsu, B. A. Merrill and M. J. Tauber, *J. Phys. Chem. B*, 2012, **116**, 10617-10630.
229. V. Kumar, G. A. Baker and S. Pandey, *Chem. Commun.*, 2011, **47**, 4730-4732.
230. P. C. Xue, Y. Zhang, J. H. Jia, D. F. Xu, X. F. Zhang, X. L. Liu, H. P. Zhou, P. Zhang, R. Lu, M. Takafuji and H. Ihara, *Soft Matter*, 2011, **7**, 8296-8304.
231. S. Yagai, Y. Nakano, S. Seki, A. Asano, T. Okubo, T. Isoshima, T. Karatsu, A. Kitamura and Y. Kikkawa, *Angew. Chem. Int. Edit.*, 2010, **49**, 9990-9994.
232. V. Karunakaran, D. D. Prabhu and S. Das, *J. Phys. Chem. C*, 2013, **117**, 9404-9415.
233. M. A. Drobizhev, M. N. Sapozhnikov, I. G. Scheblykin, O. P. Varnavsky, M. Van der Auweraer and A. G. Vitukhnovsky, *Chemical Physics*, 1996, **211**, 455-468.
234. A. Lohr, M. Lysetska and F. Würthner, *Angew. Chem. Int. Edit.*, 2005, **44**, 5071-5074.
235. K. Haraguchi, T. Takehisa and S. Fan, *Macromolecules*, 2002, **35**, 10162-10171.
236. D. Buenger, F. Topuz and J. Groll, *Prog. Polym. Sci.*, 2012, **37**, 1678-1719.
237. K. Ueno, K. Matsubara, M. Watanabe and Y. Takeoka, *Adv. Mater.*, 2007, **19**, 2807-2812.
238. S. Sutton, N. L. Campbell, A. I. Cooper, M. Kirkland, W. J. Frith and D. J. Adams, *Langmuir*, 2009, **25**, 10285-10291.
239. N. Willis-Fox, A. T. Marques, J. Arlt, U. Scherf, L. D. Carlos, H. D. Burrows and R. C. Evans, *Chem. Sci.*, 2015, **6**, 7227-7237.
240. A. Kaniyoor, B. McKenna, S. Comby and R. C. Evans, *Adv. Opt. Mater.*, 2015, 444-456.
241. M. Cross and H. Greenside, *Pattern Formation and Dynamics in Nonequilibrium Systems*, Cambridge University Press, 2009.
242. V. Castets, E. Dulos, J. Boissonade and P. Dekepper, *Phys. Rev. Lett.*, 1990, **64**, 2953-2956.
243. J. M. Köhler and S. C. Müller, *J. Phys. Chem.*, 1995, **99**, 980-983.
244. W. Hanke, M. Sieber, P. Spencer, J. Schwertner and V. M. F. de Lima, *Microgravity Sci. Technol.*, 2009, **21**, 239-246.
245. N. Tompkins, N. Li, C. Girabawe, M. Heymann, G. B. Ermentrout, I. R. Epstein and S. Fraden, *Proc. Natl. Acad. Sci. U.S.A.*, 2014, **111**, 4397-4402.
246. J. H. Jung, J. H. Lee, J. R. Silverman and G. John, *Chem. Soc. Rev.*, 2013, **42**, 924-936.
247. A. Y. Y. Tam and V. W. W. Yam, *Chem. Soc. Rev.*, 2013, **42**, 1540-1567.
248. J. W. Steed, *Chem. Soc. Rev.*, 2009, **38**, 506-519.
249. T. Fujigaya, D. L. Jiang and T. Aida, *Chem. Asian J.*, 2007, **2**, 106-113.
250. J. C. Wu, T. Yi, T. M. Shu, M. X. Yu, Z. G. Zhou, M. Xu, Y. F. Zhou, H. J. Zhang, J. T. Han, F. Y. Li and C. H. Huang, *Angew. Chem. Int. Edit.*, 2008, **47**, 1063-1067.
251. Z. Yang, G. Liang and B. Xu, *Acc. Chem. Res.*, 2008, **41**, 315-326.
252. L. A. Haines, K. Rajagopal, B. Ozbas, D. A. Salick, D. J. Pochan and J. P. Schneider, *J. Am. Chem. Soc.*, 2005, **127**, 17025-17029.
253. J. J. Zhang, Q. Zou and H. Tian, *Adv. Mater.*, 2013, **25**, 378-399.
254. X. Z. Yan, F. Wang, B. Zheng and F. H. Huang, *Chem. Soc. Rev.*, 2012, **41**, 6042-6065.
255. S. Yagai, T. Nakajima, K. Kishikawa, S. Kohmoto, T. Karatsu and A. Kitamura, *J. Am. Chem. Soc.*, 2005, **127**, 11134-11139.
256. M. Moriyama, N. Mizoshita and T. Kato, *Bull. Chem. Soc. Jpn.*, 2006, **79**, 962-964.
257. S. Lee, S. Oh, J. Lee, Y. Malpani, Y. S. Jung, B. Kang, J. Y. Lee, K. Ozasa, T. Isoshima, S. Y. Lee, M. Hara, D. Hashizume and J. M. Kim, *Langmuir*, 2013, **29**, 5869-5877.
258. Z. L. Pianowski, J. Karcher and K. Schneider, *Chem. Commun.*, 2016, **52**, 3143-3146.
259. Y. P. Wu, S. Wu, X. J. Tian, X. Wang, W. X. Wu, G. Zou and Q. J. Zhang, *Soft Matter*, 2011, **7**, 716-721.

260. X. Ran, H. T. Wang, P. Zhang, B. L. Bai, C. X. Zhao, Z. X. Yu and M. Li, *Soft Matter*, 2011, **7**, 8561-8566.
261. N. Koumura, M. Kudo and N. Tamaoki, *Langmuir*, 2004, **20**, 9897-9900.
262. F. Delbecq, N. Kaneko, H. Endo and T. Kawai, *J. Colloid Interface Sci.*, 2012, **384**, 94-98.
263. M. Fialkowski, K. J. M. Bishop, R. Klajn, S. K. Smoukov, C. J. Campbell and B. A. Grzybowski, *J. Phys. Chem. B*, 2006, **110**, 2482-2496.
264. J. Boekhoven, A. M. Brizard, K. N. K. Kowgi, G. J. M. Koper, R. Eelkema and J. H. van Esch, *Angew. Chem. Int. Edit.*, 2010, **49**, 4825-4828.
265. T. Seki, *Polym. J.*, 2004, **36**, 435-454.
266. E. Borré, J. F. Stumbé, S. Bellemin-Laponnaz and M. Mauro, *Angew. Chem. Int. Edit.*, 2016, **55**, 1313-1317.
267. F. Xie, L. Qin and M. H. Liu, *Chem. Commun.*, 2016, **52**, 930-933.
268. N. M. Sangeetha and U. Maitra, *Chem. Soc. Rev.*, 2005, **34**, 821-836.
269. K. P. Gan, M. Yoshio and T. Kato, *J. Mater. Chem. C*, 2016, **4**, 5073-5080.
270. Y. Zhao and X. Tong, *Adv. Mater.*, 2003, **15**, 1431-1435.
271. M. Moriyama, N. Mizoshita, T. Yokota, K. Kishimoto and T. Kato, *Adv. Mater.*, 2003, **15**, 1335-1338.
272. R. Reuter and H. A. Wegner, *Chem. Commun.*, 2013, **49**, 146-148.
273. K. Uchida, S. Yamaguchi, H. Yamada, M. Akazawa, T. Katayama, Y. Ishibashi and H. Miyasaka, *Chem. Commun.*, 2009, 4420-4422.
274. S. Yagai, T. Karatsu and A. Kitamura, *Langmuir*, 2005, **21**, 11048-11052.
275. M. de Loos, J. van Esch, R. M. Kellogg and B. L. Feringa, *Angew. Chem. Int. Edit.*, 2001, **40**, 613-616.
276. J. F. Xu, Y. Z. Chen, D. Y. Wu, L. Z. Wu, C. H. Tung and Q. Z. Yang, *Angew. Chem. Int. Edit.*, 2013, **52**, 9738-9742.
277. E. R. Draper, E. G. B. Eden, T. O. McDonald and D. J. Adams, *Nat. Chem.*, 2015, **7**, 849-853.
278. S. Miljanić, L. Frkanec, Z. Meić and M. Žinić, *Eur. J. Org. Chem.*, 2006, **5**, 1323-1334.
279. C. T. Chen, C. H. Chen and T. G. Ong, *J. Am. Chem. Soc.*, 2013, **135**, 5294-5297.
280. S. Matsumoto, S. Yamaguchi, S. Ueno, H. Komatsu, M. Ikeda, K. Ishizuka, Y. Iko, K. V. Tabata, H. Aoki, S. Ito, H. Noji and I. Hamachi, *Chem. Eur. J.*, 2008, **14**, 3977-3986.
281. L. L. Zhu, X. Li, Q. Zhang, X. Ma, M. H. Li, H. C. Zhang, Z. Luo, H. Agren and Y. L. Zhao, *J. Am. Chem. Soc.*, 2013, **135**, 5175-5182.
282. M. Herder, M. Utecht, N. Manicke, L. Grubert, M. Pätzelt, P. Saalfrank and S. Hecht, *Chem. Sci.*, 2013, **4**, 1028-1040.
283. S. Miljanić, L. Frkanec, Z. Meić and M. Žinić, *Langmuir*, 2005, **21**, 2754-2760.
284. H. Koshima, W. Matsusaka and H. T. Yu, *J. Photochem. Photobiol., A*, 2003, **156**, 83-90.
285. S. Ampornpun, S. Montha, G. Tumcharern, V. Vchirawongkwin, M. Sukwattanasinitt and S. Wacharasindhu, *Macromolecules*, 2012, **45**, 9038-9045.
286. F. Dumur, E. Contal, G. Wantz, T. N. T. Phan, D. Bertin and D. Gigmes, *Chem. Eur. J.*, 2013, **19**, 1373-1384.
287. M. de Loos, J. van Esch, I. Stokroos, R. M. Kellogg and B. L. Feringa, *J. Am. Chem. Soc.*, 1997, **119**, 12675-12676.
288. K. Sada, M. Takeuchi, N. Fujita, M. Numata and S. Shinkai, *Chem. Soc. Rev.*, 2007, **36**, 415-435.
289. S. Z. Zhang, X. J. Fu, H. Wang and Y. J. Yang, *J. Sep. Sci.*, 2008, **31**, 3782-3787.
290. M. Shirakawa, N. Fujita and S. Shinkai, *J. Am. Chem. Soc.*, 2005, **127**, 4164-4165.
291. J. R. Néabo, S. Rondeau-Gagné, C. Vigier-Carrière and J. F. Morin, *Langmuir*, 2013, **29**, 3446-3452.
292. J. Kim, J. Lee, W. Y. Kim, H. Kim, S. Lee, H. C. Lee, Y. S. Lee, M. Seo and S. Y. Kim, *Nat. Commun.*, 2015, **6**, 6959.
293. M. de Loos, A. G. J. Ligtenbarg, J. van Esch, H. Kooijman, A. L. Spek, R. Hage, R. M. Kellogg and B. L. Feringa, *Eur. J. Org. Chem.*, 2000, 3675-3678.
294. K. Aoki, M. Kudo and N. Tamaoki, *Org. Lett.*, 2004, **6**, 4009-4012.
295. J. Weiss, E. Jahnke, N. Severin, J. P. Rabe and H. Frauenrath, *Nano Lett.*, 2008, **8**, 1660-1666.
296. O. J. Dautel, M. Robitzler, J. P. Lère-Porte, F. Serein-Spirau and J. J. E. Moreau, *J. Am. Chem. Soc.*, 2006, **128**, 16213-16223.
297. M. Takizawa, A. Kimoto and J. Abe, *Dyes Pigm.*, 2011, **89**, 254-259.
298. A. Dawn, N. Fujita, S. Haraguchi, K. Sada, S. Tamaru and S. Shinkai, *Org. Biomol. Chem.*, 2009, **7**, 4378-4385.
299. G. C. Kuang, Y. Ji, X. R. Jia, Y. Li, E. Q. Chen, Z. X. Zhang and Y. Wei, *Tetrahedron*, 2009, **65**, 3496-3501.
300. H. T. Yu, H. Mizufune, K. Uenaka, T. Moritoki and H. Koshima, *Tetrahedron*, 2005, **61**, 8932-8938.
301. X. F. Wang, P. F. Duan and M. H. Liu, *Chem. Eur. J.*, 2013, **19**, 16072-16079.
302. J. He, B. Yan, L. Tremblay and Y. Zhao, *Langmuir*, 2011, **27**, 436-444.
303. J. E. Kwon and S. Y. Park, *Adv. Mater.*, 2011, **23**, 3615-3642.
304. T. H. Kim, M. S. Choi, B. H. Sohn, S. Y. Park, W. S. Lyoo and T. S. Lee, *Chem. Commun.*, 2008, 2364-2366.
305. Y. Qian, S. Y. Li, Q. Wang, X. H. Sheng, S. K. Wu, S. Q. Wang, J. Li and G. Q. Yang, *Soft Matter*, 2012, **8**, 757-764.
306. M. K. Nayak, *J. Photochem. Photobiol., A*, 2011, **217**, 40-48.
307. M. K. Nayak, B. H. Kim, J. E. Kwon, S. Park, J. Seo, J. W. Chung and S. Y. Park, *Chem. Eur. J.*, 2010, **16**, 7437-7447.
308. Y. Qian, S. Y. Li, G. Q. Zhang, Q. Wang, S. Q. Wang, H. J. Xu, C. Z. Li, Y. Li and G. Q. Yang, *J. Phys. Chem. B*, 2007, **111**, 5861-5868.
309. E. Hadjoudis and I. M. Mavridis, *Chem. Soc. Rev.*, 2004, **33**, 579-588.
310. M. Ziótek, G. Burdziński and A. Douhal, *Photochem. Photobiol. Sci.*, 2012, **11**, 1389-1400.
311. D. A. Safin, K. Robeyns and Y. Garcia, *RSC Adv.*, 2012, **2**, 11379-11388.
312. F. Robert, A. D. Naik, B. Tinant, R. Robiette and Y. Garcia, *Chem. Eur. J.*, 2009, **15**, 4327-4342.
313. R. Dobosz, A. Skotnicka, Z. Rozwadowski, T. Dziembowska and R. Gawinecki, *J. Mol. Struct.*, 2010, **979**, 194-199.
314. M. Sliwa, N. Mouton, C. Ruckebusch, L. Poisson, A. Idrissi, S. Aloïse, L. Potier, J. Dubois, O. Poizata and G. Buntinx, *Photochem. Photobiol. Sci.*, 2010, **9**, 661-669.
315. T. Sekikawa, O. Schalk, G. R. Wu, A. E. Boguslavskiy and A. Stolow, *J. Phys. Chem. A*, 2013, **117**, 2971-2979.
316. M. Z. Zgierski and E. C. Lim, *J. Phys. Chem. A*, 2011, **115**, 9689-9694.
317. F. Robert, A. D. Naik, F. Hidara, B. Tinant, R. Robiette, J. Wouters and Y. Garcia, *Eur. J. Org. Chem.*, 2010, 621-637.
318. F. Robert, P. L. Jacquemin, B. Tinant and Y. Garcia, *CrystEngComm*, 2012, **14**, 4396-4406.

319. D. A. Safin, K. Robeyns and Y. Garcia, *CrystEngComm*, 2012, **14**, 5523-5529.
320. G. K. Pierens, T. K. Venkatachalam, P. V. Bernhardt, M. J. Riley and D. C. Reutens, *Aust. J. Chem.*, 2012, **65**, 552-556.
321. M. M. Cai, Z. Q. Gao, X. H. Zhou, X. P. Wang, S. F. Chen, Y. Z. Zhao, Y. Qian, N. E. Shi, B. X. Mi, L. H. Xie and W. Huang, *Phys. Chem. Chem. Phys.*, 2012, **14**, 5289-5296.
322. J. Harada, H. Uekusa and Y. Ohashi, *J. Am. Chem. Soc.*, 1999, **121**, 5809-5810.
323. E. Hadjoudis, K. Yannakopoulou, S. D. Chatziefthimiou, A. Paulidou and I. M. Mavridis, *J. Photochem. Photobiol., A*, 2011, **217**, 293-298.
324. J. S. Xie, C. J. Chen, X. X. Ma and J. C. Wu, *Inorg. Chem. Commun.*, 2016, **65**, 41-44.
325. S. Datta and S. Bhattacharya, *Chem. Commun.*, 2012, **48**, 877-879.
326. P. Chen, R. Lu, P. C. Xue, T. H. Xu, G. J. Chen and Y. Y. Zhao, *Langmuir*, 2009, **25**, 8395-8399.
327. P. Xue, R. Lu, G. Chen, Y. Zhang, H. Nomoto, M. Takafuji and H. Ihara, *Chem. Eur. J.*, 2007, **13**, 8231-8239.
328. L. B. Zang, H. X. Shang, D. Y. Wei and S. M. Jiang, *Sens. Actuators, B*, 2013, **185**, 389-397.
329. Q. X. Jin, L. Zhang, X. F. Zhu, P. F. Duan and M. H. Liu, *Chem. Eur. J.*, 2012, **18**, 4916-4922.
330. V. I. Minkin, *Chem. Rev.*, 2004, **104**, 2751-2776.
331. S. A. Ahmed, Z. Moussa, S. Y. Al-Raqa and S. N. Alamry, *J. Phys. Org. Chem.*, 2009, **22**, 593-606.
332. Z. J. Qiu, H. T. Yu, J. B. Li, Y. Wang and Y. Zhang, *Chem. Commun.*, 2009, **23**, 3342-3344.
333. S. A. Ahmed, X. Sallenave, F. Fages, G. Mieden-Gundert, W. M. Müller, U. Müller, F. Vögtle and J. L. Pozzo, *Langmuir*, 2002, **18**, 7096-7101.
334. Q. Chen, D. Q. Zhang, G. X. Zhang, X. Y. Yang, Y. Feng, Q. H. Fan and D. B. Zhu, *Adv. Funct. Mater.*, 2010, **20**, 3244-3251.
335. Y. G. Li, K. M. C. Wong, A. Y. Y. Tam, L. X. Wu and V. W. W. Yam, *Chem. Eur. J.*, 2010, **16**, 8690-8698.
336. C. Maity, W. E. Hendriksen, J. H. van Esch and R. Eelkema, *Angew. Chem. Int. Edit.*, 2015, **54**, 998-1001.
337. V. I. Minkin, *Russ. Chem. Rev.*, 2013, **82**, 1-26.
338. G. Berkovic, V. Krongauz and V. Weiss, *Chem. Rev.*, 2000, **100**, 1741-1753.
339. M. Irie, *Chem. Rev.*, 2000, **100**, 1685-1716.
340. R. Göstl, B. Kobin, L. Grubert, M. Pätzl and S. Hecht, *Chem. Eur. J.*, 2012, **18**, 14282-14285.
341. S. Yagai, K. Ishiwatari, X. Lin, T. Karatsu, A. Kitamura and S. Uemura, *Chem. Eur. J.*, 2013, **19**, 6971-6975.
342. Y. Hotta, S. Fukushima, J. Motoyanagi and A. Tsuda, *Chem. Commun.*, 2015, **51**, 2790-2793.
343. S. C. Wei, M. Pan, Y. Z. Fan, H. L. Liu, J. Y. Zhang and C. Y. Su, *Chem. Eur. J.*, 2015, **21**, 7418-7427.
344. J. A. Foster, R. M. Parker, A. M. Belenguer, N. Kishi, S. Sutton, C. Abell and J. R. Nitschke, *J. Am. Chem. Soc.*, 2015, **137**, 9722-9729.
345. J. J. D. de Jong, P. R. Hania, A. Pugžlys, L. N. Lucas, M. de Loos, R. M. Kellogg, B. L. Feringa, K. Duppen and J. H. van Esch, *Angew. Chem. Int. Edit.*, 2005, **44**, 2373-2376.
346. Q. Chen, Y. Feng, D. Q. Zhang, G. X. Zhang, Q. H. Fan, S. N. Sun and D. B. Zhu, *Adv. Funct. Mater.*, 2010, **20**, 36-42.
347. S. Z. Xiao, Y. Zou, M. X. Yu, T. Yi, Y. F. Zhou, F. Y. Li and C. H. Huang, *Chem. Commun.*, 2007, 4758-4760.
348. J. Eastoe, M. Sánchez-Dominguez, P. Wyatt and R. K. Heenan, *Chem. Commun.*, 2004, 2608-2609.
349. A. Shumburo and M. C. Biewer, *Chem. Mater.*, 2002, **14**, 3745-3750.
350. J. J. D. de Jong, L. N. Lucas, R. M. Kellogg, J. H. van Esch and B. L. Feringa, *Science*, 2004, **304**, 278-281.
351. J. J. D. de Jong, T. D. Tiemersma-Wegman, J. H. van Esch and B. L. Feringa, *J. Am. Chem. Soc.*, 2005, **127**, 13804-13805.
352. J. J. D. de Jong, W. R. Browne, M. Walko, L. N. Lucas, L. J. Barrett, J. J. McGarvey, J. H. van Esch and B. L. Feringa, *Org. Biomol. Chem.*, 2006, **4**, 2387-2392.
353. H. Tian and S. J. Yang, *Chem. Soc. Rev.*, 2004, **33**, 85-97.
354. J. Andréasson and U. Pischel, *Chem. Soc. Rev.*, 2010, **39**, 174-188.
355. P. C. Xue, R. Lu, J. H. Jia, M. Takafuji and H. Ihara, *Chem. Eur. J.*, 2012, **18**, 3549-3558.
356. J. Andréasson, U. Pischel, S. D. Straight, T. A. Moore, A. L. Moore and D. Gust, *J. Am. Chem. Soc.*, 2011, **133**, 11641-11648.
357. Y. Liu, E. Kim, R. V. Ulijn, W. E. Bentley and G. F. Payne, *Adv. Funct. Mater.*, 2011, **21**, 1575-1580.
358. C. Yu, C. F. Wang and S. Chen, *Adv. Funct. Mater.*, 2014, **24**, 1235-1242.
359. S. C. Li, V. T. John, G. C. Irvin, S. H. Rachakonda, G. L. McPherson and C. J. O'Connor, *J. Appl. Phys.*, 1999, **85**, 5965-5967.
360. M. O. M. Piepenbrock, N. Clarke and J. W. Steed, *Soft Matter*, 2010, **6**, 3541-3547.
361. A. Zaccone, H. Wu, D. Gentili and M. Morbidelli, *Phys. Rev. E*, 2009, **80**, 051404.
362. G. J. Price, M. Ashokkumar, M. Hodnett, B. Zequiri and F. Grieser, *J. Phys. Chem. B*, 2005, **109**, 17799-17801.
363. G. Cravotto and P. Cintas, *Chem. Soc. Rev.*, 2006, **35**, 180-196.
364. K. S. Suslick and G. J. Price, *Annu. Rev. Mater. Sci.*, 1999, **29**, 295-326.
365. J. Rae, M. Ashokkumar, O. Eulaerts, C. von Sonntag, J. Reisse and F. Grieser, *Ultrason. Sonochem.*, 2005, **12**, 325-329.
366. E. B. Flint and K. S. Suslick, *Science*, 1991, **253**, 1397-1399.
367. S. J. Doktycz and K. S. Suslick, *Science*, 1990, **247**, 1067-1069.
368. D. Bardelang, *Soft Matter*, 2009, **5**, 1969-1971.
369. G. Cravotto and P. Cintas, *Chem. Soc. Rev.*, 2009, **38**, 2684-2697.
370. E. Blanco, L. Esquivias, R. Litrán, M. Piñero, M. Ramírez-del-Solar and N. de la Rosa-Fox, *Appl. Organomet. Chem.*, 1999, **13**, 399-418.
371. X. Q. Cai, Y. Wu, L. Y. Wang, N. Yan, J. Liu, X. H. Fang and Y. Fang, *Soft Matter*, 2013, **9**, 5807-5814.
372. Y. B. He, Z. Bian, C. Q. Kang, R. Z. Jin and L. X. Gao, *New J. Chem.*, 2009, **33**, 2073-2080.
373. K. M. Anderson, G. M. Day, M. J. Paterson, P. Byrne, N. Clarke and J. W. Steed, *Angew. Chem. Int. Edit.*, 2008, **47**, 1058-1062.
374. C. Baddeley, Z. Q. Yan, G. King, P. M. Woodward and J. D. Badjić, *J. Org. Chem.*, 2007, **72**, 7270-7278.
375. C. D. Dou, D. Chen, J. Iqbal, Y. Yuan, H. Y. Zhang and Y. Wang, *Langmuir*, 2011, **27**, 6323-6329.
376. R. Y. Wang, X. Y. Liu and J. L. Li, *Cryst. Growth Des.*, 2009, **9**, 3286-3291.

377. D. Bardelang, M. Giorgi, V. Hornebecq, A. Stepanov, E. Rizzato, M. B. Zaman, G. Chan, O. Ouari and P. Tordo, *RSC Adv.*, 2012, **2**, 5605-5609.
378. W. Weng, J. B. Beck, A. M. Jamieson and S. J. Rowan, *J. Am. Chem. Soc.*, 2006, **128**, 11663-11672.
379. A. J. P. Teunissen, M. M. L. Nieuwenhuizen, F. Rodríguez-Llansola, A. R. A. Palmans and E. W. Meijer, *Macromolecules*, 2014, **47**, 8429-8436.
380. T. Naota and H. Koori, *J. Am. Chem. Soc.*, 2005, **127**, 9324-9325.
381. K. Y. Liu, L. Y. Meng, S. L. Mo, M. M. Zhang, Y. Y. Mao, X. H. Cao, C. H. Huang and T. Yi, *J. Mater. Chem. C*, 2013, **1**, 1753-1762.
382. A. W. P. Fitzpatrick, G. T. Debelouchina, M. J. Bayro, D. K. Clare, M. A. Caporini, V. S. Bajaj, C. P. Jaroniec, L. C. Wang, V. Ladizhansky, S. A. Müller, C. E. MacPhee, C. A. Waudby, H. R. Mott, A. De Simone, T. P. J. Knowles, H. R. Saibil, M. Vendruscolo, E. V. Orlova, R. G. Griffin and C. M. Dobson, *Proc. Natl. Acad. Sci. U.S.A.*, 2013, **110**, 5468-5473.
383. S. Maity, P. Kumar and D. Haldar, *Soft Matter*, 2011, **7**, 5239-5245.
384. J. M. J. Paulusse, D. J. M. van Beek and R. P. Sijbesma, *J. Am. Chem. Soc.*, 2007, **129**, 2392-2397.
385. J. M. J. Paulusse, J. P. J. Huijbers and R. P. Sijbesma, *Chem. Eur. J.*, 2006, **12**, 4928-4934.
386. S. Y. Zhang, S. J. Yang, J. B. Lan, Y. R. Tang, Y. Xue and J. S. You, *J. Am. Chem. Soc.*, 2009, **131**, 1689-1691.
387. Y. B. Wang, C. L. Zhan, H. B. Fu, X. Li, X. H. Sheng, Y. S. Zhao, D. B. Xiao, Y. Ma, J. S. Ma and J. N. Yao, *Langmuir*, 2008, **24**, 7635-7638.
388. C. Deng, R. Fang, Y. F. Guan, J. L. Jiang, C. Lin and L. Y. Wang, *Chem. Commun.*, 2012, **48**, 7973-7975.
389. S. M. Park and B. H. Kim, *Soft Matter*, 2008, **4**, 1995-1997.
390. D. M. Ke, C. L. Zhan, X. Li, X. Wang, Y. Zeng and J. N. Yao, *J. Colloid Interface Sci.*, 2009, **337**, 54-60.
391. W. G. Weng, J. B. Beck, A. M. Jamieson and S. J. Rowan, *J. Am. Chem. Soc.*, 2006, **128**, 11663-11672.
392. J. Lyklema, *Fundamentals of Interface and Colloid Science: Particulate Colloids*, Morgan Kaufmann, 2005.
393. K. Hyun, S. H. Kim, K. H. Ahn and S. J. Lee, *J. Non-Newtonian Fluid Mech.*, 2002, **107**, 51-65.
394. K. Hyun, J. G. Nam, M. Wilhelm, K. H. Ahn and S. J. Lee, *Rheol. Acta*, 2006, **45**, 239-249.
395. M. O. M. Piepenbrock, N. Clarke and J. W. Steed, *Soft Matter*, 2011, **7**, 2412-2418.
396. X. D. Yu, X. H. Cao, L. M. Chen, H. C. Lan, B. Liu and T. Yi, *Soft Matter*, 2012, **8**, 3329-3334.
397. W. H. Shih, W. Y. Shih, S. I. Kim, J. Liu and I. A. Aksay, *Phys. Rev. A*, 1990, **42**, 4772-4779.
398. N. M. Sangeetha, S. Bhat, A. R. Choudhury, U. Maitra and P. Terech, *J. Phys. Chem. B*, 2004, **108**, 16056-16063.
399. Z. Y. Xu, J. X. Peng, N. Yan, H. Yu, S. S. Zhang, K. Q. Liu and Y. Fang, *Soft Matter*, 2013, **9**, 1091-1099.
400. L. J. Gibson and M. F. Ashby, *Proc. R. Soc. London, A*, 1982, **382**, 43-49.
401. G. O. Lloyd, M. O. M. Piepenbrock, J. A. Foster, N. Clarke and J. W. Steed, *Soft Matter*, 2012, **8**, 204-216.
402. C. E. Stanley, N. Clarke, K. M. Anderson, J. A. Elder, J. T. Lenthall and J. W. Steed, *Chem. Commun.*, 2006, **30**, 3199-3201.
403. S. Paavilainen, J. L. McWhirter, T. Rog, J. Jarvinen, I. Vattulainen and J. A. Ketoja, *Nord. Pulp Paper Res. J.*, 2012, **27**, 282-286.
404. A. Gautieri, M. J. Buehler and A. Redaelli, *J. Mech. Behav. Biomed. Mater.*, 2009, **2**, 130-137.
405. J. Y. Chen, B. Yuan, Z. Y. Li, B. Tang, E. Ankers, X. G. Wang and J. L. Li, *Langmuir*, 2016, **32**, 1171-1177.
406. S. K. Tang, X. Y. Liu and C. S. Strom, *Adv. Funct. Mater.*, 2009, **19**, 2252-2259.
407. J. L. Li, X. Y. Liu, R. Y. Wang and J. Y. Xiong, *J. Phys. Chem. B*, 2005, **109**, 24231-24235.
408. M. Djabourov, K. Nishinari and S. B. Ross-Murphy, *Physical Gels from Biological and Synthetic Polymers*, Cambridge University Press, 2013.
409. N. W. Tschoegl, *The Phenomenological Theory of Linear Viscoelastic Behaviour: An Introduction*, Springer-Verlag, 2012.
410. P. Sollich, *Phys. Rev. E*, 1998, **58**, 738-759.
411. T. Ozdemir and F. Sozmen, *RSC Adv.*, 2016, **6**, 10601-10605.
412. Y. Shi, M. Wang, C. B. Ma, Y. Q. Wang, X. P. Li and G. H. Yu, *Nano Lett.*, 2015, **15**, 6276-6281.
413. P. Sahoo, R. Sankolli, H. Y. Lee, S. R. Raghavan and P. Dastidar, *Chem. Eur. J.*, 2012, **18**, 8057-8063.
414. J. L. Yan, J. Liu, H. R. Lei, Y. Kang, C. Zhao and Y. Fang, *J. Colloid Interface Sci.*, 2015, **448**, 374-379.
415. G. W. Huang, Q. L. Yu, M. R. Cai, F. Zhou and W. M. Liu, *Adv. Mater. Interfaces*, 2016, **3**, 10.
416. Q. L. Yu, D. M. Li, M. R. Cai, F. Zhou and W. M. Liu, *Tribol. Lett.*, 2016, **61**, 16.
417. A. Dawn, T. Shiraki, H. Ichikawa, A. Takada, Y. Takahashi, Y. Tsuchiya, L. T. N. Lien and S. Shinkai, *J. Am. Chem. Soc.*, 2012, **134**, 2161-2171.
418. K. Q. Liu and J. W. Steed, *Soft Matter*, 2013, **9**, 11699-11705.
419. P. Terech, M. H. Yan, M. Maréchal, G. Royal, J. Galvez and S. K. P. Velu, *Phys. Chem. Chem. Phys.*, 2013, **15**, 7338-7344.
420. P. Bartlett, L. J. Teece and M. A. Faers, *Phys. Rev. E*, 2012, **85**, 021404.
421. C. S. O'Hern, L. E. Silbert, A. J. Liu and S. R. Nagel, *Phys. Rev. E*, 2003, **68**, 011306.
422. K. Pogoda, L. Chin, P. C. Georges, F. J. Byfield, R. Bucki, R. Kim, M. Weaver, R. G. Wells, C. Marcinkiewicz and P. A. Janmey, *New J. Phys.*, 2014, **16**, 075002.
423. V. V. Yashin, O. Kuksenok and A. C. Balazs, *J. Phys. Chem. B*, 2010, **114**, 6316-6322.
424. A. S. van Oosten, M. Vahabi, A. J. Licup, A. Sharma, P. A. Galie, F. C. MacKintosh and P. A. Janmey, *Sci. Rep.*, 2016, **6**, 19270.
425. O. V. Kim, R. I. Litvinov, J. W. Weisel and M. S. Alber, *Biomaterials*, 2014, **35**, 6739-6749.
426. U. S. Schwarz and S. A. Safran, *Rev. Mod. Phys.*, 2013, **85**, 1327-1381.
427. P. A. Janmey and R. T. Miller, *J. Cell Sci.*, 2010, **124**, 9-18.
428. I. Levental, P. C. Georges and P. A. Janmey, *Soft Matter*, 2007, **3**, 299-306.
429. H. Kang, Q. Wen, P. A. Janmey, J. X. Tang, E. Conti and F. C. MacKintosh, *J. Phys. Chem. B*, 2009, **113**, 3799-3805.
430. M. L. Gardel, J. H. Shin, F. C. MacKintosh, L. Mahadevan, P. Matsudaira and D. A. Weitz, *Science*, 2004, **304**, 1301-1305.

431. J. R. Blundell and E. M. Terentjev, *Macromolecules*, 2009, **42**, 5388-5394.
432. R. H. Pritchard, Y. Y. Huang and E. M. Terentjev, *Soft Matter*, 2014, **10**, 1864-1884.
433. M. Jaspers, M. Dennison, M. F. J. Mabesoone, F. C. MacKintosh, A. E. Rowan and P. H. J. Kouwer, *Nat. Commun.*, 2014, **5**, 5808.
434. C. G. Pappas, P. Frederix, T. Mutasa, S. Fleming, Y. M. Abul-Haija, S. M. Kelly, A. Gachagan, D. Kalafatovic, J. Trevino, R. V. Uljijn and S. Bai, *Chem. Commun.*, 2015, **51**, 8465-8468.
435. Y. Hotta, S. Suiko, J. Motoyanagi, H. Onishi, T. Ihozaki, R. Arakawa and A. Tsuda, *Chem. Commun.*, 2014, **50**, 5615-5618.
436. H. M. M. ten Eikelder, A. J. Markvoort, T. F. A. de Greef and P. A. J. Hilbers, *J. Phys. Chem. B*, 2012, **116**, 5291-5301.
437. W. L. Noorduin, T. Izumi, A. Millemaggi, M. Leeman, H. Meekes, W. J. P. Van Enckevort, R. M. Kellogg, B. Kaptein, E. Vlieg and D. G. Blackmond, *J. Am. Chem. Soc.*, 2008, **130**, 1158-1159.
438. L. Pérez-García and D. B. Amabilino, *Chem. Soc. Rev.*, 2002, **31**, 342-356.
439. J. W. Steed and J. L. Atwood, *Supramolecular Chemistry*, John Wiley & Sons, 2013.
440. Y. Saito and H. Hyuga, *Rev. Mod. Phys.*, 2013, **85**, 603-621.
441. Z. El-Hachemi, J. Crusats, J. M. Ribó and S. Veintemillas-Verdaguer, *Cryst. Growth Des.*, 2009, **9**, 4802-4806.
442. D. K. Kondepudi, R. J. Kaufman and N. Singh, *Science*, 1990, **250**, 975-976.
443. J. Crusats, Z. El-Hachemi and J. M. Ribó, *Chem. Soc. Rev.*, 2010, **39**, 569-577.
444. D. B. Amabilino, *Nat. Mater.*, 2007, **6**, 924-925.
445. C. Escudero, J. Crusats, I. Díez-Pérez, Z. El-Hachemi and J. M. Ribó, *Angew. Chem. Int. Edit.*, 2006, **45**, 8032-8035.
446. S. Azeroual, J. Surprenant, T. D. Lazzara, M. Kocun, Y. Tao, L. A. Cuccia and J. M. Lehn, *Chem. Commun.*, 2012, **48**, 2292-2294.
447. M. Wolffs, S. J. George, Ž. Tomović, S. C. J. Meskers, A. P. H. J. Schenning and E. W. Meijer, *Angew. Chem. Int. Edit.*, 2007, **46**, 8203-8205.
448. A. Tsuda, M. A. Alam, T. Harada, T. Yamaguchi, N. Ishii and T. Aida, *Angew. Chem. Int. Edit.*, 2007, **46**, 8198-8202.
449. J. Liu, P. L. He, J. L. Yan, X. H. Fang, J. X. Peng, K. Q. Liu and Y. Fang, *Adv. Mater.*, 2008, **20**, 2508-2511.
450. J. Brinksma, B. L. Feringa, R. M. Kellogg, R. Vreeker and J. van Esch, *Langmuir*, 2000, **16**, 9249-9255.
451. J. C. Wu, T. Yi, Q. Xia, Y. Zou, F. Liu, H. Dong, T. M. Shu, F. Y. Li and C. H. Huang, *Chem. Eur. J.*, 2009, **15**, 6234-6243.
452. Y. Zhang, H. Ding, Y. F. Wu, C. X. Zhang, B. L. Bai, H. T. Wang and M. Li, *Soft Matter*, 2014, **10**, 8838-8845.
453. X. Y. Liu and P. D. Sawant, *Adv. Mater.*, 2002, **14**, 421-426.
454. P. Byrne, D. R. Turner, G. O. Lloyd, N. Clarke and J. W. Steed, *Cryst. Growth Des.*, 2008, **8**, 3335-3344.
455. X. F. Sui, X. L. Feng, M. A. Hempenius and G. J. Vancso, *J. Mater. Chem. B*, 2013, **1**, 1658-1672.
456. C. Wang, Q. Chen, F. Sun, D. Zhang, G. Zhang, Y. Huang, R. Zhao and D. Zhu, *J. Am. Chem. Soc.*, 2010, **132**, 3092-3096.
457. P. F. Duan, Y. G. Li, L. C. Li, J. G. Deng and M. H. Liu, *J. Phys. Chem. B*, 2011, **115**, 3322-3329.
458. C. X. Liu, D. Yang, Q. X. Jin, L. Zhang and M. H. Liu, *Adv. Mater.*, 2016, **28**, 1644-1649.
459. R. Pardo, M. Zayat and D. Levy, *Chem. Soc. Rev.*, 2011, **40**, 672-687.
460. J. L. Yan, J. Liu, P. Jing, C. K. Xu, J. M. Wu, D. Gao and Y. Fang, *Soft Matter*, 2012, **8**, 11697-11703.
461. D. J. Cornwell and D. K. Smith, *Mater. Horiz.*, 2015, **2**, 279-293.
462. J. A. Foster, R. M. Edkins, G. J. Cameron, N. Colgin, K. Fucke, S. Ridgeway, A. G. Crawford, T. B. Marder, A. Beeby, S. L. Cobb and J. W. Steed, *Chem. Eur. J.*, 2014, **20**, 279-291.
463. K. Miyamoto, H. Jintoku, T. Sawada, M. Takafuji, T. Sagawa and H. Ihara, *Tetrahedron Lett.*, 2011, **52**, 4030-4035.
464. E. Wang, M. S. Desai and S. W. Lee, *Nano Lett.*, 2013, **13**, 2826-2830.
465. Y. Okumura and K. Ito, *Adv. Mater.*, 2001, **13**, 485-487.
466. P. C. Xue, R. Lu, L. Zhao, D. F. Xu, X. F. Zhang, K. C. Li, Z. G. Song, X. C. Yang, M. Takafuji and H. Ihara, *Langmuir*, 2010, **26**, 6669-6675.
467. K. L. Morris, L. Chen, J. Raeburn, O. R. Sellick, P. Cotanda, A. Paul, P. C. Griffiths, S. M. King, R. K. O'Reilly, L. C. Serpell and D. J. Adams, *Nat. Commun.*, 2013, **4**, 1480.
468. J. Raeburn, B. Alston, J. Kroeger, T. O. McDonald, J. R. Howse, P. J. Cameron and D. J. Adams, *Mater. Horiz.*, 2014, **1**, 241-246.
469. C. Colquhoun, E. R. Draper, E. G. B. Eden, B. N. Cattoz, K. L. Morris, L. Chen, T. O. McDonald, A. E. Terry, P. C. Griffiths, L. C. Serpell and D. J. Adams, *Nanoscale*, 2014, **6**, 13719-13725.
470. J. P. Gong, *Soft Matter*, 2010, **6**, 2583-2590.
471. M. A. Haque, T. Kurokawa and J. P. Gong, *Polymer*, 2012, **53**, 1805-1822.
472. G. E. Fantner, T. Hassenkam, J. H. Kindt, J. C. Weaver, H. Birkedal, L. Pechenik, J. A. Cutroni, G. A. G. Cidade, G. D. Stucky, D. E. Morse and P. K. Hansma, *Nat. Mater.*, 2005, **4**, 612-616.
473. A. S. Gladman, E. A. Matsumoto, R. G. Nuzzo, L. Mahadevan and J. A. Lewis, *Nat. Mater.*, 2016, **15**, 413-418.
474. J. W. Li, I. Cvrtila, M. Colomb-Delsuc, E. Otten and S. Otto, *Chem. Eur. J.*, 2014, **20**, 15709-15714.
475. T. T. H. Pham, J. Y. Wang, M. W. T. Werten, F. Snijkers, F. A. de Wolf, M. A. C. Stuart and J. van der Gucht, *Soft Matter*, 2013, **9**, 8923-8930.
476. R. T. Woodward, C. I. Olariu, E. A. Hasan, H. H. P. Yiu, M. J. Rosseinsky and J. V. M. Weaver, *Soft Matter*, 2011, **7**, 4335-4340.
477. R. M. Yang, S. H. Peng and T. C. Hughes, *Soft Matter*, 2014, **10**, 2188-2196.
478. T. T. H. Pham, F. A. de Wolf, M. A. C. Stuart and J. van der Gucht, *Soft Matter*, 2013, **9**, 8737-8744.